Heedong Goh

Lecture Notes for

Structural Analysis

Department of Civil and Environmental Engineering
Seoul National University
2025

Preface

These lecture notes are written for the courses *Structural Analysis 1 and 2* offered in the Department of Civil and Environmental Engineering at Seoul National University. The composition of the notes is heavily based on the courses *Structural Analysis 1 and 2* taught by Professor Hae Sung Lee from year 1993 to 2022 [Lee, 2022a, Lee, 2022b].

These lecture notes are a working manuscript, subject to ongoing refinement and enhancement; I welcome and greatly appreciate any reports regarding errors, typos, or any other inaccuracies found within the notes.

Double-crested cormorants near DB Drawbridge, Secaucus, NJ, USA.

Contents

Part I

Chapter 1

Preliminaries

1.1 Algebraic and differential equations

An engineering problem often takes a form of equation solving, which is a deductive process of unraveling unknowns out of an implicit information hidden in equations. The operators of algebraic equations are $+$, $-$, $\times$, and $\div$. For example, a system of linear algebraic equations reads:
Given $A \in \mathbb{R}^{M\times N}$ and $b \in \mathbb{R}^M$, find $x \in \mathbb{R}^N$ such that $Ax = b$ or

$$\begin{cases} A_{11}x_1 + A_{12}x_2 + \ldots + A_{1N}x_N = b_1 \\ A_{21}x_1 + A_{22}x_2 + \ldots + A_{2N}x_N = b_2 \\ \qquad\qquad\qquad \vdots \\ A_{M1}x_1 + A_{M2}x_2 + \ldots + A_{MN}x_N = b_M \end{cases} \tag{1.1}$$

or

$$\sum_{j=1}^{N} A_{ij}x_j = b_i,\ i = 1, 2, \ldots, M. \tag{1.2}$$

The unknowns of algebraic equations x_j, are *numbers*, where the number of unknowns, or *dimension*, N is typically finite. We also have a finite number of equations denoted by M. Thanks to the linearity, we can find out whether the problem is solvable by counting the number of independent equations, i.e.,

$$\begin{cases} N > M & \text{no unique solution (underdetermined system)} \\ N = M & \text{unique solution} \\ N < M & \text{no solution (overdetermined system)} \end{cases}.$$

Consider a linearly suspended mass-spring system. The equilibrium equation for each mass m_i is

$$k_i\left(x_i - x_{i-1}\right) - k_{i+1}\left(x_{i+1} - x_i\right) - m_i g = 0, \quad i = 0, 1, 2, \ldots, N. \tag{1.3}$$

Let $x_0 = 0$; we have a system of linear algebraic equations,

$$\begin{bmatrix} k_1+k_2 & -k_2 & 0 & \dots & 0 \\ -k_1 & k_2+k_3 & -k_3 & \dots & 0 \\ 0 & -k_2 & k_2+k_3 & \dots & 0 \\ \vdots & \vdots & \vdots & \ddots & \vdots \\ 0 & 0 & 0 & \dots & k_N \end{bmatrix} \begin{pmatrix} x_1 \\ x_2 \\ x_3 \\ \vdots \\ x_N \end{pmatrix} = \begin{pmatrix} m_1 g \\ m_2 g \\ m_3 g \\ \vdots \\ m_N g \end{pmatrix}. \tag{1.4}$$

On the other hand, we seek for *functions* when solving differential equations, which involves with differential operators. For example:
Given $L : \mathcal{V} \to \mathcal{W}$ and $f \in \mathcal{W}$, find $u \in \mathcal{V}$ such that

$$\begin{cases} Lu(x) \equiv \dfrac{d^2 u(x)}{dx^2} = f(x), \quad x \in (0,1) & \text{(governing equation)} \\ u(0) = u(1) = 0 & \text{(boundary conditions)} \end{cases}. \tag{1.5}$$

In the above, the unknown function $u : \mathbb{R} \to \mathbb{R}$ and the corresponding governing equation are defined over an interval $x \in (0,1)$, which excludes boundaries. The function values at the boundaries are explicitly given as boundary conditions. Unlike the algebraic equations, the dimension of a function space, such as $\mathcal{W}$ and $\mathcal{V}$, is infinite. When defining a function space, we consider a set of *admissible functions* to satisfy physical/mathematical constraints such as continuity and differentiability. Rigorous studies on function space or the existence and the uniqueness of differential equations are out of our scope.

We require n number of boundary conditions for a n-th order differential equation. For each boundary, we can specify upto $(n-1)$-th derivatives, where the higher half,

$$u\big|_{x=0} = g_0, \tag{1.6a}$$
$$\left.\frac{du}{dx}\right|_{x=0} = g_1, \tag{1.6b}$$
$$\vdots \tag{1.6c}$$
$$\left.\frac{d^{n/2}u}{dx^{n/2}}\right|_{x=0} = g_{n/2}, \tag{1.6d}$$

are called the *Dirichlet boundary conditions*. They are also called *essential boundary conditions* or *displacement boundary conditions*. The lower half

$$\left.\frac{d^{n/2+1}u}{dx^{n/2+1}}\right|_{x=0} = g_{n/2+1}, \tag{1.7a}$$
$$\left.\frac{d^{n/2+2}u}{dx^{n/2+2}}\right|_{x=0} = g_{n/2+2}, \tag{1.7b}$$
$$\vdots \tag{1.7c}$$
$$\left.\frac{d^{n-1}u}{dx^{n-1}}\right|_{x=0} = g_{n-1}, \tag{1.7d}$$

are called the *Neumann boundary conditions*. They are also called *natural boundary conditions* or *force boundary conditions*.

Consider the Newton's second law, $F = m\ddot{u}$. The general solution u can be obtained by integrating the equation twice, which gives

$$u = \frac{1}{2}\frac{F}{m}t^2 + C_1 t + C_2. \tag{1.8}$$

In the above, we are left with two undetermined constants, C_1 and C_2. The boundary, or the initial, conditions completes the analysis, e.g.,

$$u(0) = u_0 \quad \text{and} \quad \dot{u}(0) = v_0 \tag{1.9}$$

gives $C_1 = v_o$ and $C_2 = u_0$. Here, we specified both Dirichlet and Neumann data at $t = 0$, which are called *Cauchy boundary conditions*.

We will later study another type of boundary condition, known as the *Robin boundary condition*, which prescribes a linear relationship between Dirichlet and Neumann data. For instance, in the context of a second-order differential equation, it may take the form

$$\left(\alpha u + \beta \frac{du}{dx}\right)\Big|_{x=0} = g, \tag{1.10}$$

where, α and β are given numbers and g is a given function.

1.2 Miscellanies

- *Vector*s, as elements of a *vector space*, are objects that can be added to each other and scaled by numbers to produce new vectors.

- *Inner product* between two real-valued vectors/functions are denoted by

$$(u, v) = \int_\Omega uv \, d\Omega. \tag{1.11}$$

- *Differentiation* is defined as

$$\frac{df}{dx} = \lim_{\Delta x \to 0} \frac{f(x + \Delta x) - f(x)}{\Delta x}. \tag{1.12}$$

- *Integration by parts* states:

$$\int_a^b u\frac{dv}{dx}dx = [uv]_{x=a}^{x=b} - \int_a^b \frac{du}{dx}v dx, \tag{1.13}$$

  where $[A(x)]_{x=a}^{x=b} = A(x)|_{x=b} - A(x)|_{x=a} = A(b) - A(a)$.

- *Functional* is an operator that takes functions as arguments and returns a number. For example, a bending energy is a functional such that

$$E[M] = \frac{1}{2}\int_0^L \frac{M^2}{EI}dx. \tag{1.14}$$

- *Gateaux derivative* is a derivative of a functional F with respect to a function u, i.e.,

$$dF\left[u\right]\left(\tilde{u}\right)=\lim_{\varepsilon\to 0}\frac{F\left[u+\varepsilon\tilde{u}\right]-F\left[u\right]}{\varepsilon}=\frac{d}{d\varepsilon}F\left[u+\varepsilon\tilde{u}\right]\Big|_{\varepsilon=0}. \tag{1.15}$$

In the above, $\tilde{u}$ is a direction of the derivative. There exists a gradient g when the map $\tilde{u}\to dF\left[u\right]\left(\tilde{u}\right)$ is linear. Then, we have [Stone and Goldbart, 2009]

$$dF\left[u\right]\left(\tilde{u}\right)=\left(g,\tilde{u}\right). \tag{1.16}$$

- *Dirac delta function* $\delta\left(x-x_o\right)$ is not a traditional function. As a *generalized function*, or a *distribution*, acting on a regular function $f(x)$, it is defined such that [Gel'Fand and Shilov, 1964]

$$\left(f(x),\delta(x-x_o)\right)=\int_{-\infty}^{\infty}f(x)\delta(x-x_o)dx=f(x_o). \tag{1.17}$$

The above relation is called *sifting property*. The Dirac delta function can also be loosely considered as a "function" with the following properties:

$$\delta\left(x-x_o\right)=\begin{cases}\infty, & x=x_o\\ 0, & \text{otherwise}\end{cases}\quad\text{and}\quad\int_{-\infty}^{\infty}\delta\left(x-x_o\right)dx=1. \tag{1.18}$$

In the above, ∞ is not a unique value; thus, $\delta(x-x_o)$ is not a function in the conventional sense. Figure 1.1 illustrates "one", i.e., not unique, representation of the Dirac delta function. Then, we can verify that

$$\begin{aligned}\int_{-\infty}^{\infty}\delta\left(x-x_o\right)&=\lim_{\varepsilon\to 0}\left[\int_{-\infty}^{x_o-\varepsilon}0dx+\int_{x_o-\varepsilon}^{x_o+\varepsilon}\frac{1}{2\varepsilon}dx+\int_{x_o+\varepsilon}^{\infty}0dx\right]\\&=\lim_{\varepsilon\to 0}\frac{1}{2\varepsilon}2\varepsilon=1\quad\text{and}\end{aligned} \tag{1.19}$$

$$\begin{aligned}\int_{-\infty}^{\infty}f\left(x\right)\delta\left(x-x_o\right)&=\lim_{\varepsilon\to 0}\left[\int_{-\infty}^{x_o-\varepsilon}f\left(x\right)0dx+\int_{x_o-\varepsilon}^{x_o+\varepsilon}\frac{f\left(x\right)}{2\varepsilon}dx\right.\\&\qquad\left.+\int_{x_o+\varepsilon}^{\infty}f\left(x\right)0dx\right]\\&=\lim_{\varepsilon\to 0}\frac{F\left(x_o+\varepsilon\right)-F\left(x_o-\varepsilon\right)}{2\varepsilon}\\&=F'\left(x_o\right)=f\left(x_o\right).\end{aligned} \tag{1.20}$$

Derivatives of Dirac delta function have following operations:

$$\begin{aligned}\left(f(x),\delta'(x-x_o)\right)&=\int_{-\infty}^{\infty}f(x)\delta'(x-x_o)dx\\&=f(x)\delta(x-x_o)|_{-\infty}^{\infty}-\int_{-\infty}^{\infty}f'(x)\delta(x-x_o)dx\\&=-f'(x_o),\end{aligned} \tag{1.21}$$

$$\left(f(x),\delta''(x-x_o)\right)=f''(x_o), \tag{1.22}$$

$$\vdots$$

$$\left(f(x),\delta^{(n)}(x-x_o)\right)=(-1)^{(n)}f^{(n)}(x_o),\quad n=0,1,2,\ldots. \tag{1.23}$$

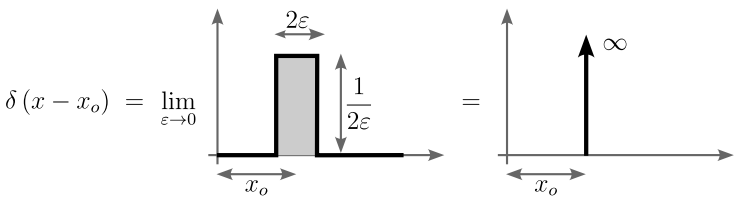

Figure 1.1: Dirac delta function defined with a limiting process.

Chapter 2

Introduction to Structural Analysis

2.1 Structures and structural analysis

A structure is an object that deforms under an external load: springs elongate by pulling forces, bridges deflect due to gravity, etc. As engineers, we analyze/predict the force-deformation interaction and design structures for various purposes.

In this course, we consider structures composed of elements with "long" aspect ratio that can be approximated by (locally) one-dimensional objects, which are common in civil engineering applications (Figure 2.1). Common types of civil structures includes *trusses*, *beams*, *frames*, and *cables*.

We mainly consider three types of deformation (Figure 2.2): 1) axial deformation by axial force; 2) torsion by torsional moment; and 3) deflection by shear force and/or bending moment. The governing equations for the above deformations are

- Axial deformation:

$$\frac{d}{dx}\left[EA\frac{du}{dx}\right] + f = 0, \quad x \in (0, L), \tag{2.1}$$

  where u is the axial deformation, f is the distributed load per unit length, E is the Young's modulus and A is the cross-sectional area. Other physical quantities are defined as

$$F = EA\frac{du}{dx} \quad \text{(axial force)}. \tag{2.2}$$

- Torsion:

$$\frac{d}{dx}\left[GJ\frac{d\varphi}{dx}\right] + m = 0, \quad x \in (0, L), \tag{2.3}$$

  where φ is the angle of rotation, m is the distributed moment per unit length, G is the shear modulus and J is the the second polar moment of

area. In addition, we have

$$T = GJ\frac{d\varphi}{dx} \quad \text{(torsional moment)}. \tag{2.4}$$

- Deflection:

$$\frac{d^2}{dx^2}\left[EI\frac{d^2w}{dx^2}\right] - q = 0, \quad x \in (0, L), \tag{2.5}$$

where w is the deflection, q is the distributed load per unit length, and I the cross-sectional moment of inertia. The derivatives of w represents the following physical quantities (for a small w):

$$\theta = \frac{dw}{dx} \quad \text{(slope or deflection angle)}, \tag{2.6}$$

$$M = EI\frac{d^2w}{dx^2} \quad \text{(bending moment), and} \tag{2.7}$$

$$V = \frac{d}{dx}\left[EI\frac{d^2w}{dx^2}\right] \quad \text{(shear force)}. \tag{2.8}$$

The above equations are based on the right-handed coordinate system; for the left-handed coordinate system, we have $M = -EId^2w/dx^2$ and $V = -(d/dx)(EIdw^2/dx^2)$. Note that some notations are overused, a practice with which we should all be familiar.

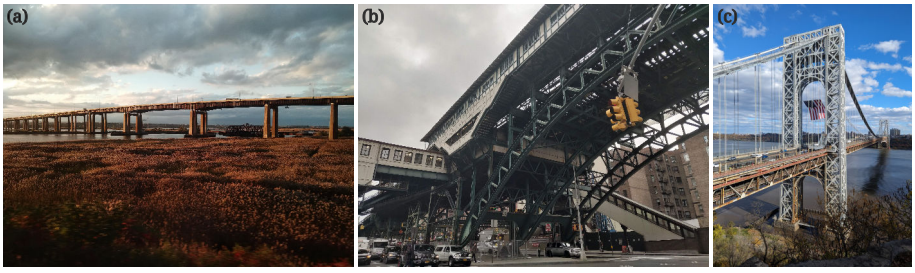

Figure 2.1: Civil structures with long aspect ratio. (a) I-95 near DB Drawbridge, Secaucus, NJ. (b) 125st Station, New York, NY. (c) George Washington Bridge, Fort Lee, NJ.

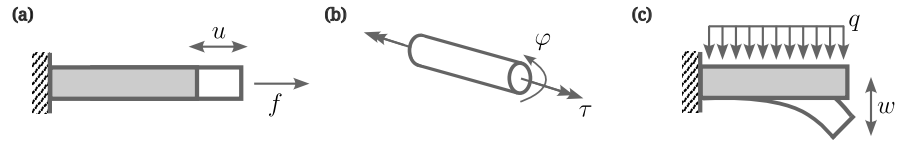

Figure 2.2: Deformations of one-dimensional objects. (a) Axial deformation. (b) Torsion. (c) Deflection.

As discussed earlier, boundary conditions are important as well as the governing equations. In structural analysis, they are manifested as *supports* (Figure 2.3).

- Fixed support: all motions, horizontal, vertical, and rotational, are constrained. Thus, we expect horizontal, vertical, and moment reaction forces.

- Hinge support: horizontal and vertical motions are constrained but rotational motions are allowed. We expect horizontal and vertical reaction forces.

- Roller support: vertical motions are constrained, while other motions are allowed. We expect a vertical reaction force only.

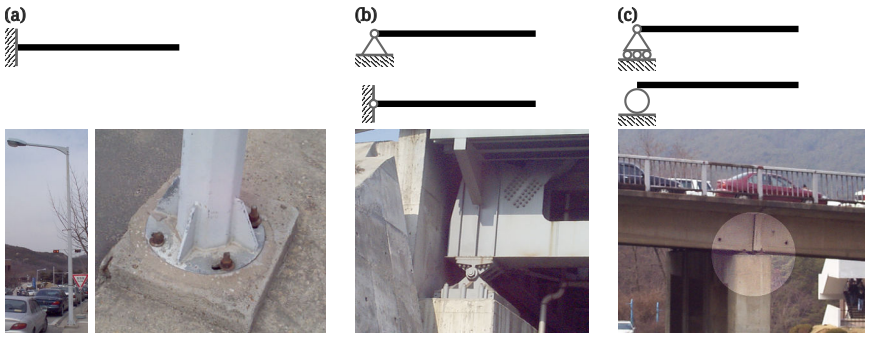

Figure 2.3: Three types of support. (a) Fixed support. (b) Hinge support. (c) Roller support (bridge over a tennis court at Seoul National University). Images courtesy of Hae Sung Lee.

Now, let's solve a beam equation for the structure shown in Figure 2.4. From the figure, we can identify that the deflection is constrained to be zero at $x = 0, L, 2L$. The corresponding governing equations and the boundary conditions reads:
Given a constant EI and a uniform load q, find $w_1(x)$ and $w_2(x)$ such that

$$EI\frac{d^4w_1}{dx^4} = -q, \quad x \in (0, L) \quad \text{and} \tag{2.9a}$$

$$EI\frac{d^4w_2}{dx^4} = -q, \quad x \in (L, 2L) \tag{2.9b}$$

with boundary conditions of

$$w_1(0) = 0, \tag{2.10a}$$
$$w_1(L) = 0, \tag{2.10b}$$
$$EI\frac{d^2 w_1(0)}{dx^2} = 0, \tag{2.10c}$$
$$w_2(L) = 0, \tag{2.10d}$$
$$w_2(2L) = 0, \tag{2.10e}$$
$$EI\frac{d^2 w_2(2L)}{dx^2} = 0, \tag{2.10f}$$
$$\frac{dw_1(L)}{dx} = \frac{dw_2(L)}{dx}, \quad \text{and} \tag{2.10g}$$
$$EI\frac{d^2 w_1(L)}{dx^2} = EI\frac{d^2 w_2(L)}{dx^2}. \tag{2.10h}$$

Let $y = 2L - x$, the general solutions to the above governing equations are

$$w_1(x) = -\frac{qx^4}{24EI} + a_1 x^3 + b_1 x^2 + c_1 x + d_1 \quad \text{and} \tag{2.11a}$$
$$w_2(y) = -\frac{qy^4}{24EI} + a_2 y^3 + b_2 y^2 + c_2 y + d_2. \tag{2.11b}$$

Then, the eight integration constants are determined by the boundary conditions, which are

$$a_1 = a_2 = \frac{3qL}{48EI}, \quad c_1 = c_2 = -\frac{qL^3}{48EI}, \quad \text{and} \quad b_1 = b_2 = d_1 = d_2 = 0. \tag{2.12}$$

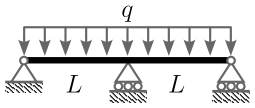

Figure 2.4: A beam with three supports under a uniform load. EI is constant.

Structural analysis, however, is not merely about solving differential equations. Throughout this notes, we will cover various elegant methods, which founded on solid physical and mathematical reasoning.

2.2 Elasticity, linearity, and reciprocity

Elasticity means that the structure recovers the original shape from the deformation when the external loads are removed. Note that elasticity does not imply a linear force-deformation relation, although we assume linearity in this notes.

Linearity is a powerful and reasonable assumption that allows exploiting the superposition principle:

$$f(x_1 + x_2) = f(x_1) + f(x_1) \quad \text{(additivity)} \quad \text{and} \tag{2.13a}$$
$$f(\alpha x) = \alpha f(x) \quad \text{(homogeneity)}, \tag{2.13b}$$

where α is a scalar. To understand its usefulness, let us assume that we are given with solutions of the two identical *simply supported beams* of length $2L$ with two different loading conditions: 1) a uniform distributed load q (Figure 2.5(a)) and 2) a concentrated load p at the center (Figure 2.5(b)). The corresponding deflections at the center of the beam are $\delta_{(a)} = 5q(2L)^4/(384EI)$ and $\delta_{(b)} = p(2L)^3/(48EI)$, respectively. With this information, we can analyze a different structure with an additional support at the center under a uniform distributed load q (Figure 2.5(c)). In this case, the center support can be regarded as a concentrated load that balances out the deflection at the center, i.e., $\delta_{(c)} = \delta_{(a)} + \delta_{(b)} = 0$. Thus, we can easily calculate the reaction force at the center $p = -5qL/4$.

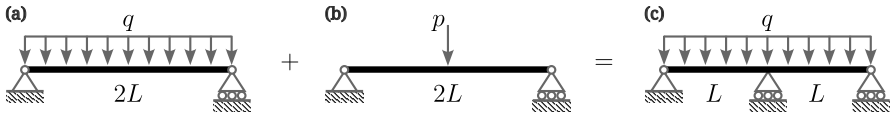

Figure 2.5: Exploiting linearity. (a) A simple beam with a uniform load. (b) With a concentrated load. (c) A beam with three supports that is a linear superposition of the two preceding cases.

Reciprocity follows from the *self-adjoint* nature of our linear operator of interest. Given two pairs of "input" f_i and "output" u_i, $i = 1, 2$, the reciprocity simply states:

$$u_1 f_2 = u_2 f_1. \tag{2.14}$$

Thus, for a given pair of force and displacement, we can easily obtain another force-displacement pair without additional analysis. For example, consider a frame with fixed supports (Figure 2.6). Let us assume that we are given with a pair of force and displacement $(p_1, \theta_1) = (1.0, -3.57)$. Then, for an arbitrary moment m_2, we can calculate the horizontal displacement $\delta_{x,2}$ by computing $\theta_1 m_2 = \delta_{x,2} p_1$ or $\delta_{x,2} = -3.57 m_2$.

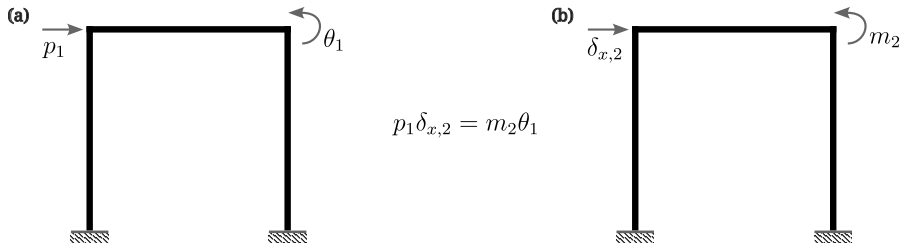

Figure 2.6: Exploiting reciprocity. (a) A frame with a horizontal load. (b) A frame with a moment.

2.3 Stability

Stability ensures the existence of a unique solution. In structural analysis, a lack of stability—referred to as *instability*—is associated with rigid body motions.

As a clear example, a structure with all supports removed may undergo rigid body motions, in which case its position is not uniquely determined in the context of statics. However, prescribing supports does not always guarantee stability. For instance, a bar with Neumann boundary conditions at both ends exhibits non-unique deformation, indicating that the structure is unstable. Try to solve for u from the following setup:

$$\begin{cases} EA\dfrac{d^2u}{dx^2} + f = 0 \quad x \in (0, L) \\ EA\dfrac{du}{dx}\Big|_{x=0} = 0, \\ EA\dfrac{du}{dx}\Big|_{x=L} = 0 \end{cases} \tag{2.15}$$

The above examples are classified as cases of *external instability*. In contrast, *internal instability* arises from local instability within the structure. We will examine this more closely in the context of truss problems.

2.4 Sign conventions

In this note, we use a variety of coordinate systems depending on the geometry of structures in consideration. Right-handed coordinate system is the most widely used convention. On the other hand, Left-handed coordinate system is also useful giving positive values for downwards, which is the typical direction for displacements under gravity. We will be flexible when choosing the coordinate system. However, we will consistently use one sign convention for the internal forces as shown in Figure 2.7.

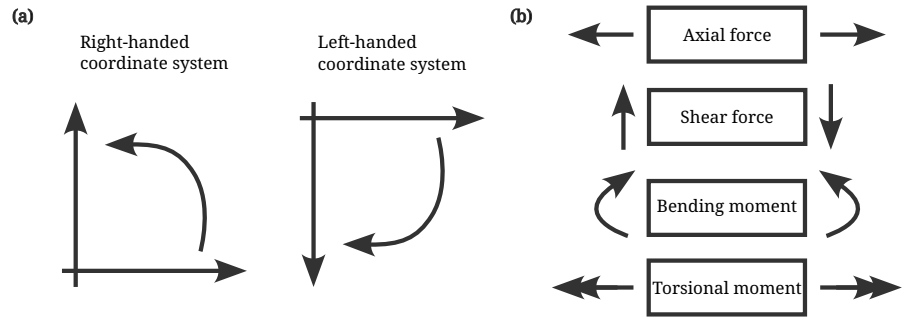

Figure 2.7: Sign conventions. (a) Coordinate systems. (b) Internal forces acting on an infinitesimally small element. Arrows indicate positive directions.

Chapter 3

Reactions and Internal Forces by Freebody Diagrams

3.1 Freebody diagrams

Freebody diagrams are graphical representations of an object and all forces acting upon on the object (Figure 3.1). Any supports can be replaced by reaction forces. In addition, a subset of an object can be considered in separate from the whole object when the influences of the removed parts are replaced by internal forces. Importantly, all forces, translational and rotational, must be balanced for all versions of freebody diagrams.

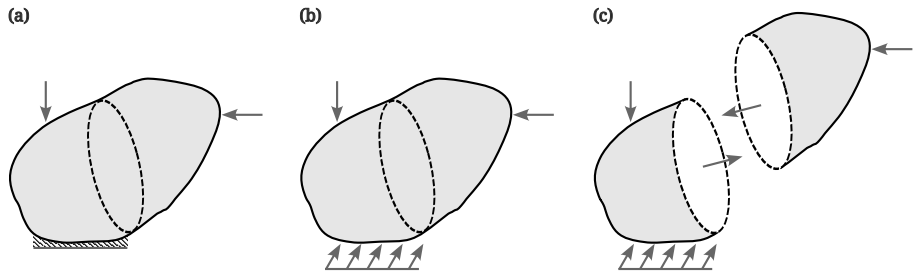

Figure 3.1: Freebody diagrams. (a) A potato under external loads. (b) A support replaced by a reaction force. (c) A sliced potato showing internal forces.

Determinate structures can be easily analyzed by freebody diagrams. First, we identify all unknowns, i.e., reaction forces, based on the type of supports, or boundary conditions. Second, we calculate reaction forces from the equations we have such as balance of translational and rotational forces. We can determine internal forces, such as shear forces and bending moments, by applying the aforementioned process to a specific section of the structure, which is sliced at the desired location.

3.2 Beams

Beam is a structural element that resists shear forces and bending moments to support slabs or floors in bridges and buildings (Figure 3.2).

Figure 3.2: Beam structure. I-95 near DB Drawbridge, Secaucus, NJ.

Consider a simply-supported beam with a uniform load q (Figure 3.3). We can identify two vertical reaction forces at supports. The hinged supports guarantee that there is no moment reaction. The two reaction forces R_A and R_B can be easily calculated by the balance of vertical forces and moment at the left end of the structure, i.e.,

$$0 = \sum F_V = R_A + R_B - qL \quad \text{and} \tag{3.1}$$

$$0 = \sum M_A = LR_B - \frac{L}{2}qL. \tag{3.2}$$

As shown above, we have two unknowns and two equations, which gives $R_A = R_B = qL/2$. Internal forces V and M at an arbitrary position of the beam can be identified as (Figure 3.3(C))

$$0 = \sum F_V = R_A - V - qx \quad \text{and} \tag{3.3}$$

$$0 = \sum M_A = -Vx + M - \frac{1}{2}qx^2. \tag{3.4}$$

Thus, we have $V(x) = q\,(x - L/2)$ and $M(x) = qx^2/2 - q(x - L/2)x$. Let's do a coherence check. We expect that the magnitude of shear force V become equal to the those of the reaction forces at both ends: $\lim_{x\to 0} V(x) = q\,(0 - L/2) = -qL/2$ and $\lim_{x\to L} V(x) = q\,(L - L/2) = qL/2$. We also expect that the moment vanishes at both ends: $\lim_{x\to 0} M(x) = 0$ and $\lim_{x\to L} M(x) = qL^2/2 - q(L - L/2)L = 0$. Then, we can draw the shear force diagram (SFD) and bending moment diagram (BMD) as shown in Figure 3.4.

A *Gerber beam* is a beam that hosts hinges within its girder. Consider a structure shown in Figure 3.5. At a glance, the structure seems to be structurally indeterminant (Figure 3.5(a)): we have three unknowns, R_A, R_B, and R_C, but with only two equations, $\sum F_V = 0$ and $\sum M_A = 0$. However, the structure is determinant when we utilize the fact that bending moments always vanish at hinges; each hinge effectively provides an additional equation. Figure 3.5(b) shows an alternative freebody diagram separating the structure at the hinge. Note that the shear force is carried by R_H between the bodies; however, there

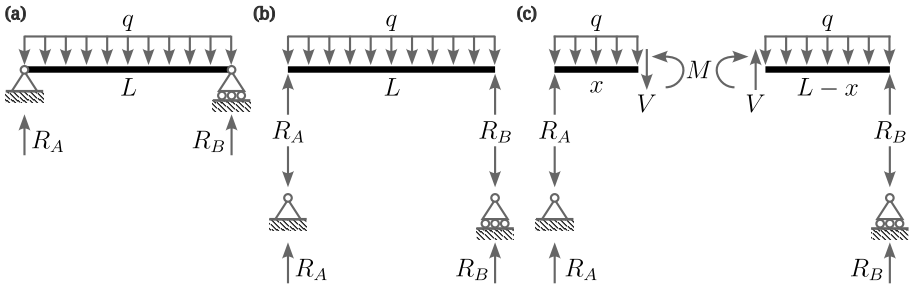

Figure 3.3: Freebody diagrams of a simple beam. (a) A beam under a uniform load. (b) Separated diagrams of beam and supports. (c) A beam sliced at x revealing internal forces.

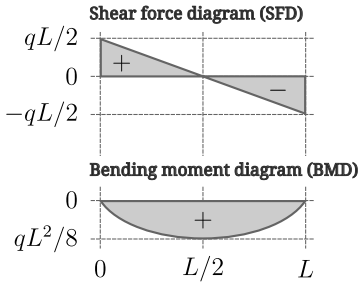

Figure 3.4: Shear force diagram (SFD) and bending moment diagram (BMD) correspond to Figure 3.3.

is no bending moment carried at the interface (because it is zero). Thus, we can construct following equilibrium equations:

$$0 = \sum F_V = R_A + R_B - R_H, \tag{3.5}$$

$$0 = \sum M_A = -LR_B + \frac{5L}{4}R_H, \quad \text{and} \tag{3.6}$$

$$0 = \sum F_V = R_H + R_C - P, \tag{3.7}$$

$$0 = \sum M_C = -\frac{3L}{4}R_H + \frac{L}{2}P. \tag{3.8}$$

The above equations give $R_A = -P/6$, $R_B = 5P/6$, $R_C = P/3$, and $R_H = 2P/3$. The corresponding SFD, BMD, and deflected shape is shown in Figure 3.5(c). Note that there is slope discontinuity at the hinge.

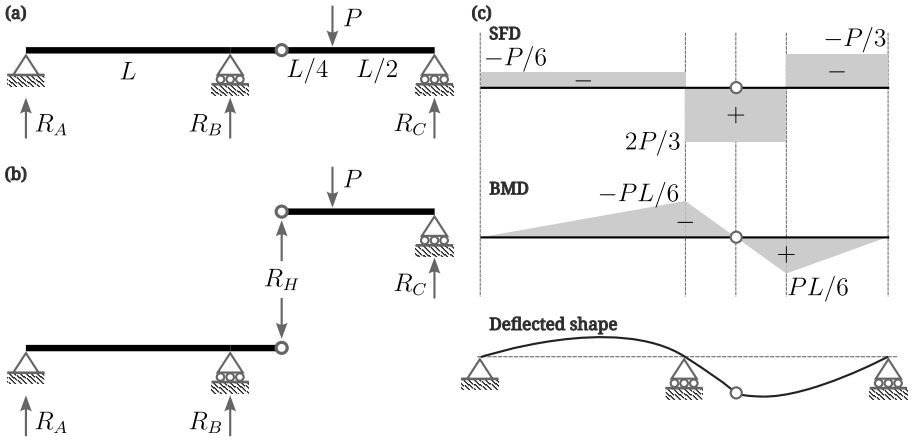

Figure 3.5: Freebody diagrams of a gerber beam. Bending moment vanishes at the hinge. (a),(b) Freebody diagrams. (c) SFD, BMD, and deflected shape. Shear force is continuous across the hinge, while the slope of the deflection is discontinuous.

Another example of a Gerber beam with two hinges is shown in Figure 3.6. Similarly to above, we can separate the structures at the hinges, which gives two cantilevers and one simple beam (Figure 3.6(b)).

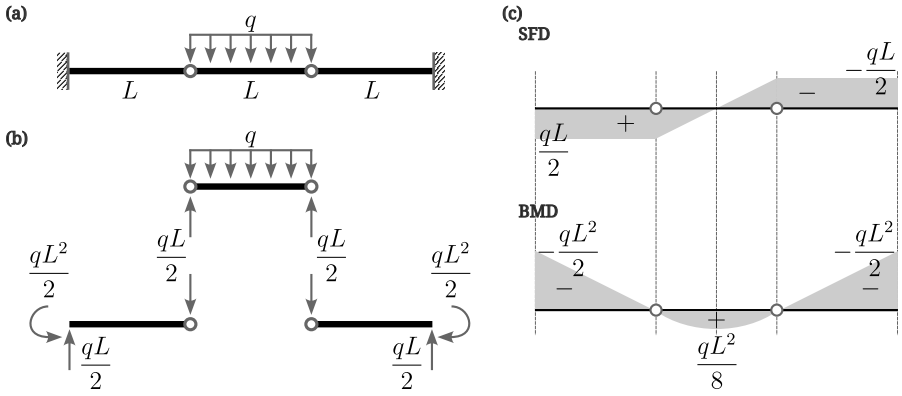

Figure 3.6: Gerber beam with two hinges (a) Structure. (b) Freebody diagram. (c) SFD and BMD.

3.3 Trusses

Truss is a structure that is designed to allow only axial deformations. Thus, a truss is free from shear forces and bending moments, with which most structures are vulnerable; however, it occupies a large space in general (Figure 3.7).

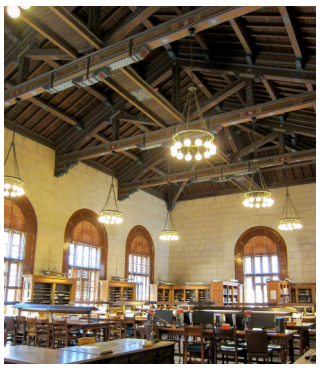

Figure 3.7: Truss structure. Architecture and Planning Library at the University of Texas at Austin, Austin, TX.

We need few assumptions for trusses to carry axial forces only:

1. all joints are hinges;
2. all members are straight;
3. all external loads are applied only at joints; and
4. all deformations are small.

From the above second, third, and fourth assumptions, we have

$$\frac{d^2M}{dx^2} = q = 0 \Rightarrow M(x) = C_1 x + C_2. \tag{3.9}$$

The first assumption implies that $M(0) = M(L) = 0$; then, we have

$$C_1 = C_2 = 0 \Rightarrow M(x) = V(x) = 0. \tag{3.10}$$

Thus, we have only axial forces in a truss.

Consider a truss illustrated in Figure 3.8; the reaction forces at supports are already given. Next, we disassemble all joints and members to find all internal forces (Figure 3.9). Thanks to the assumptions above, the internal forces within a member is constant. Thus, we can focus only on the joints when solving for the internal forces, which is called *method of joints*:

$$\text{Joint (4)} \begin{cases} 0 = \sum_{(4)} F_x = F_4 \\ 0 = \sum_{(4)} F_y = -F_1 \end{cases} \Rightarrow F_1 = F_4 = 0, \tag{3.11a}$$

$$\text{Joint (6)} \begin{cases} 0 = \sum_{(6)} F_x = -F_8 \\ 0 = \sum_{(6)} F_y = -F_9 \end{cases} \Rightarrow F_8 = F_9 = 0, \tag{3.11b}$$

$$\text{Joint (1)} \begin{cases} 0 = \sum_{(1)} F_x = F_2 + F_3/\sqrt{2} \\ 0 = \sum_{(1)} F_y = F_1 + F_3/\sqrt{2} + P/2 \end{cases} \Rightarrow F_2 = \frac{1}{2}P,\ F_3 = -\frac{\sqrt{2}}{2}P, \tag{3.11c}$$

$$\text{Joint (2)} \begin{cases} 0 = \sum_{(2)} F_x = -F_2 + F_6 \\ 0 = \sum_{(2)} F_y = F_5 - P \end{cases} \Rightarrow F_5 = P,\ F_6 = \frac{1}{2}P, \tag{3.11d}$$

$$\text{Joint (3)} \begin{cases} 0 = \sum_{(3)} F_x = -F_6 - F_7/\sqrt{2} \\ 0 = \sum_{(3)} F_y = F_7/\sqrt{2} + F_9 + P/2 \end{cases} \Rightarrow F_7 = -\frac{\sqrt{2}}{2}P, \quad \text{and} \tag{3.11e}$$

$$\text{Joint (5)} \begin{cases} 0 = \sum_{(5)} F_x = -F_4 - F_3/\sqrt{2} + F_7/\sqrt{2} + F_8 \\ 0 = \sum_{(5)} F_y = -F_3/\sqrt{2} - F_5 - F_7/\sqrt{2} \end{cases} \Rightarrow \text{coherence checked!} \tag{3.11f}$$

It is easier to start at a joint with two unknowns, e.g., joint (4) and (6) in the given example, and subsequently look for other joints with two unknowns. We can always verify the coherence of the calculations at the final joint, where the equilibrium equations should be automatically satisfied.

We can verify that, for the given loading condition, there are no internal forces at member 1, 4, 8, and 9; therefore, they are redundant. Additionally, all internal forces show a symmetry about the member 5 because of the symmetry in both the geometry and the external forces.

As hinted above, we can select any cross-section to perform a freebody analysis when calculating the internal forces. The *method of sections* draws a line in between members in which we are interested in calculating their internal forces. For example, consider a *Werren truss* in Figure 3.11. Suppose we are only interested in the internal forces of members 4, 5, and 6. We can selectively find those forces by cutting the structure through the members (Figure 3.11(c)). Then, we have

$$\begin{cases} 0 = \sum F_x = F_6 + F_5/\sqrt{2} + F_4 \\ 0 = \sum F_y = F_5/\sqrt{2} + 2P/3 - P \\ 0 = \sum M_A = LF_6 + LP - 3L \cdot 2P/3 \end{cases} \Rightarrow F_4 = \frac{4P}{3},\ F_5 = \frac{\sqrt{2}P}{3},\ F_6 = P. \tag{3.12}$$

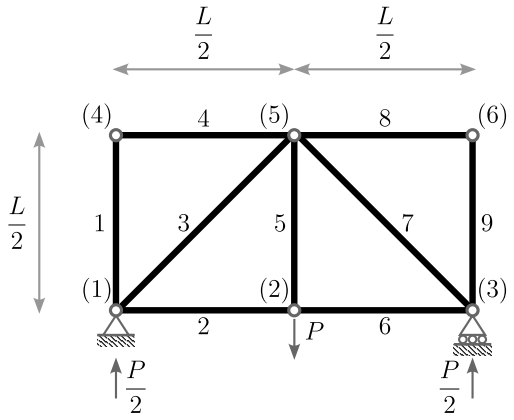

Figure 3.8: A truss with 9 members and 6 joints.

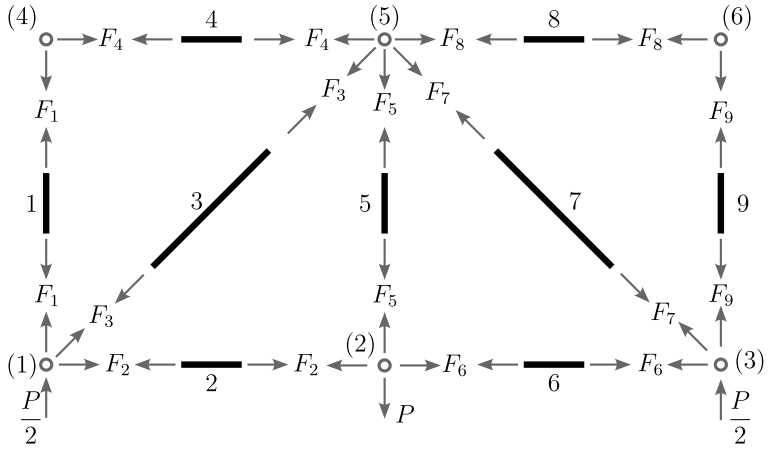

Figure 3.9: A freebody diagram of the truss shown in Figure 3.8. The directions of the arrows are chosen such that positive value implies tension for the corresponding truss member.

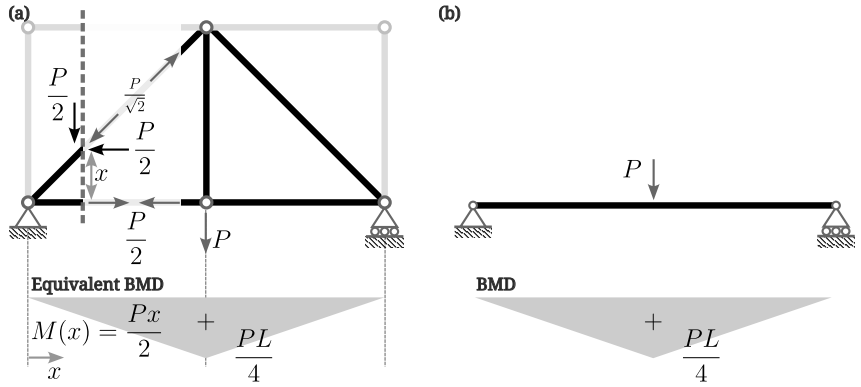

Figure 3.10: Equivalent beam action of the truss shown in Figure 3.8. (a) Equivalent BMD and (b) Beam problem.

Similarly, we can use the freebody diagram in Figure 3.11(d) to find the forces F_8, F_9, and F_{10} as

$$\begin{cases} 0 = \sum F_y = -F_9/\sqrt{2} + P/3 \\ 0 = \sum M_B = -LF_{10} + LP/3 \\ 0 = \sum M_C = LF_8 + 2LP/3 \end{cases} \Rightarrow F_8 = -\frac{2P}{3},\ F_9 = \frac{\sqrt{2}P}{3},\ F_{10} = \frac{P}{3}. \tag{3.13}$$

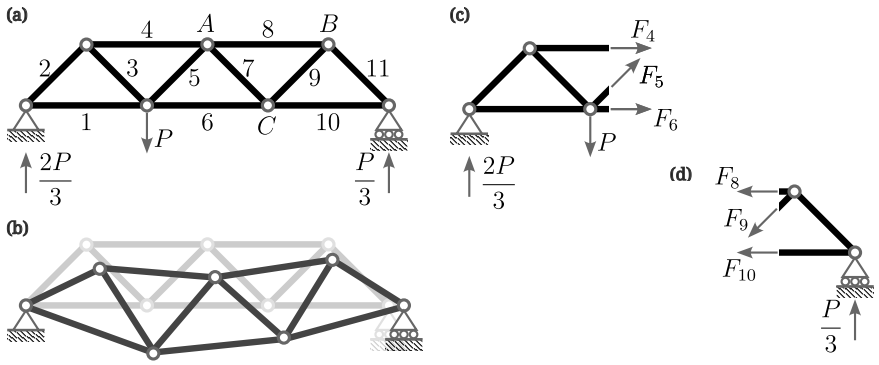

Figure 3.11: Warren truss. (a) Geometry and external forces. (b) Deformed shape. (c),(d) Freebody diagrams with different cross-sections.

3.4 Frames

Frame consists of bending elements connected with an angle not necessarily straight like beams (see the portal-like substructures in Figure 3.12). It carries axial forces as well; however, the axial deformation is small compared to the deflection from bending, and, thus, neglected in general.

Figure 3.12: Frame structure. Roberta Crenshaw Bridge, Austin, TX.

For example, consider a three-hinged frame illustrated in Figure 3.13. First we compute the reaction forces from the balance of forces and moments, i.e.,

$$\begin{cases} 0 = \sum F_x = H_A + H_B \\ 0 = \sum F_y = R_A + R_B - qL/2 \\ 0 = \sum M_{h,L} = L \cdot H_A - L/2 \cdot R_A + L/4 \cdot qL/2 \\ 0 = \sum M_{h,R} = L \cdot H_B + L/2 \cdot R_B \end{cases} \tag{3.14}$$

$$\Rightarrow \begin{cases} H_A = \dfrac{qL}{16},\ H_B = -\dfrac{qL}{16}, \\ R_A = \dfrac{3qL}{8},\ R_B = \dfrac{qL}{8}. \end{cases} \tag{3.15}$$

Then, we can compute the internal forces as

$$\text{Member AC} \begin{cases} F_{A,y} = F_{C,y} = -R_A = -3qL/8 \\ F_{A,x} = F_{C,x} = -H_A = -qL/16 \\ M_C = F_{C,x} L = -qL^2/16 \end{cases}, \tag{3.16}$$

$$\text{Member CD} \begin{cases} F_{D,x} = F_{C,x} = -qL/16 \\ F_{D,y} = F_{C,y} + qL/2 = qL/8 \\ M_D = -L/2 \cdot F_{D,y} = -qL^2/16 \end{cases}, \text{ and} \tag{3.17}$$

$$\text{Member DB} \begin{cases} F_{B,x} = F_{D,x} = H_B = -qL/16 \\ F_{B,y} = -F_{D,y} = -R_B = -qL/8 \\ M_D = L F_{B,x} = -qL^2/16 \end{cases}. \tag{3.18}$$

In the above, the internal forces of the member DB are automatically given by the previous computations, which gives a good coherence check.

The corresponding axial force, shear force, and bending moment diagrams are given in Figure 3.14. Note that the shear force of the member CD vanishes at $x = qL/8$ in the local coordinate, which becomes an inflection point for the bending moment as shown below:

$$V(x) = -qx + \frac{3qL}{8}, \quad 0 < x < \frac{L}{2} \quad \text{and} \tag{3.19}$$

$$\begin{aligned} M(x) &= -\frac{q}{2}x^2 + \frac{3qL}{8}x - \frac{qL^2}{16} \\ &= -\frac{q}{2}\left(x - \frac{3L}{8}\right)^2 + \frac{7qL^2}{32}, \quad 0 < x < \frac{L}{2}. \end{aligned} \tag{3.20}$$

Another example below (Figure 3.15) is given for readers to exercise.

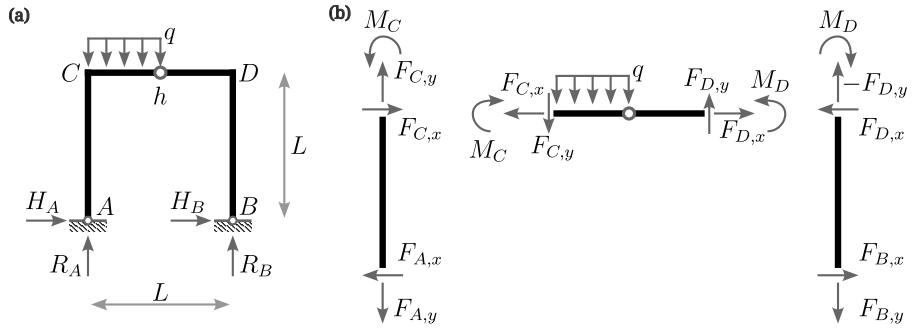

Figure 3.13: Three-hinged frame. (a) External and reaction forces. (b) Internal forces.

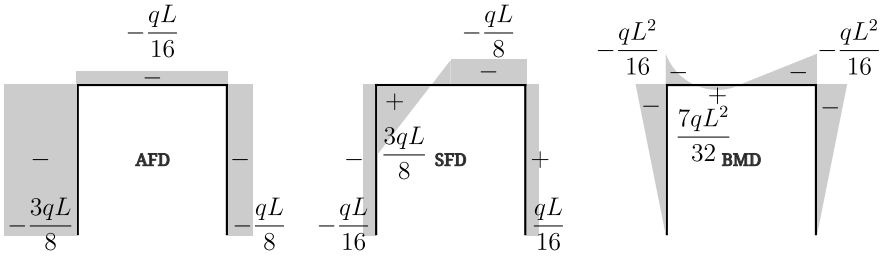

Figure 3.14: Axial force, shear force, and bending moment diagrams.

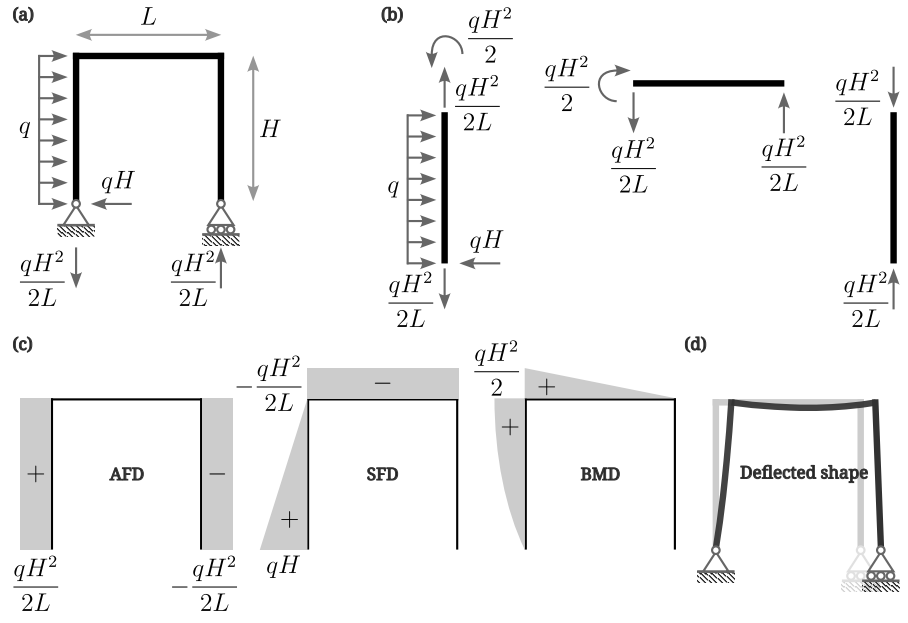

Figure 3.15: A frame under a horizontal load. (a) External and reaction forces. (b) Internal forces. (c) Axial force, shear force, and bending moment diagrams. (d) Deflected shape.

3.5 Arches

Arches are curved structures that provide large open spaces underneath them with minimal bending moments (Figure 3.16). An ideal arch only carries axial forces through out the structure, which are balanced by reaction forces at supports.

Figure 3.16: Arch structures. (a) South Congress Bridge, Austin, TX. (b) Butterfly Bridge, Austin, TX. (c) The Assembly Chamber at New York State Capitol, Albany, NY.

First, let's analyze the following three-hinged arch with a point load (Figure 3.17). The geometry of the arch is given as

$$\frac{y}{h} = 1 - \left(\frac{x}{l}\right)^2, \quad x \in (-l, l). \tag{3.21}$$

The reaction forces are calculated as

$$\begin{cases} 0 = \sum F_x = H_A + H_B \\ 0 = \sum F_y = R_A + R_B - P \\ 0 = \sum M_{h,L} = hH_A - lR_A \\ 0 = \sum M_{h,R} = hH_B + lR_B \end{cases} \tag{3.22}$$

$$\Rightarrow H_A = \frac{Pl}{2h},\ H_B = -\frac{Pl}{2h},\ R_A = \frac{P}{2},\ R_B = \frac{P}{2}. \tag{3.23}$$

Next, we compute the internal forces using the freebody diagram Figure 3.17(b). For an arbitrary position $x \in (-l, 0)$, we have

$$\begin{cases} 0 = \sum F_x = H_A + H \\ 0 = \sum F_y = R_A + V \\ 0 = \sum M_A = (l + x)\, V - \left(h - hx^2/l^2\right) H + M \end{cases} \tag{3.24}$$

$$\Rightarrow \begin{cases} H = -\dfrac{Pl}{2h},\ V = -\dfrac{P}{2}, \\ M = \left[\dfrac{x}{l} + \left(\dfrac{x}{l}\right)^2\right] \dfrac{Pl}{2}. \end{cases} \tag{3.25}$$

We can see that the maximum bending moment is $M_{\max} = -Pl/8$ at $x = -l/2$. The axial and shear forces can be computed from rotating V and H with an angle θ such that (Figure 3.17(c))

$$\begin{pmatrix} A \\ S \end{pmatrix} = \begin{bmatrix} \cos\theta & \sin\theta \\ -\sin\theta & \cos\theta \end{bmatrix} \begin{pmatrix} H \\ V \end{pmatrix}. \tag{3.26}$$

In the above, $\tan\theta = dy/dx = 2hx/l^2$, which gives $\cos\theta = (l/h)/\sqrt{(l/h)^2 + 4(x/l)^2}$ and $\sin\theta = (-2x/l)/\sqrt{(l/h)^2 + 4(x/l)^2}$. Then,

$$S = \frac{-Pl/h}{\sqrt{(l/h)^2 + 4(x/l)^2}} \left(\frac{1}{2} + \frac{x}{l}\right) \quad \text{and} \tag{3.27}$$

$$A = \frac{-P/2}{\sqrt{(l/h)^2 + 4(x/l)^2}} \left[\left(\frac{l}{h}\right)^2 - 2\left(\frac{x}{l}\right)\right]. \tag{3.28}$$

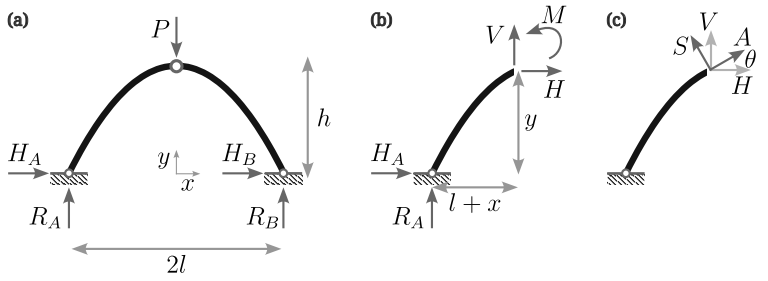

Figure 3.17: Three-hinged arch with a point load. (a) External and reaction forces. (b),(c) Internal forces.

Next, we consider an arbitrary geometry of $y/h = f(x)$ in replacement of the geometry given in (3.21). Then, with the similar procedure above, we have the bending moment at an arbitrary position $x \in (-l, 0)$ as

$$M = \frac{Pl}{2}\left(1 + \frac{x}{l} - f(x)\right). \tag{3.29}$$

The above bending moment can be vanished entirely by an appropriate function $f(x)$, i.e.,

$$f(x) = 1 + \frac{x}{l}. \tag{3.30}$$

Note that the above geometry gives a truss structure, which is consistent with its assumptions and design goals: no bending moments when point loads are applied at hinges.

Let's consider a case of a uniform distributed load applied at the same three-hinged arch (Figure 3.18). The reaction forces are

$$R_A = R_B = ql \quad \text{and} \quad H_A = -H_B = \frac{ql^2}{2h}. \tag{3.31}$$

The bending moment ($x \in (-l, 0)$) is calculated by

$$0 = \sum M_x = M + yH_A - (l + x)\, R_A + \frac{l + x}{2} q\,(l + x) \Rightarrow M = 0. \tag{3.32}$$

Thus, we conclude that a parabola is an optimal geometry for a uniform distributed load. Similarly, we can design different geometries for different loading conditions.

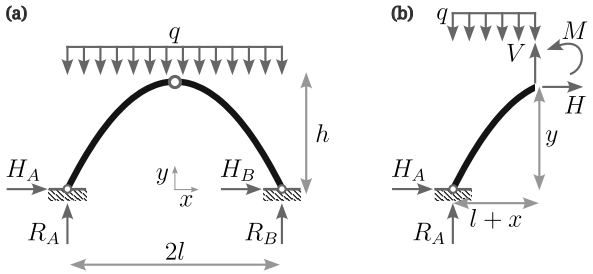

Figure 3.18: Three-hinged arch with a distributed load. (a) External and reaction forces. (b) Internal forces.

Chapter 4

Governing Equations

4.1 Bar equation

Consider an infinitesimally small element subjected to an external axial load f (Figure 4.1). The balance of force reads

$$0 = \sum F = -F + f\Delta x + F + \Delta F. \tag{4.1}$$

By taking the limit of $\Delta x \to 0$, we have

$$0 = \lim_{\Delta x \to 0} \left(\frac{\Delta F}{\Delta x} + f \right) \Rightarrow \frac{dF}{dx} = -f. \tag{4.2}$$

Thus, we have the relation between the external load f and the internal axial force F.

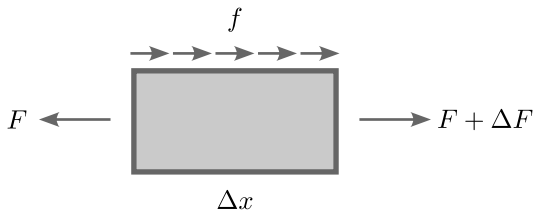

Figure 4.1: Infinitesimally small element for bar equation.

Let u denote the axial displacement; then, the strain-displacement relation is given by

$$\varepsilon = \frac{du}{dx}. \tag{4.3}$$

We assume Hooke's law $\sigma = E\varepsilon$ for the constitutive relation, which gives

$$\sigma = E\frac{du}{dx}. \tag{4.4}$$

Then, we compute the axial force by integrating the normal stress over the cross-section, i.e.,

$$F = \int_A \sigma dA = \int_A E\frac{du}{dx}dA = E\frac{du}{dx}\int_A dA = EA\frac{du}{dx}. \tag{4.5}$$

Thus, we derived the bar equation as

$$\frac{d}{dx}\left[EA\frac{du}{dx}\right] + f = 0. \tag{4.6}$$

4.2 Beam equation

We derive the beam equation from the equilibrium equations of an infinitesimal element (Figure 4.2). First, we identify two equilibrium equations:

$$0 = \sum F_y = V - (V + \Delta V) + q \cdot \Delta x \quad \text{and} \tag{4.7a}$$

$$0 = \sum M_R = -M + (M + \Delta M) - V \cdot \Delta x - \frac{1}{2}q\left(\Delta x\right)^2. \tag{4.7b}$$

Then, we take the limit of $\Delta x \to 0$ that keeps linear terms only

$$0 = \lim_{\Delta x \to 0}\left(\frac{\Delta V}{\Delta x} - q\right) \Rightarrow \frac{dV}{dx} = q \quad \text{and} \tag{4.8a}$$

$$0 = \lim_{\Delta x \to 0}\left(\frac{\Delta M}{\Delta x} - V - \frac{1}{2}q\Delta x\right) \Rightarrow \frac{dM}{dx} = V. \tag{4.8b}$$

Thus, the above result gives the relation between external load and shear forces and bending moment, i.e.,

$$\frac{d^2M}{dx^2} = \frac{dV}{dx} = q. \tag{4.9}$$

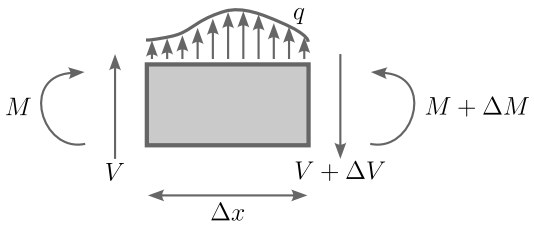

Figure 4.2: Infinitesimal beam element.

Next, we consider geometrical quantities w, u, and θ, under deformation. Figure 4.3 shows how the angle θ is related to the normal displacement u and deflection w. Under a small deformation, we assume that the cross-section rotates but remains flat; then, we have the following *strain-displacement relation*:

$$\left.\begin{aligned} &\lim_{\Delta x \to 0}\frac{\Delta w}{\Delta x} = \frac{dw}{dx} = \tan\theta \ (\approx \theta) \\ &u = -y\tan\theta = -\frac{dw}{dx}y \end{aligned}\right\} \Rightarrow \varepsilon \equiv \frac{du}{dx} = -\frac{d^2w}{dx^2}y. \tag{4.10}$$

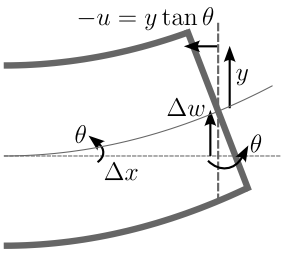

Figure 4.3: Geometrical quantities under deformation.

In the above, ε is the normal strain.

Then, the final piece we need is the relation between the geometrical quantities and the forces, i.e., a *constitutive relation*. Here, we use the *Hooke's law*:

$$\sigma \equiv E\varepsilon = -E\frac{d^2w}{dx^2}y. \tag{4.11}$$

In the above, σ is the normal stress at the cross-section, where the definition of moment states

$$M \equiv -\int_A \sigma y dA = -\int_A E\varepsilon y dA = \int_A E\frac{d^2w}{dx^2}y^2 dA = EI\frac{d^2w}{dx^2}. \tag{4.12}$$

Thus, we have derived the beam equation:

$$\frac{d^2}{dx^2}\left[EI\frac{d^2w}{dx^2}\right] = q. \tag{4.13}$$

4.3 Strong and weak formulations

Strong formulation, or strong form, states a pointwise condition when defining a function. For example, a beam equation in a strong form reads:
Given EI and q, find w such that

$$\frac{d^2}{dx^2}\left(EI\frac{d^2w}{dx^2}\right) - q = 0, \quad x \in (0, L) \tag{4.14}$$

and, on the boundary,

$$w\big|_{x=0} = 0, \tag{4.15a}$$

$$EI\frac{d^2w}{dx^2}\bigg|_{x=0} = 0, \tag{4.15b}$$

$$w\big|_{x=L} = 0, \quad \text{and} \tag{4.15c}$$

$$EI\frac{d^2w}{dx^2}\bigg|_{x=L} = 0. \tag{4.15d}$$

Thus, to test a *trial function* w, we need to evaluate the governing equation (4.14) for all x within the domain as well as the boundary conditions (4.15) at all boundaries. However, testing a function for such an infinite number of points are generally intractable.

On the other hand, *Weak formulation*, or weak form, provides a relaxed condition by an action of a generalized function. First, we need to convince ourselves that the 0 on the right-hand-side of the governing equation (4.14) is not a number but a function with a constant return value $\forall x \in (0, L)$. Then, the function, or a *vector*, 0 can be defined equivalently via an inner product such that

$$(0, v) \equiv \int_0^L 0 \cdot v \, dx = 0, \quad \forall v \in \mathcal{V}. \tag{4.16}$$

In the above, v is an arbitrary *test function* in a function space $\mathcal{V}$ and the right-hand-side 0 is a number. Thus, the function 0 is defined such that it returns a number 0 when inner-producted with any function $v \in \mathcal{V}$. Then, the function space $\mathcal{V}$ can be constructively approximated and provides tractable evaluations, which is out-of-scope for this notes. Thus, the weak form of the beam equation can be stated as:
Given EI and q, find $w \in \mathcal{W}$ such that

$$\left(\frac{d^2}{dx^2} \left[EI \frac{d^2 w}{dx^2} \right] - q, v \right) = 0, \quad \forall v \in \mathcal{V}. \tag{4.17}$$

In the above, $\mathcal{W}$ and $\mathcal{V}$ are *admissible* function spaces that satisfies certain boundary conditions and integrability conditions. Physically, an admissible functions are a smooth and continuous function with certain boundary conditions; there is no beam with discontinuity or hanging in the air without supports. It is very important to understand the equivalence of the strong form and the weak form when tested with all possible test function v. One easy way to think about is using a Dirac delta function as a test function, i.e., $v = \delta(x - x_o)$. Then, evaluating the weak form for an arbitrary $x_o \in (0, L)$ becomes the same procedure of testing the strong form as previously discussed:

$$\left(\frac{d^2}{dx^2} \left[EI \frac{d^2 w}{dx^2} \right] - q, \delta(x - x_o) \right) = \frac{d^2}{dx^2} \left[EI \frac{d^2 w}{dx^2} \right] - q \Big|_{x = x_o} = 0. \tag{4.18}$$

Chapter 5

Principle of Virtual Work

5.1 Beams

5.1.1 From weighted residual

A weak form exhibits its usefulness when it is integrated by parts. Let's denote a test function as $\overline{w}$ and all related quantities with the overline. Physically, we can consider the test function $\overline{w}$ as a solution of the same structure, i.e., the same governing equation, with (not necessarily) different boundary conditions and external forces. Then, we have

$$\begin{aligned}
0 &= \int_0^L \left[\frac{d^2}{dx^2}\left(EI\frac{d^2w}{dx^2}\right) - q\right]\overline{w}dx \\
&= \left[\frac{d}{dx}\left(EI\frac{d^2w}{dx^2}\right)\overline{w}\right]_{x=0}^{x=L} - \left[\left(EI\frac{d^2w}{dx^2}\right)\frac{d\overline{w}}{dx}\right]_{x=0}^{x=L} \\
&\quad + \int_0^L \frac{d^2w}{dx^2}EI\frac{d^2\overline{w}}{dx^2}dx - \int_0^L q\overline{w}dx \\
&= [V\overline{w}]_{x=0}^{x=L} - \left[M\overline{\theta}\right]_{x=0}^{x=L} + \int_0^L \frac{d^2w}{dx^2}EI\frac{d^2\overline{w}}{dx^2}dx - \int_0^L q\overline{w}dx. \qquad (5.1)
\end{aligned}$$

In the above, a boundary term is denoted by $[\cdot]_{x=0}^{x=L} \equiv \cdot|_{x=L} - \cdot|_{x=0}$. Then, we can rewrite the above equation, which gives the *Principle of virtual work*:

$$\underbrace{\int_0^L \frac{M\overline{M}}{EI}dx}_{=\delta W_{\text{int}}} - \underbrace{\left(\int_0^L q\overline{w}dx - [V\overline{w}]_{x=0}^{x=L} + \left[M\overline{\theta}\right]_{x=0}^{x=L}\right)}_{=\delta W_{\text{ext}}} = 0 \qquad (5.2)$$

or $\delta W_{\text{int}} = \delta W_{\text{ext}}$. Thus, the above equation states that the internal virtual work δW_{int} balances out with the external virtual work δW_{ext}. We call them "virtual" because they are cross-operated with their counterparts.

On the other hand, we can follow the same procedure above for $\overline{w}$ treating w as a test function, which gives

$$\int_0^L \frac{\overline{M}M}{EI}dx - \left(\int_0^L \overline{q}wdx - \left[\overline{V}w\right]_{x=0}^{x=L} + \left[\overline{M}\theta\right]_{x=0}^{x=L}\right) = 0. \qquad (5.3)$$

Let both systems, w and $\overline{w}$, satisfy the same boundary condition (4.15). Then, the boundary terms in (5.2) and (5.3) vanish, which leads to the *Betti-Maxwell Reciprocal Theorem* as

$$\int_0^L \frac{M\overline{M}}{EI}dx = \int_0^L \frac{\overline{M}M}{EI}dx \Rightarrow \int_0^L q\overline{w}dx = \int_0^L \overline{q}wdx. \tag{5.4}$$

The above result can also be derived by integrating-by-parts twice on (5.1).

5.1.2 From energy

Here, we derive the principle of virtual work from the *conservation of energy*, i.e., $W_{\text{ext}} = W_{\text{int}}$. For example, it can be shown in for a simply supported beam as

$$\begin{aligned}
W_{\text{ext}} &= \frac{1}{2}\int_0^L wqdx \\
&= \frac{1}{2}\int_0^L wEI\frac{d^4w}{dx^4}dx \\
&= \left[\frac{1}{2}wEI\frac{d^3w}{dx^3}\right]_{x=0}^{x=L} - \left[\frac{1}{2}\frac{dw}{dx}EI\frac{d^2w}{dx^2}\right]_{x=0}^{x=L} + \frac{1}{2}\int_0^L \frac{d^2w}{dx^2}EI\frac{d^2w}{dx^2} \\
&= \underbrace{\left[\frac{1}{2}wV\right]_{x=0}^{x=L}}_{=0} - \underbrace{\left[\frac{1}{2}\theta M\right]_{x=0}^{x=L}}_{=0} + \frac{1}{2}\int_0^L \frac{M^2}{EI}dx = W_{\text{int}}.
\end{aligned} \tag{5.5}$$

Next, we consider a two loading case q and $\overline{q}$; then, the conservation of energy respectively gives

$$\frac{1}{2}\int_0^L \frac{M^2}{EI}dx = \frac{1}{2}\int_0^L qwdx \quad \text{and} \quad \frac{1}{2}\int_0^L \frac{\overline{M}^2}{EI}dx = \frac{1}{2}\int_0^L \overline{q}\overline{w}dx. \tag{5.6}$$

In case q and $\overline{q}$ are simultaneously applied, we have

$$\frac{1}{2}\int_0^L \frac{\left(M+\overline{M}\right)^2}{EI}dx = \frac{1}{2}\int_0^L \left(q+\overline{q}\right)\left(w+\overline{w}\right)dx, \tag{5.7}$$

which reduces to

$$\int_0^L \frac{M\overline{M}}{EI}dx = \frac{1}{2}\int_0^L \left(q\overline{w}+\overline{q}w\right)dx. \tag{5.8}$$

Note that the total work must be identical either q and $\overline{q}$ are simultaneously applied or q is applied first then $\overline{q}$ is applied later, i.e.,

$$\begin{aligned}
&\frac{1}{2}\int_0^L qwdx + \frac{1}{2}\int_0^L \overline{q}\overline{w}dx + \int_0^L q\overline{w}dx = \frac{1}{2}\int_0^L \left(q+\overline{q}\right)\left(w+\overline{w}\right)dx \\
&\Rightarrow \int_0^L q\overline{w}dx = \int_0^L \overline{q}wdx.
\end{aligned} \tag{5.9}$$

In the above, we arrived at the Betti-Maxwell Reciprocal Theorem. Note that the virtual work term on the left-hand-side of the equation does not have 1/2;

can you explain this physically or graphically? What do you expect if we switch the order of loadings? Finally, we have the principle of virtual work from (5.8) and (5.9) as:

$$\int_0^L \frac{M\overline{M}}{EI}dx = \int_0^L q\overline{w}dx = \int_0^L \overline{q}wdx. \tag{5.10}$$

It is worth noting that the principle of virtual work can be derived alternatively from the *principle of the minimum potential energy*. Here, the principle of virtual work is identified as the Gateaux derivative, or *variation*, of the potential energy, while the governing differential equation is its Fréchet derivative.

5.1.3 Applications

Suppose we are interested in calculating displacement at specific locations of a simple beam under a uniform distributed load, (4.14) and (4.15). The principle of virtual work (5.3) gives an elegant tool to compute such displacements with an appropriated chosen virtual system.

For example, we can calculate the deflection at x_o by choosing $\overline{q} = \delta(x - x_o)$, i.e., a unit concentrated load, subjected to the same boundary condition:

$$\begin{cases} EI\dfrac{d^4\overline{w}}{dx^4} = \delta\left(x - x_o\right), & x \in (0, L) \\ \overline{w}\left(0\right) = \overline{w}\left(L\right) = 0 \\ \overline{M}\left(0\right) = \overline{M}\left(L\right) = 0 \end{cases} \tag{5.11}$$

Then, (5.3) gives

$$\begin{aligned} 0 &= \int_0^L \frac{\overline{M}M}{EI}dx + \left[\overline{V}w\right]_{x=0}^{x=L} - \left[\overline{M}\theta\right]_{x=0}^{x=L} - \int_0^L \delta(x - x_o)wdx \\ \Rightarrow w\left(x_o\right) &= \int_0^L \frac{\overline{M}M}{EI}dx. \end{aligned} \tag{5.12}$$

In case of $x_o = L/2$ (Figure 5.1(b)), we have

$$\begin{aligned} w\left(\frac{L}{2}\right) &= \int_0^{\frac{L}{2}} \left[-\frac{q}{2}\left(x - \frac{L}{2}\right)^2 + \frac{qL^2}{8}\right]\frac{1}{EI}\left(-\frac{x}{2}\right)dx \\ &\quad + \int_{\frac{L}{2}}^L \left[-\frac{q}{2}\left(x - \frac{L}{2}\right)^2 + \frac{qL^2}{8}\right]\frac{1}{EI}\left(\frac{x}{2} - \frac{L}{2}\right)dx \\ &= -\frac{5}{384}\frac{qL^4}{EI}. \end{aligned} \tag{5.13}$$

Similarly, we can calculate the slope θ by choosing $\overline{q} = -\delta'(x - x_o)$, i.e., a unit concentrated moment:

$$\begin{cases} EI\dfrac{d^4\overline{w}}{dx^4} = -\delta'\left(x - x_o\right), & x \in (0, L) \\ \overline{w}\left(0\right) = \overline{w}\left(L\right) = 0 \\ \overline{M}\left(0\right) = \overline{M}\left(L\right) = 0 \end{cases} \tag{5.14}$$

Then, we have

$$0 = \int_0^L \frac{\overline{M}M}{EI}dx + \left[\overline{V}w\right]_{x=0}^{x=L} - \left[\overline{M}\theta\right]_{x=0}^{x=L} + \int_0^L \delta'(x-x_o)wdx$$
$$\Rightarrow \theta\left(x_o\right) = \int_0^L \frac{\overline{M}M}{EI}dx. \tag{5.15}$$

For $x = x_o$, we have (Figure 5.1(c))

$$\begin{aligned}\theta\left(\frac{L}{2}\right) = &\int_0^{\frac{L}{2}} \left[-\frac{q}{2}\left(x-\frac{L}{2}\right)^2 + \frac{qL^2}{8}\right]\frac{1}{EI}\left(\frac{x}{L}\right)dx \\ &+ \int_{\frac{L}{2}}^L \left[-\frac{q}{2}\left(x-\frac{L}{2}\right)^2 + \frac{qL^2}{8}\right]\frac{1}{EI}\left(\frac{x}{L}-1\right)dx \\ &= 0.\end{aligned} \tag{5.16}$$

When interested on boundaries, we can choose a virtual system with non-homogeneous boundary conditions. For example, we choose

$$\begin{cases} EI\dfrac{d^4\overline{w}}{dx^4} = 0, \quad x \in (0,L) \\ \overline{w}\left(0\right) = \overline{w}\left(L\right) = 0 \\ \overline{M}\left(0\right) = -1, \quad \overline{M}\left(L\right) = 0 \end{cases} \tag{5.17}$$

to compute the slope at the left boundary (Figure 5.1(d)), i.e.,

$$0 = \int_0^L \frac{\overline{M}M}{EI}dx + \left[\overline{V}w\right]_{x=0}^{x=L} - \overline{M}\theta\big|_{x=L} + \underbrace{\overline{M}}_{=-1}\theta\Big|_{x=0} - \int_0^L 0 \cdot wdx$$
$$\Rightarrow \theta\left(0\right) = \int_0^L \frac{\overline{M}M}{EI}dx. \tag{5.18}$$

Then, we have

$$\theta\left(0\right) = \int_0^L \left[-\frac{q}{2}\left(x-\frac{L}{2}\right)^2 + \frac{qL^2}{8}\right]\frac{1}{EI}\left(\frac{x}{L}-1\right)dx = -\frac{qL^3}{24EI}. \tag{5.19}$$

Table 5.1 shows the integration formulae for a product of two functions with various shapes, which can be used for virtual work calculation. For example, the previous calculation (5.13) can be calculated using the table as

$$w\left(\frac{L}{2}\right) = \frac{L}{3EI}\left(1+\frac{1}{4}\right)\underbrace{\frac{qL^2}{8}}_{=M_1}\underbrace{\left(-\frac{L}{4}\right)}_{=M_3} = -\frac{5}{384}\frac{qL^4}{EI}. \tag{5.20}$$

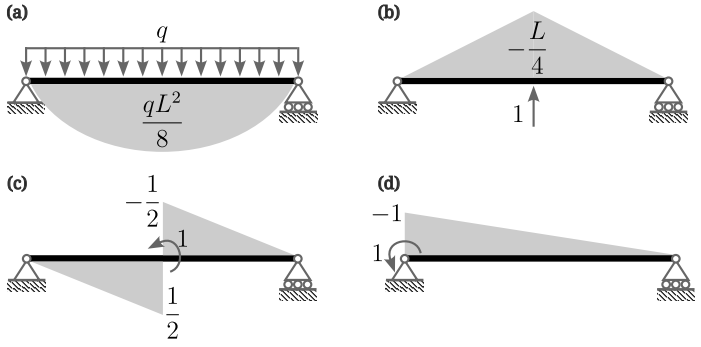

Figure 5.1: Bending moment diagrams for (a) w system and (b),(c),(d) three $\overline{w}$ systems.

Table 5.1: Integration formulae for a product of two functions $\int_0^L M_A M_B dx$.

M_A \ M_B	M_1 (L)	M_1, M_2 (L)	M_1 (a, b; L)	M_1 (L)
M_3 (L)	$\frac{L}{2}M_1M_3$	$\frac{L}{2}(M_1+M_2)M_3$	$\frac{L}{2}M_1M_3$	$\frac{2L}{3}M_1M_3$
M_3 (L)	$\frac{L}{3}M_1M_3$	$\frac{L}{6}(M_1+2M_2)M_3$	$\frac{L}{6}\left(1+\frac{a}{L}\right)M_1M_3$	$\frac{L}{3}M_1M_3$
M_3 (L)	$\frac{L}{6}M_1M_3$	$\frac{L}{6}(2M_1+M_2)M_3$	$\frac{L}{6}\left(1+\frac{b}{L}\right)M_1M_3$	$\frac{L}{3}M_1M_3$
M_3, M_4 (L)	$\frac{L}{6}M_1(M_3+2M_4)$	$\frac{L}{6}M_1(2M_3+M_4)$ $+\frac{L}{6}M_2(M_3+2M_4)$	$\frac{L}{6}\left(1+\frac{b}{L}\right)M_1M_3$ $+\frac{L}{6}\left(1+\frac{a}{L}\right)M_1M_4$	$\frac{L}{3}M_1(M_3+M_4)$
M_3 (c, d; L)	$\frac{L}{6}\left(1+\frac{c}{L}\right)M_1M_3$	$\frac{L}{6}\left(1+\frac{d}{L}\right)M_1M_3$ $+\frac{L}{6}\left(1+\frac{c}{L}\right)M_2M_3$	for $c \le a$, $\frac{L}{3}M_1M_3$ $-\frac{L(a-c)^2}{6ad}M_1M_3$	$\frac{L}{3}\left(1+\frac{cd}{L^2}\right)M_1M_3$
M_3 (L)	$\frac{L}{3}M_1M_3$	$\frac{L}{3}(M_1+M_2)M_3$	$\frac{L}{3}\left(1+\frac{ab}{L^2}\right)M_1M_3$	$\frac{8L}{15}M_1M_3$
M_3 (L)	$\frac{L}{4}M_1M_3$	$\frac{L}{12}(M_1+3M_2)M_3$	$\frac{L}{12}\left(1+\frac{a}{L}+\frac{a^2}{L^2}\right)M_1M_3$	$\frac{L}{5}M_1M_3$

5.2 General elastic bodies

5.2.1 Weighted residual method for linear elasticity

Here, we derive the principle of virtual work for linear elasticity using weighted residual method. The governing equations are

$$\begin{cases} \operatorname{div}\sigma + b = 0 & \text{(equilibrium equation)} \\ \sigma = C\left[\varepsilon\right], & \text{(stress-strain relation)} \\ \varepsilon = \operatorname{grad}_{\text{sym.}} u & \text{(strain-displacement relation)} \end{cases} \tag{5.21}$$

or, when combined in terms of u,

$$\operatorname{div} C\left[\operatorname{grad} u\right] + b = 0. \tag{5.22}$$

In the above, $u \in \mathbb{R}^3$ is the displacement, $\varepsilon \in \mathbb{R}^{3\times3}$ is the strain, $\sigma \in \mathbb{R}^{3\times3}$ is the stress, $C \in \mathbb{R}^{3\times3\times3\times3}$ is the elasticity tensor, and $b \in \mathbb{R}^3$ is the body force. The $\operatorname{grad}_{\text{sym.}}\cdot \equiv (1/2)[\operatorname{grad}\cdot + (\operatorname{grad}\cdot)^T]$ is the symmetric part of the gradient, which is replaced with the regular gradient in the displacement-only formulation called *Navier equation* (5.22) due to the symmetry inherit in the elasticity tensor C. For a linear isotropic medium, C is composed of two parameters E and $G = E/(2(1+\nu))$, where ν is the *Poisson's ratio*. Equivalently, the two parameters can be expressed with a different set of parameters, $\lambda = E\nu/((1+\nu)(1-2\nu))$ and $\mu = G$, called *Lamé parameters*, which gives

$$C\left[\,\right] = \mu\left[\,\right] + \mu\left[\,\right]^T + \lambda \operatorname{tr}\left[\,\right] I. \tag{5.23}$$

In the above, $\operatorname{tr}[\,] : \mathbb{R}^{3\times3} \to \mathbb{R}$ is a trace operator, i.e., $\operatorname{tr}[A] = \sum_i A_{ii}$, and $I \in \mathbb{R}^{3\times3}$ is the identity tensor.

Multiplying the (5.22) with a test function $\overline{u}$ and integrating by parts, we have

$$\begin{aligned} 0 &= \int_\Omega \overline{u} \cdot \left(\operatorname{div} C\left[\operatorname{grad} u\right] + b\right) d\Omega \\ &= \int_\Gamma \overline{u} \cdot C\left[\operatorname{grad} u\right] n d\Gamma + \int_\Omega \overline{u} \cdot b d\Omega - \int_\Omega \operatorname{grad}\overline{u} : C\left[\operatorname{grad} u\right] d\Omega \\ &= \underbrace{\int_\Gamma \overline{u} \cdot T d\Gamma + \int_\Omega \overline{u} \cdot b d\Omega}_{=\delta W_{\text{ext}}} - \underbrace{\int_\Omega \overline{\varepsilon} : \sigma d\Omega}_{=\delta W_{\text{int}}}. \end{aligned} \tag{5.24}$$

In the above, Ω is the domain and its boundary is denoted by $\Gamma \equiv \partial\Omega$; n is the outward-normal vector. Single and double contractions are denoted by $\cdot$ and $:$, respectively. The boundary term implies that we can either apply the Dirichlet boundary condition, i.e., the displacement boundary condition

$$u = u_o \quad x \in \Gamma \tag{5.25}$$

or the Neumann boundary condition, i.e., the traction boundary condition,

$$T \equiv C\left[\operatorname{grad} u\right] n = T_o \quad x \in \Gamma. \tag{5.26}$$

5.2.2 One-dimensional approximation for structural analysis

Now, let's deduce from the above result to structural analysis. We will decompose the internal virtual work by its contribution to bending moment, axial deformation, shear stress, and torsion.

- Bending moment (normal stress):
  Here, we assume a non-uniform normal strain and stress in a cross-section due to a bending, i.e.,

$$\overline{\varepsilon} = -\frac{d^2\overline{w}}{dx^2} y \hat{e}_x \hat{e}_x \quad \text{and} \quad \sigma = -E\frac{d^2 w}{dx^2} y \hat{e}_x \hat{e}_x. \tag{5.27}$$

  Then, we have

$$\begin{aligned}
\int_\Omega \overline{\varepsilon} : \sigma d\Omega &= \int_\Omega \left(-\frac{d^2\overline{w}}{dx^2} y\right)\left(-E\frac{d^2 w}{dx^2} y\right) d\Omega \\
&= \int_0^L \frac{d^2\overline{w}}{dx^2} E \left(\int_A y^2 dA\right) \frac{d^2 w}{dx^2} dx \\
&= \int_0^L \frac{d^2\overline{w}}{dx^2} EI \frac{d^2 w}{dx^2} dx \\
&= \int_0^L \frac{\overline{M} M}{EI} dx.
\end{aligned} \tag{5.28}$$

- Axial deformation (normal stress):
  Here, we assume a uniform normal strain and stress in a cross-section , i.e.,

$$\overline{\varepsilon} = \frac{d\overline{u}}{dx} \hat{e}_x \hat{e}_x \quad \text{and} \quad \sigma = E\frac{du}{dx} \hat{e}_x \hat{e}_x. \tag{5.29}$$

  Then, we have

$$\begin{aligned}
\int_\Omega \overline{\varepsilon} : \sigma d\Omega &= \int_\Omega \frac{d\overline{u}}{dx} E \frac{du}{dx} d\Omega \\
&= \int_0^L \frac{d\overline{u}}{dx} E \left(\int_A dA\right) \frac{du}{dx} dx \\
&= \int_0^L \frac{d\overline{u}}{dx} EA \frac{du}{dx} dx \\
&= \int_0^L \frac{\overline{F} F}{EA} dx.
\end{aligned} \tag{5.30}$$

- Shear strain from bending (a posteriori shear stress correction):
  Here, we assume a non-uniform shear strain and stress in a cross-section due to a bending, i.e.,

$$\overline{\varepsilon} = \frac{1}{G}\frac{\overline{V} Q}{Ib} \hat{e}_y \hat{e}_x \quad \text{and} \quad \sigma = \frac{VQ}{Ib} \hat{e}_y \hat{e}_x \tag{5.31}$$

In the above, $b(y)$ is the cross-sectional width and $Q(x,y) = \int_y^a y dA$. Then, we have

$$\begin{aligned}\int_\Omega \overline{\varepsilon} : \sigma d\Omega &= \int_\Omega \left(\frac{1}{G}\frac{\overline{V}Q}{Ib}\right)\left(\frac{VQ}{Ib}\right) d\Omega \\ &= \int_0^L \frac{\overline{V}V}{G}\left(\int_A \frac{Q^2}{I^2 b^2} dA\right) dx \\ &= \int_0^L f_s \frac{\overline{V}V}{GA} dx \end{aligned} \tag{5.32}$$

Here, the *form factor* f_s is defined as

$$f_s(x) = \frac{A(x)}{I^2(x)} \int_A \frac{Q^2(x,y)}{b^2(y)} dA, \tag{5.33}$$

where for a rectangle $f_s = 6/5$, for a circle $f_s = 10/9$, and for a thin-walled tube $f_s = 2$.

- Torsion (shear stress):
  Here, we assume a non-uniform shear strain and stress in a cross-section due to a torsion, i.e.,

$$\overline{\varepsilon} = \frac{1}{2}\rho\frac{d\overline{\varphi}}{dx}\hat{e}_\theta\hat{e}_\rho + \frac{1}{2}\rho\frac{d\overline{\varphi}}{dx}\hat{e}_\rho\hat{e}_\theta \quad \text{and} \tag{5.34}$$

$$\sigma = \frac{1}{2}G\rho\frac{d\varphi}{dx}\hat{e}_\theta\hat{e}_\rho + \frac{1}{2}G\rho\frac{d\varphi}{dx}\hat{e}_\rho\hat{e}_\theta. \tag{5.35}$$

  In the above, ρ is the radial distance from the cross-sectional center. Then, we have

$$\begin{aligned}\int_\Omega \overline{\varepsilon} : \sigma d\Omega &= \int_\Omega \left(\rho\frac{d\overline{\varphi}}{dx}\right)\left(G\rho\frac{d\varphi}{dx}\right) d\Omega \\ &= \int_0^L \frac{d\overline{\varphi}}{dx} G\left(\int_A \rho^2 dA\right)\frac{d\varphi}{dx} dx \\ &= \int_0^L \frac{d\overline{\varphi}}{dx} GJ\frac{d\varphi}{dx} dx \\ &= \int_0^L \frac{\overline{T}T}{GJ} dx. \end{aligned} \tag{5.36}$$

Thus, considering all strains, the displacement at $x = x_o$ can be calculated as

$$w(x_o) = \int_0^L \frac{\overline{M}M}{EI} dx + \int_0^L \frac{\overline{F}F}{EA} dx + \int_0^L f_s \frac{\overline{V}V}{GA} dx + \int_0^L \frac{\overline{T}T}{GJ} dx. \tag{5.37}$$

As an example, let's compute the deflection at a center of a simply supported beam under a uniform load $-q$. From the previous calculation (5.20), we know the deflection due to the normal stress is

$$w_m = \int_0^L \frac{\overline{M}M}{EI} dx = -\frac{5}{384}\frac{qL^4}{EI}. \tag{5.38}$$

On the other hand, the deflection due to the shear stress is

$$w_s = \int_0^L f_s \frac{\overline{V}V}{GA} dx = \frac{f_s}{GA}\left(-\frac{L}{4}\frac{1}{2}\frac{qL}{2} - \frac{L}{4}\frac{1}{2}\frac{qL}{2}\right) = -\frac{1}{8}\frac{f_s q L^2}{GA}. \tag{5.39}$$

For a rectangular cross-section ($h \times b$), we have $f_s = 6/5$, $I = bh^3/12$, and $A = bh$. We have $E/G = 2(1+\nu) = 2.6$ assuming a Poisson's ratio of $\nu = 0.3$. Then, the ratio between the two contributions are

$$\frac{w_s}{w_m} = \frac{f_s}{L^2}\frac{384EI}{40GA} \approx 2.5\left(\frac{h}{L}\right)^2. \tag{5.40}$$

Thus, the deflection due to the shear stress w_s can be neglected for a small aspect ratio h/L. For example, we have $w_s/w_m \approx 0.625\%$ for $h/L = 1/20$.

5.3 Trusses

5.3.1 From general expression

In this section, we apply the principle of virtual work to solve a displacement of a truss. We start with the general expression, i.e.,

$$\int_S \overline{q} \cdot w dS = \sum_{e=1}^{N_{\text{member}}} \left(\int_0^{L_e} \frac{\overline{M}M}{EI} dx + \int_0^{L_e} \frac{\overline{F}F}{EA} dx + \int_0^{L_e} f_s \frac{\overline{V}V}{GA} dx + \int_0^{L_e} \frac{\overline{T}T}{GJ} dx \right). \tag{5.41}$$

In the above, N_{member} is the total number of members and $\sum_{e=1}$ is a summation for all members, where L_e is the length of each member. Let $\overline{q} = \delta(s - s_o)n$, where s_o is one of the nodes and $n = (\cos\alpha)\hat{e}_x + (\sin\alpha)\hat{e}_y$ is a normal vector. Then, the left-hand-side of the above equation becomes

$$\int_S \overline{q} \cdot w dS = \|w_o\| \cos\alpha = \sqrt{u_o^2 + v_o^2}\cos\alpha, \tag{5.42}$$

where w_o is a vector-valued displacement of node s_o and its horizontal and vertical components are denoted by u_o and v_o, respectively. On the other hand, the assumptions of truss structures leave member-wise constant axial forces only, which gives

$$\sqrt{u_o^2 + v_o^2}\cos\alpha = \sum_{e=1}^{N_{\text{member}}} \int_0^{L_e} \frac{\overline{F}F}{EA} dx = \sum_{e=1}^{N_{\text{member}}} \frac{\overline{F}_e F_e}{E_e A_e} L_e. \tag{5.43}$$

5.3.2 From weighted residual

Next, we derive the principle directly from weighted residual. Let $F_j^{(i)}$ denote an internal force acting on a node i due to a member j. For each node i, we

have $N^{(i)}_{\text{member}}$ number of members connected. Thus, an equilibrium equations at a node i reads

$$\begin{cases} X^{(i)} + \displaystyle\sum_{j=1}^{N^{(i)}_{\text{member}}} F^{(i)}_j \cos\theta^{(i)}_j = 0 \\ Y^{(i)} + \displaystyle\sum_{j=1}^{N^{(i)}_{\text{member}}} F^{(i)}_j \sin\theta^{(i)}_j = 0 \end{cases} \qquad i = 1, 2, \ldots, N_{\text{node}}. \tag{5.44}$$

In the above, $X^{(i)}$ and $Y^{(i)}$ are horizontal and vertical external loads acting on a node (i), respectively. N_{node} is the total number of nodes and $\theta^{(i)}_j$ are the angle of the member j at node i. Denoting $\overline{u}^{(i)}$ and $\overline{v}^{(i)}$ as test functions, or virtual displacements, in horizontal and vertical directions, we have

$$\begin{aligned} 0 = & -\sum_{i=1}^{N_{\text{node}}} \left[\left(X^{(i)} + \sum_{j=1}^{N^{(i)}_{\text{member}}} F^{(i)}_j \cos\theta^{(i)}_j \right) \overline{u}^{(i)} \right. \\ & \qquad \left. + \left(Y^{(i)} + \sum_{j=1}^{N^{(i)}_{\text{member}}} F^{(i)}_j \sin\theta^{(i)}_j \right) \overline{v}^{(i)} \right] \\ = & \underbrace{\sum_{i=1}^{N_{\text{node}}} \left(-\overline{u}^{(i)} \sum_{j=1}^{N^{(i)}_{\text{member}}} F^{(i)}_j \cos\theta^{(i)}_j - \overline{v}^{(i)} \sum_{j=1}^{N^{(i)}_{\text{member}}} F^{(i)}_j \sin\theta^{(i)}_j \right)}_{=\delta W_{\text{int}}} \\ & \underbrace{- \sum_{i=1}^{N_{\text{node}}} \left(X^{(i)} \overline{u}^{(i)} + Y^{(i)} \overline{v}^{(i)} \right)}_{=\delta W_{\text{ext}}}. \end{aligned} \tag{5.45}$$

Let N_{member} the total number of members, we rearrange the nodal summations with member-wise summations for the internal virtual work, e.g. (Figure 5.2),

$$\begin{aligned} & u^{(i)} F^{(i)} \cos\theta^{(i)} + v^{(i)} F^{(i)} \sin\theta^{(i)} + u^{(i+1)} F^{(i+1)} \cos\theta^{(i+1)} + v^{(i+1)} F^{(i+1)} \sin\theta^{(i+1)} \\ & \qquad = u^A_e F_e \cos\theta_e + v^A_e F_e \sin\theta_e - u^B_e F_e \cos\theta_e - v^B_e F_e \sin\theta_e \\ & \qquad = -F_e \left[\left(u^B_e - u^A_e \right) \cos\theta_e + \left(v^B_e - v^A_e \right) \sin\theta_e \right] \\ & \qquad = -F_e \Delta L_e. \end{aligned} \tag{5.46}$$

Then, we have

$$\begin{aligned} \delta W_{\text{int}} = & \sum_{e=1}^{N_{\text{member}}} \left[F_e \cos\theta_e \left(\overline{u}^B_e - \overline{u}^A_e \right) + F_e \sin\theta_e \left(\overline{v}^B_e - \overline{v}^A_e \right) \right] \\ = & \sum_{e=1}^{N_{\text{member}}} F_e \Delta \overline{L}_e = \sum_{e=1}^{N_{\text{member}}} F_e \frac{\overline{F}_e L_e}{E_e A_e}. \end{aligned} \tag{5.47}$$

In the above, F_e are the axial force at member e inclined with an angle θ_e. u^A_e and u^B_e are the horizontal displacements at two nodes of a member e; v^A_e and v^B_e

are similarly defined. The deformation at a member e is $\Delta L_e = F_e L_e/(E_e A_e)$. Then, by applying the Betti-Maxwell reciprocal theorem and a virtual force at a single node o, we have

$$\sum_{i=1}^{N_{\text{node}}} \left(\overline{X}^{(i)} u^{(i)} + \overline{Y}^{(i)} v^{(i)} \right) = \sqrt{u_o^2 + v_o^2} \cos\alpha = \sum_{e=1}^{N_{\text{member}}} \frac{\overline{F}_e F_e}{E_e A_e} L_e. \tag{5.48}$$

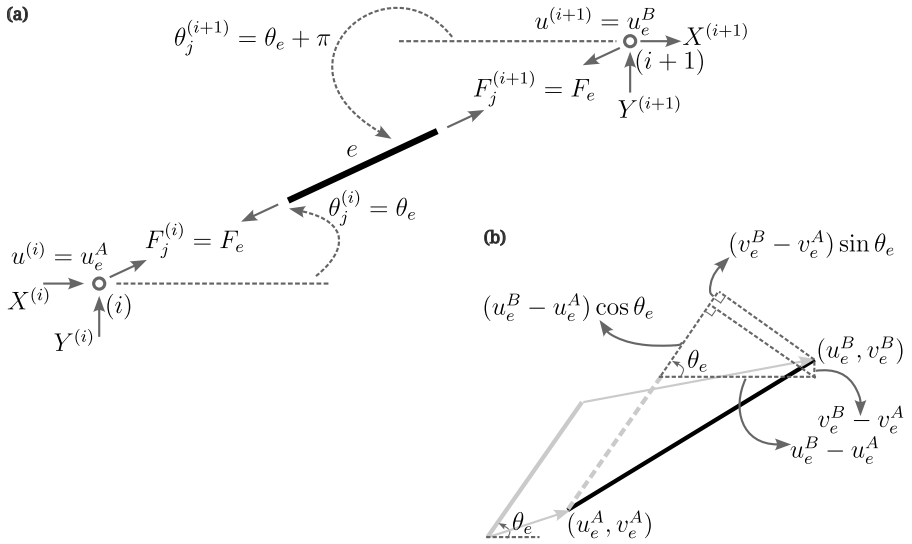

Figure 5.2: Truss member under deformation. (a) Nodal vs. member-wise forces and the corresponding (b) Elongation $\Delta L_e = (u_e^B - u_e^A)\cos\theta_e + (v_e^B - v_e^A)\sin\theta_e$.

5.3.3 From energy

The conservation of energy for trusses reads

$$\begin{aligned}
W_{\text{ext}} &= \frac{1}{2} \sum_{i=1}^{N_{\text{node}}} \Delta^{(i)} \cdot P^{(i)} \\
&= \frac{1}{2} \sum_{i=1}^{N_{\text{node}}} \left(u^{(i)} X^{(i)} + v^{(i)} Y^{(i)} \right) \\
&= \frac{1}{2} \sum_{i=1}^{N_{\text{node}}} \left(-u^{(i)} \sum_{j=1}^{N_{\text{member}}^{(i)}} F_j^{(i)} \cos\theta_j^{(i)} - v^{(i)} \sum_{j=1}^{N_{\text{member}}^{(i)}} F_j^{(i)} \sin\theta_j^{(i)} \right) \\
&= \frac{1}{2} \sum_{e=1}^{N_{\text{member}}} \left[F_e \cos\theta_e \left(u_e^B - u_e^A \right) + F_e \sin\theta_e \left(v_e^B - v_e^A \right) \right] \\
&= \frac{1}{2} \sum_{e=1}^{N_{\text{member}}} \frac{F_e^2 L_e}{E_e A_e} = W_{\text{int}}.
\end{aligned} \tag{5.49}$$

Then, we write the above equation for two loads applied simultaneously

$$\frac{1}{2}\sum_{e=1}^{N_{\text{member}}}\frac{\left(F_e+\overline{F}_e\right)^2 L_e}{E_e A_e}=\frac{1}{2}\sum_{i=1}^{N_{\text{node}}}\left(\Delta^{(i)}+\overline{\Delta}^{(i)}\right)\cdot\left(P^{(i)}+\overline{P}^{(i)}\right)$$
$$\Rightarrow\sum_{e=1}^{N_{\text{member}}}\frac{F_e\overline{F}_e L_e}{E_e A_e}=\frac{1}{2}\sum_{i=1}^{N_{\text{node}}}\left(\Delta^{(i)}\cdot\overline{P}^{(i)}+\overline{\Delta}^{(i)}\cdot P^{(i)}\right). \tag{5.50}$$

By comparing with another case when P is applied first, we have (Figure 5.3)

$$\frac{1}{2}\sum_{i=1}^{N_{\text{node}}}\Delta^{(i)}\cdot P^{(i)}+\sum_{i=1}^{N_{\text{node}}}\overline{\Delta}^{(i)}\cdot P^{(i)}+\frac{1}{2}\sum_{i=1}^{N_{\text{node}}}\overline{\Delta}^{(i)}\cdot\overline{P}^{(i)}$$
$$=\frac{1}{2}\sum_{i=1}^{N_{\text{node}}}\left(\Delta^{(i)}+\overline{\Delta}^{(i)}\right)\cdot\left(P^{(i)}+\overline{P}^{(i)}\right)$$
$$\Rightarrow\sum_{i=1}^{N_{\text{node}}}\overline{\Delta}^{(i)}\cdot P^{(i)}=\sum_{i=1}^{N_{\text{node}}}\Delta^{(i)}\cdot\overline{P}^{(i)}. \tag{5.51}$$

Thus, we conclude

$$\sum_{e=1}^{N_{\text{member}}}\frac{F_e\overline{F}_e}{E_e A_e}L_e=\sum_{i=1}^{N_{\text{node}}}\overline{\Delta}^{(i)}\cdot P^{(i)}=\sum_{i=1}^{N_{\text{node}}}\Delta^{(i)}\cdot\overline{P}^{(i)}. \tag{5.52}$$

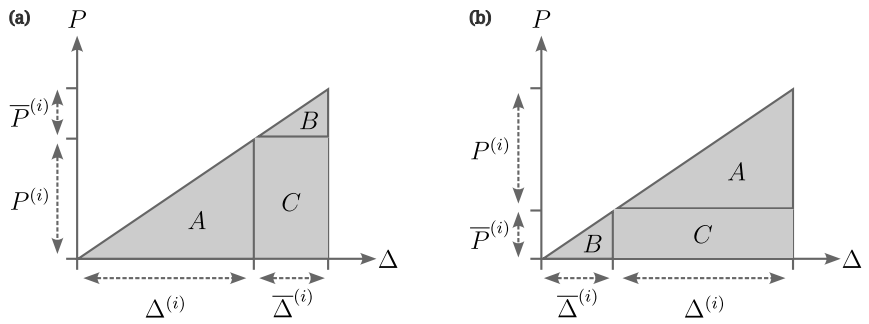

Figure 5.3: Betti-Maxwell reciprocal theorem illustrated by sequential loadings; $A = P^{(i)}\Delta^{(i)}/2$ and $B = \overline{P}^{(i)}\overline{\Delta}^{(i)}/2$ indicate works done by $P^{(i)}$ and $\overline{P}^{(i)}$, respectively; notice that the areas of the cross term $C = P^{(i)}\overline{\Delta}^{(i)} = \overline{P}^{(i)}\Delta^{(i)}$ are the same for both loading cases. (a) P-first case. (b) $\overline{P}$-first case.

5.4 Examples

Consider a truss shown in Figure 5.4. We can calculate the displacement along the direction of the virtual force by computing internal forces for both real and virtual system. As an example, Table 5.2 is prepared below, which gives the displacement of $130 + 60\sqrt{2}$.

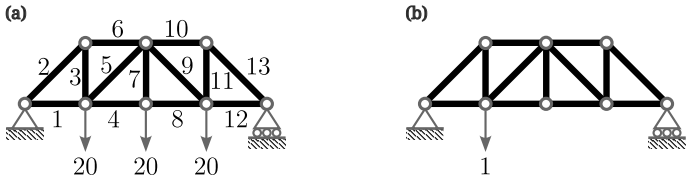

Figure 5.4: Truss example. (a) Real system. (b) Virtual system.

Table 5.2: Table for the displacement calculation of a truss (Figure 5.4).

Member	$L/(EA)$	F	$\overline{F}$	$F\overline{F}L/(EA)$
1	1	30	0.75	22.5
2	$\sqrt{2}$	$-30\sqrt{2}$	$-0.75\sqrt{2}$	$45\sqrt{2}$
3	1	30	0.75	22.5
4	1	40	0.50	20
5	$\sqrt{2}$	$-10\sqrt{2}$	$0.25\sqrt{2}$	$-5\sqrt{2}$
6	1	-30	-0.75	22.5
7	1	20	0	0
8	1	40	0.5	20
9	$\sqrt{2}$	$-10\sqrt{2}$	$-0.25\sqrt{2}$	$5\sqrt{2}$
10	1	-30	-0.25	7.5
11	1	30	0.25	7.5
12	1	30	0.25	7.5
13	$\sqrt{2}$	$-30\sqrt{2}$	$-0.25\sqrt{2}$	$15\sqrt{2}$
$\sum$				$130 + 60\sqrt{2}$

Next, consider a three-hinged frame with a concentrated load (Figure 5.5). Using the principle of virtual work, we can compute the displacement at any location by

$$w\left(x_o\right)=\sum_e\int_0^{L_e}\frac{\overline{M}M}{EI}dx+\sum_e\int_0^{L_e}\frac{\overline{F}F}{EA}dx+\sum_e\int_0^{L_e}f_s\frac{\overline{V}V}{GA}dx. \tag{5.53}$$

Then, the amount of displacement downward at the hinge can be calculated by

$$\Delta=\Delta_m+\Delta_s+\Delta_a=\frac{PL^3}{16EI}\left(1+\frac{6f_sEI}{GAL^2}+\frac{9I}{AL^2}\right), \tag{5.54}$$

where, using the integration table,

$$\Delta_m=\sum_e\int_0^{L_e}\frac{\overline{M}M}{EI}dx=\frac{2}{EI}\left(\frac{L}{3}\frac{PL}{4}\frac{L}{4}+\frac{L}{6}\frac{PL}{4}\frac{L}{4}\right)=\frac{PL^3}{16EI}, \tag{5.55a}$$

$$\Delta_s=\sum_e\int_0^{L_e}f_s\frac{\overline{V}V}{GA}dx=\frac{2f_s}{GA}\left(L\frac{P}{4}\frac{1}{4}+\frac{L}{2}\frac{P}{2}\frac{1}{2}\right)=\frac{3}{8}\frac{f_sPL}{EA}, \quad \text{and} \tag{5.55b}$$

$$\Delta_a=\sum_e\int_0^{L_e}\frac{\overline{F}F}{EA}dx=\frac{2}{EA}\left(L\frac{P}{2}\frac{1}{2}+\frac{L}{2}\frac{P}{4}\frac{1}{4}\right)=\frac{9}{16}\frac{PL}{EA}. \tag{5.55c}$$

We assume a rectangular cross-section ($h\times b$) and Poisson's ratio of $\nu=0.3$, which give $f_s=6/5$, $I=bh^3/12$, $A=bh$, and $E/G=2(1+\nu)=2.6$. Then, the displacement (5.54) reads

$$\Delta=\Delta_m+\Delta_s+\Delta_a\approx\frac{PL^3}{16EI}\left[1+1.56\left(\frac{h}{L}\right)^2+0.75\left(\frac{h}{L}\right)^2\right]. \tag{5.56}$$

Again, we confirm that the contributions from shear and axial forces are negligible for small h/L ratio, i.e.,

$$\Delta\approx\Delta_m=\sum_e\int_0^{L_e}\frac{\overline{M}M}{EI}dx. \tag{5.57}$$

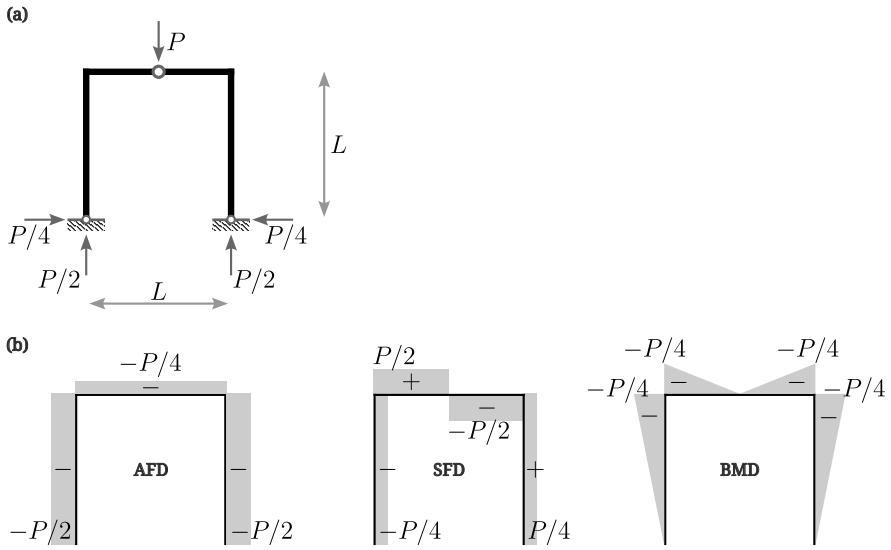

Figure 5.5: Frame example. (a) Reaction forces. (b) Axial force, shear force, and bending moment diagrams.

Chapter 6

Statically Indeterminate Structures

6.1 Beams

In this and following sections, we will study *statically indeterminate structures*. Statically indeterminate structures can not be analyzed as they are because the number of unknowns are larger than the number of equations. Instead, we often necessary to divide them into simpler determinate substructures, or *primary structures*. Then, the response of the original structure is a linear combination of primary structures, which leads to a *compatibility condition* that takes a general form of

$$\delta_{i0} + \sum_{j=1}^{N} \delta_{ij} X_j = \Delta_j, \quad i = 1, 2, \ldots, N. \tag{6.1}$$

In the above, N is the number of primary structures, δ_{ij} are known physical quantities of primary structures, X_j are the unknowns to be determined, and Δ_i are known quantities from the original structure. Such method of analyzing indeterminate structures are called the *flexibility method*, where the above expression will be more clearer as we study specific examples.

6.1.1 Propped cantilever beam

Consider a following statically indeterminate beam (Figure 6.1). Here, we have three unknowns, M_A, R_A, and R_B, whereas two equilibrium equations are given:

$$R_A + R_B - qL = 0 \quad \text{and} \tag{6.2}$$

$$-M_A - \frac{qL^2}{2} + LR_B = 0. \tag{6.3}$$

First, we release the support B so that the original structure is represented by a superposition of two identical cantilevers with different loading condition (Figure 6.2). Then, the compatibility condition reads

$$\delta_0 + R_B \delta_1 = 0. \tag{6.4}$$

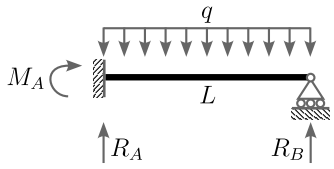

Figure 6.1: Indeterminate beam.

The two determinate beams can be solved using the principle of virtual work, i.e.,

$$\delta_0 = \int_0^L \frac{M\overline{M}}{EI}dx = \frac{1}{EI}\int_0^L \quad \cdot \quad dx$$

$$= \frac{1}{EI}\frac{L}{4}\left(-\frac{qL^2}{2}\right)L = -\frac{qL^4}{8EI} \quad \text{and} \tag{6.5}$$

$$\delta_1 = \int_0^L \frac{M\overline{M}}{EI}dx = \frac{1}{EI}\int_0^L \quad \cdot \quad dx$$

$$= \frac{1}{EI}\frac{L}{3}LL = \frac{L^3}{3EI}. \tag{6.6}$$

Thus, we have $R_B = 3qL/8$, $R_A = 5qL/8$, and $M_A = -qL^2/8$.

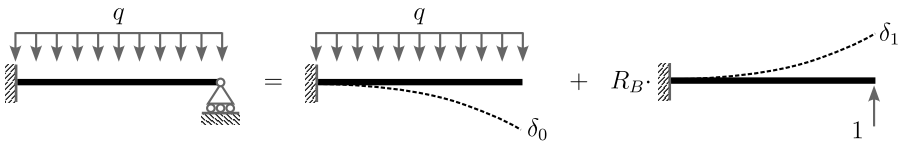

Figure 6.2: Indeterminate beam as a superposition of two determinate beams.

As for the displacement, which formed the compatibility condition, other physical quantities such as bending moment can be superposed.

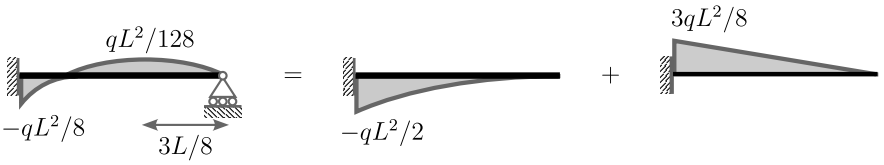

Figure 6.3: Superposition of bending moments.

Alternatively, we can release the left-hand-side moment M_A (Figure 6.4). The corresponding compatibility condition is

$$\theta_0 + M_A\theta_1 = 0. \tag{6.7}$$

The above angles can be calculated by

$$\theta_0 = \int_0^L \frac{M\overline{M}}{EI}dx = \frac{1}{EI}\int_0^L \quad \cdot \quad dx$$
$$= \frac{1}{EI}\frac{L}{3}\frac{qL^2}{8}\cdot(-1) = -\frac{qL^3}{24EI} \quad \text{and} \tag{6.8}$$
$$\theta_1 = \int_0^L \frac{M\overline{M}}{EI}dx = \frac{1}{EI}\int_0^L \quad \cdot \quad dx$$
$$= \frac{1}{EI}\frac{L}{3}(1)\cdot(-1) = -\frac{L}{3EI}. \tag{6.9}$$

Then, we have $M_A = -qL^2/8$.

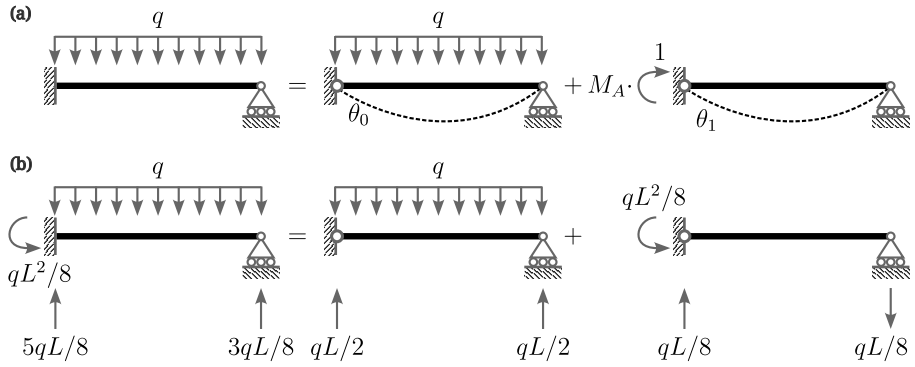

Figure 6.4: Alternative choice of superposition. (a) Compatibility condition. (b) Superposition of reaction forces.

Before we move on to different examples, let's check the contribution of shear forces on the reactions. First, we rewrite the compatibility condition (6.4) as

$$\delta_0 + R_B\delta_1 = \left(\delta_0^M + \delta_0^S\right) + R_B\left(\delta_1^M + \delta_1^S\right) = 0. \tag{6.10}$$

In the above, the superscript M and S denote contributions from bending moment and shear force, respectively. We previously calculated $\delta_0^M = -qL^4/(8EI)$ and $\delta_1^M = L^3/(3EI)$; below, we have

$$\delta_0^S = \int_0^L f_s\frac{V\overline{V}}{GA}dx = \frac{f_s}{GA}\int_0^L \quad \cdot \quad dx$$
$$= \frac{f_s}{GA}\frac{L}{2}qL\cdot(-1) = -\frac{f_sqL^2}{2GA} \quad \text{and} \tag{6.11}$$
$$\delta_1^S = \int_0^L f_s\frac{V\overline{V}}{GA}dx = \frac{f_s}{GA}\int_0^L \quad \cdot \quad dx$$
$$= \frac{f_s}{GA}\frac{L}{2}(-1)\cdot(-1) = \frac{f_sL}{GA}. \tag{6.12}$$

Then, the reaction force is

$$R_B = \frac{\frac{qL^4}{8EI} + \frac{f_sqL^2}{2GA}}{\frac{L^3}{3EI} + \frac{f_sL}{GA}} = \frac{3qL}{8}\frac{1+4\frac{f_sEI}{GAL^2}}{1+3\frac{f_sEI}{GAL^2}} \approx \frac{3qL}{8}\frac{1+2.1(h/L)^2}{1+1.56(h/L)^2}, \tag{6.13}$$

where, for rectangular section, we have

$$\frac{f_s EI}{GAL^2} = \frac{6}{5}\frac{E\frac{bh^3}{12}}{\frac{E}{2(1+\nu)}hbL^2} \approx 0.52(h/L)^2. \tag{6.14}$$

Thus, for $h/L = 1/20$, we have $R_B \approx 1.0014 \cdot 3qL/8$, which gives about 0.14% error when shear effect is omitted.

6.1.2 Cantilever beam with spring support

Here, we replace the roller support with a vertical spring (Figure 6.5(a)), which introduces a new type of boundary condition called *Robin boundary condition*. Instead of specifying either Dirichlet or Neumann data, this type defines a relation between the two data. For example, we have a relation between shear force and the deflection at $x = L$ such that (Figure 6.5(b))

$$EI\frac{d^3w}{dx^3}\bigg|_{x=L} - k \cdot w|_{x=L} = 0. \tag{6.15}$$

In the above, k is the spring constant.

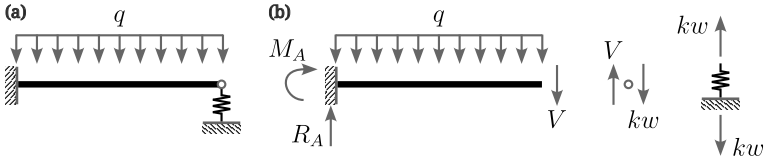

Figure 6.5: Cantilever beam with spring support. (a) Structure and load. (b) Freebody diagram.

We take the primary structures as shown in Figure 6.6. Then, the corresponding compatibility equation reads

$$\delta_0 + R_B(\delta_1 + \delta_s) = 0 \quad \text{or} \quad \delta_0 + R_B\delta_1 = -R_B\delta_s, \tag{6.16}$$

which gives

$$-\frac{qL^4}{8EI} + R_B\left(\frac{L^3}{3EI} + \frac{1}{k}\right) = 0 \quad \text{or} \quad R_B = \frac{3qL}{8}\frac{kL^3}{kL^3 + 3EI}. \tag{6.17}$$

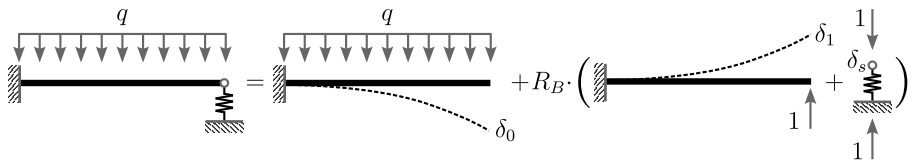

Figure 6.6: Compatibility condition.

If we consider $3EI/L^3$ as an effective spring constant of the cantilever beam at the free end, then the above $L^3/(3EI) + 1/k$ can be regarded as the inverse

of the equivalent spring constant of two springs in series. In addition, the two limiting cases of k, $k \to 0$ and $k \to \infty$, recover cases of free and fixed support, respectively as

$$\lim_{k\to 0} R_B = 0 \quad \text{and} \quad \lim_{k\to\infty} R_B = \frac{3qL}{8}. \tag{6.18}$$

The deflected shape for $k = 100EI/L^3$ is shown in Figure 6.7.

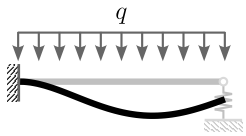

Figure 6.7: Deflected shape when $k = 100EI/L^3$.

6.1.3 Support settlement

Structures are subject to stresses when one of their supports are displaced even without any external load. Figure 6.8 illustrates a case of support settlement and its primary structures. Let Δ denote the amount of settlement downward, the corresponding compatibility condition reads

$$\delta_0 + R_B\delta_1 = -\Delta, \tag{6.19}$$

which gives

$$0 + R_B\frac{L^3}{3EI} = -\Delta \quad \text{or} \quad R_B = -\frac{3EI}{L^3}\Delta. \tag{6.20}$$

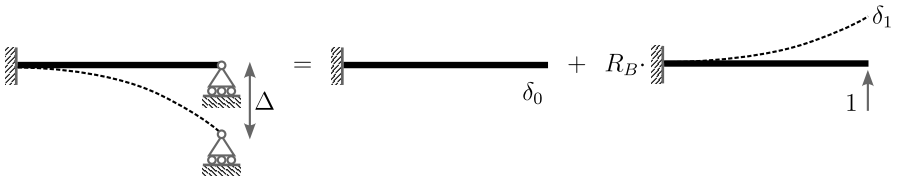

Figure 6.8: Compatibility condition for support settlement

6.1.4 Temperature gradient

Similarly to the support settlement, a temperature difference between top and bottom of a beam can also induce deformation. A linear temperature gradient gives a uniform curvature gradient (Figure 6.9), i.e.,

$$h d\theta = \alpha\,(T_2 - T_0)\,dx - \alpha\,(T_1 - T_0)\,dx \tag{6.21}$$

or

$$\frac{d\theta}{dx} = \frac{\alpha\,(T_2 - T_1)}{h} = \frac{d^2w}{dx^2}. \tag{6.22}$$

In the above, α is the thermal constant. Then, the general solution reads

$$w = \frac{\alpha\,(T_2 - T_1)}{2h} x^2 + C_0 x + C_1. \tag{6.23}$$

For example, we have $C_0 = -\alpha\,(T_2 - T_1)\,L/\,(2h)$ and $C_1 = 0$ for a simple beam ($w(0) = w(L) = 0$).

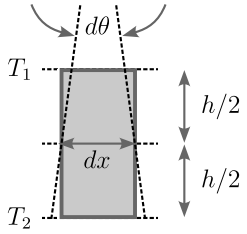

Figure 6.9: Curvature due to temperature gradient.

Let's consider a propped cantilever beam under a linear temperature gradient (Figure 6.10). The compatibility condition reads

$$\theta_0 + M_A \theta_1 = 0. \tag{6.24}$$

Then, using the solution above, we have

$$-\frac{\alpha\,(T_2 - T_1)\,L}{2h} + M_A \left(-\frac{L}{3EI}\right) = 0 \quad \text{or} \quad M_A = -\frac{3}{2}\frac{\alpha\,(T_2 - T_1)}{h} EI. \tag{6.25}$$

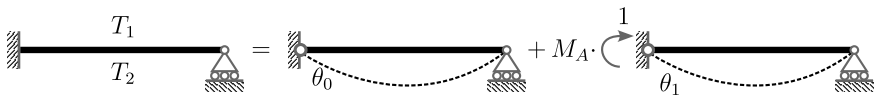

Figure 6.10: Compatibility condition for temperature gradient.

6.1.5 Other examples

Two-span continuous beam

Consider a two-span continuous beam (Figure 6.11). Here, we choose to release a moment at the middle support, which gives the following compatibility condition due to the slope continuity:

$$\theta_0^L + M_B \theta_1^L = -\left(\theta_0^R + M_B \theta_1^R\right) \quad \Rightarrow \quad \left(\theta_0^L + \theta_0^R\right) + M_B \left(\theta_1^L + \theta_1^R\right) = 0. \tag{6.26}$$

Then, from the principle of virtual work, we have

$$\begin{aligned}
\theta_0^L + \theta_0^R &= \int_0^{2L} \frac{M\overline{M}}{EI} dx \\
&= \frac{1}{EI}\int_0^L \text{▲}\cdot\text{▲}\,dx + \frac{1}{EI}\int_0^L \text{◠}\cdot\text{▲}\,dx \\
&= \frac{1}{EI}\frac{L}{6}\left(1+\frac{1}{2}\right)\frac{qL^2}{4}\cdot 1 + \frac{1}{EI}\frac{L}{3}\frac{qL^2}{8}\cdot 1 = \frac{5}{48}\frac{qL^3}{EI} \quad \text{and} \qquad (6.27)\\
\theta_1^L + \theta_1^R &= \int_0^{2L} \frac{M\overline{M}}{EI} dx \\
&= \frac{1}{EI}\int_0^L \text{▲}\cdot\text{▲}\,dx + \frac{1}{EI}\int_0^L \text{◺}\cdot\text{◺}\,dx \\
&= \frac{1}{EI}\frac{L}{3} + \frac{1}{EI}\frac{L}{3} = \frac{2}{3}\frac{L}{EI}. \qquad (6.28)
\end{aligned}$$

Thus, we computed the moment $M_B = -5qL^2/32$.

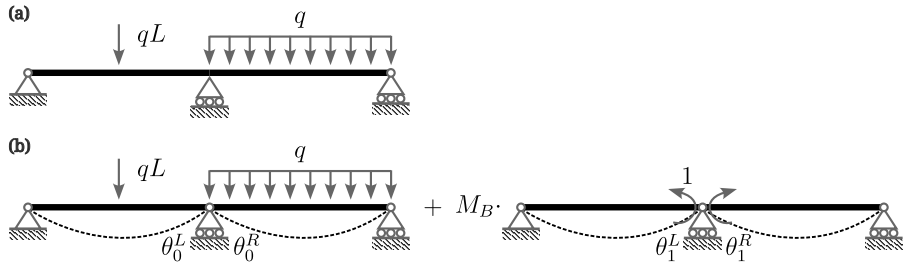

Figure 6.11: Two-span continuous beam. (a) Structure and loads. (b) Primary structures.

Three-span continuous beam

Three-span continuous beam is nothing more complex than the previous two-span example other than the increased number of primary structures (Figure 6.12). The corresponding compatibility condition reads

$$\begin{cases} \theta_{10}^L + M_1\theta_{11}^L = -\left(\theta_{10}^R + M_1\theta_{11}^R + M_2\theta_{12}^R\right) \\ \theta_{20}^L + M_1\theta_{21}^L + M_2\theta_{22}^L = -\left(\theta_{20}^R + M_2\theta_{22}^R\right) \end{cases} \qquad (6.29)$$

or

$$\begin{cases} \underbrace{\left(\theta_{10}^L + \theta_{10}^R\right)}_{=\delta_{10}} + M_1\underbrace{\left(\theta_{11}^L + \theta_{11}^R\right)}_{=\delta_{11}} + M_2\underbrace{\left(0 + \theta_{12}^R\right)}_{=\delta_{12}} = 0 \\ \underbrace{\left(\theta_{20}^L + \theta_{20}^R\right)}_{=\delta_{20}} + M_1\underbrace{\left(\theta_{21}^L + 0\right)}_{=\delta_{21}} + M_2\underbrace{\left(\theta_{22}^L + \theta_{22}^R\right)}_{=\delta_{22}} = 0 \end{cases} . \qquad (6.30)$$

Then, we have

$$\delta_{10} = \delta_{20} = \int_0^{2L} \frac{M\overline{M}}{EI} dx$$

$$= \frac{1}{EI_1} \int_0^{L} \quad \cdot \quad dx + \frac{1}{EI_2} \int_0^{L} \quad \cdot \quad dx$$

$$= + \frac{1}{EI_1} \frac{L}{3} \frac{qL^2}{8} \cdot 1 + \frac{1}{EI_2} \frac{L}{3} \frac{qL^2}{8} \cdot 1 = \frac{qL^3}{24EI_1} \left(1 + \frac{I_1}{I_2}\right), \tag{6.31}$$

$$\delta_{11} = \delta_{22} = \int_0^{2L} \frac{M\overline{M}}{EI} dx$$

$$= \frac{1}{EI_1} \int_0^{L} \quad \cdot \quad dx + \frac{1}{EI_2} \int_0^{L} \quad \cdot \quad dx$$

$$= \frac{1}{EI_1} \frac{L}{3} + \frac{1}{EI_2} \frac{L}{3} = \frac{L}{3EI_1} \left(1 + \frac{I_1}{I_2}\right), \quad \text{and} \tag{6.32}$$

$$\delta_{12} = \delta_{21} = \int_0^{L} \frac{M\overline{M}}{EI_2} dx$$

$$= \frac{1}{EI_2} \int_0^{L} \quad \cdot \quad dx$$

$$= \frac{L}{6EI_2}. \tag{6.33}$$

Notice that the reciprocity gives the symmetrical response of $\delta_{12} = \delta_{21}$, while $\delta_{10} = \delta_{20}$ and $\delta_{11} = \delta_{22}$ are due to the geometrical symmetry. Finally, the above compatibility equations yield to

$$\begin{bmatrix} \frac{L}{3EI_1}\left(1 + \frac{I_1}{I_2}\right) & \frac{L}{6EI_2} \\ \frac{L}{6EI_2} & \frac{L}{3EI_1}\left(1 + \frac{I_1}{I_2}\right) \end{bmatrix} \begin{pmatrix} M_1 \\ M_2 \end{pmatrix} = \begin{pmatrix} -\frac{qL^3}{24EI_1}\left(1 + \frac{I_1}{I_2}\right) \\ -\frac{qL^3}{24EI_1}\left(1 + \frac{I_1}{I_2}\right) \end{pmatrix}. \tag{6.34}$$

For $I_1 = I_2$, we have $M_1 = M_2 = -qL^2/10$.

Three-span continuous beam with a spring support

Here, we are interest in a three-span beam with a temperature gradient, concentrated and distributed loads, and a spring support (Figure 6.13). Releasing moments at supports B and C, the compatibility equations read

$$\delta_{10} + M_B\delta_{11} + M_C\delta_{12} = 0 \quad \text{and} \tag{6.35}$$

$$\delta_{20} + M_B\delta_{21} + M_C\delta_{22} = 0. \tag{6.36}$$

In the above, $\delta_{ij} = \theta_{ij}^L + \theta_{ij}^R$. Note that we need to consider the bending of beams as well as the deformation of the spring when using the principle of virtual work

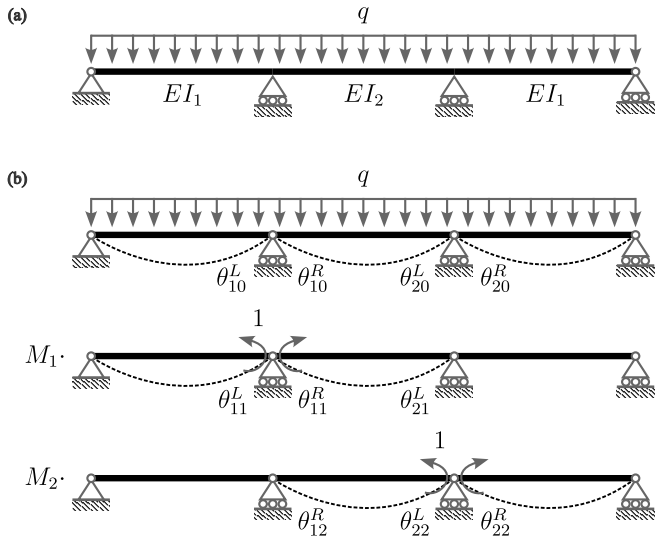

Figure 6.12: Three-span continuous beam. (a) Structure and loads. (b) Primary structures.

to calculate δ_{ij}. Specifically,

$$\begin{aligned}
\delta_{10} &= \left(\theta_{10}^{L}\right)^{\text{temp.}} + \int \frac{M_1 M_0}{EI} dx + \frac{F_1 F_0}{k} \\
&= \frac{\alpha L \Delta T}{2h} + \frac{L}{4EI} \cdot 1 \cdot \frac{PL}{4} + \left(-\frac{1}{L}\right) \cdot \left(-\frac{P+qL}{2}\right) \cdot \frac{L^3}{EI} \\
&= \frac{\alpha L \Delta T}{2h} + \frac{PL^2}{16EI} + \frac{(P+qL)\,L^2}{2EI}, \qquad (6.37) \\
\delta_{20} &= \int \frac{M_2 M_0}{EI} dx + \frac{F_2 F_0}{k} \\
&= \frac{L}{4EI} \cdot 1 \cdot \frac{PL}{4} + \frac{L}{3EI} \cdot 1 \cdot \frac{qL^2}{8} + \frac{2}{L} \cdot \left(-\frac{P+qL}{2}\right) \cdot \frac{L^3}{EI} \\
&= \frac{PL^2}{16EI} + \frac{qL^3}{24EI} - \frac{(P+qL)\,L^2}{EI}, \qquad (6.38) \\
\delta_{11} &= \int \frac{M_1 M_1}{EI} dx + \frac{F_1 F_1}{k} \\
&= \frac{2L}{3EI} + \frac{L}{EI}, \qquad (6.39) \\
\delta_{12} = \delta_{21} &= \int \frac{M_1 M_2}{EI} dx + \frac{F_1 F_2}{k} \\
&= \frac{L}{6EI} - \frac{2L}{EI}, \quad \text{and} \qquad (6.40) \\
\delta_{22} &= \int \frac{M_2 M_2}{EI} dx + \frac{F_2 F_2}{k} \\
&= \frac{2L}{3EI} + \frac{4L}{EI}. \qquad (6.41)
\end{aligned}$$

Here, F_i is the internal force of the spring. Then, the compatibility equations become

$$\frac{L}{EI}\begin{bmatrix} 5/3 & -11/6 \\ -11/6 & 14/3 \end{bmatrix}\begin{pmatrix} M_B \\ M_C \end{pmatrix} = -\frac{L^2}{EI}\begin{pmatrix} \alpha EI\Delta T/(2hL) + P/16 + (P+qL)/2 \\ P/16 + qL/24 - (P+qL) \end{pmatrix}. \tag{6.42}$$

As a side note, the contributions of the spring on δ_{ij} calculations can be considered geometrically (Figure 6.14): $\theta \approx \tan\theta = \Delta/L = F/(kL)$. For example, the spring contribution for δ_{10} is calculated as

$$\delta_{10}^{\text{spring}} = \left(\theta_{10}^{R}\right)^{\text{spring}} = \frac{F}{kL} = \frac{P+qL}{2}\cdot\frac{L^2}{EI}. \tag{6.43}$$

Such geometrical approach is useful, but not necessary, when dealing with a support settlement.

Fixed-fixed end beam

For the next example, we consider a beam with homogeneous Dirichlet boundary conditions on both ends (Figure 6.15). The Figures 6.15(b),(c) are two different choices of primary structures. The compatibility condition for the first case (Figure 6.15(b)) reads

$$\begin{cases} \delta_{10} + R_B\delta_{11} + M_B\delta_{12} = 0 \\ \delta_{20} + R_B\delta_{21} + M_B\delta_{22} = 0 \end{cases}. \tag{6.44}$$

The corresponding displacements are

$$\delta_{10} = \frac{1}{EI}\frac{L}{4}\left(-\frac{qL^2}{2}\right)\cdot L = -\frac{qL^4}{8EI}, \tag{6.45}$$

$$\delta_{20} = \frac{1}{EI}\frac{L}{3}\left(-\frac{qL^2}{2}\right)\cdot 1 = -\frac{qL^3}{6EI}, \tag{6.46}$$

$$\delta_{11} = \frac{L^3}{3EI}, \tag{6.47}$$

$$\delta_{21} = \delta_{12} = \frac{L^2}{2EI}, \quad \text{and} \tag{6.48}$$

$$\delta_{22} = \frac{L}{EI}. \tag{6.49}$$

Then, we have

$$\frac{L}{EI}\begin{bmatrix} \frac{L^2}{3} & \frac{L}{2} \\ \frac{L}{2} & 1 \end{bmatrix}\begin{pmatrix} R_B \\ M_B \end{pmatrix} = \frac{qL^3}{EI}\begin{pmatrix} \frac{L}{8} \\ \frac{1}{6} \end{pmatrix} \tag{6.50}$$

or

$$R_B = \frac{qL}{2} \quad \text{and} \quad M_B = -\frac{qL^2}{12}. \tag{6.51}$$

On the other hand (Figure 6.15(c)), we have

$$\begin{cases} \delta_{10} + M_A\delta_{11} + M_B\delta_{12} = 0 \\ \delta_{20} + M_A\delta_{21} + M_B\delta_{22} = 0 \end{cases}. \tag{6.52}$$

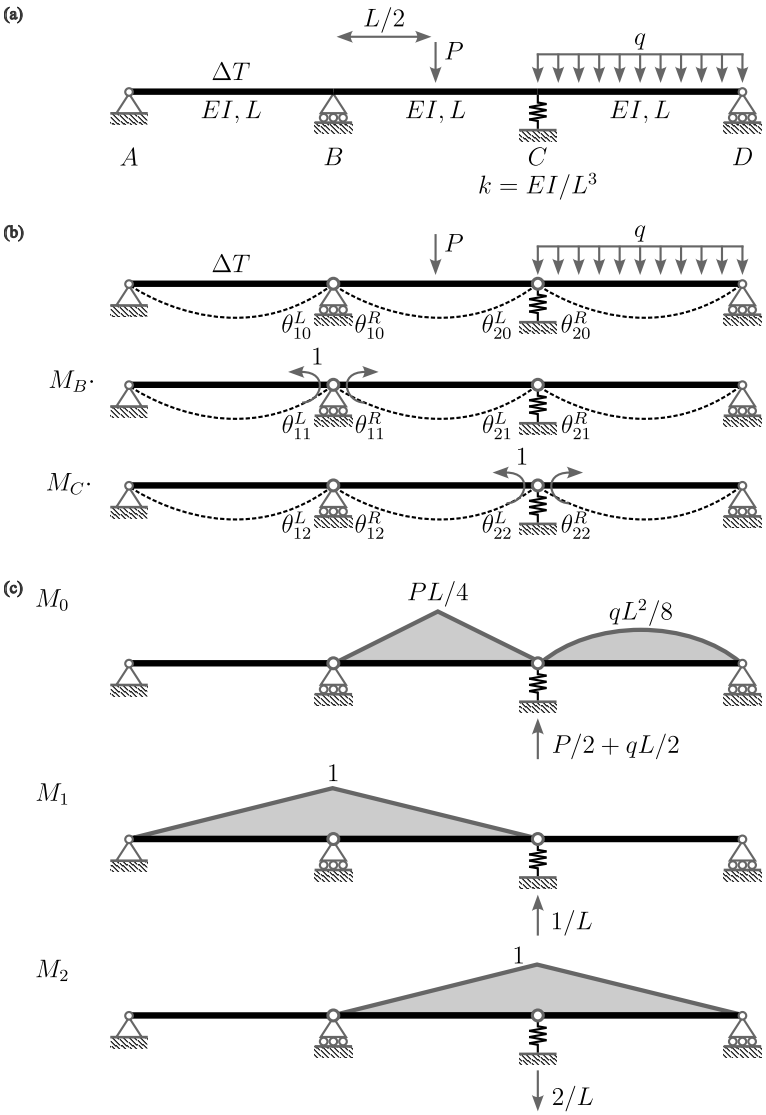

Figure 6.13: Three-span beam with various loads. (a) Structure and Loads. (b) Primary structures. (c) Corresponding bending moment diagrams, M_0, M_1, and M_2, and reaction forces at support C.

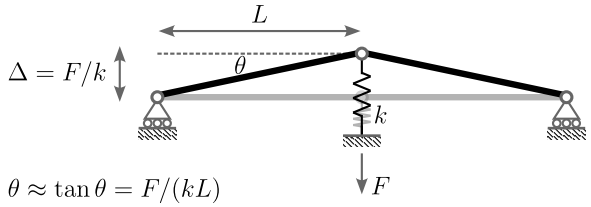

Figure 6.14: Geometrical representation of the slope due to a spring support.

The corresponding displacements are

$$\delta_{10} = \delta_{20} = \frac{qL^3}{24EI}, \tag{6.53}$$

$$\delta_{11} = \delta_{22} = \frac{L}{3EI}, \quad \text{and} \tag{6.54}$$

$$\delta_{21} = \delta_{12} = \frac{L}{6EI}. \tag{6.55}$$

Then, we have

$$\frac{L}{EI}\begin{bmatrix} \frac{1}{3} & \frac{1}{6} \\ \frac{1}{6} & \frac{1}{3} \end{bmatrix}\begin{pmatrix} R_B \\ M_B \end{pmatrix} = -\frac{qL^3}{24EI}\begin{pmatrix} 1 \\ 1 \end{pmatrix} \tag{6.56}$$

or

$$M_A = M_B = -\frac{qL^2}{12}. \tag{6.57}$$

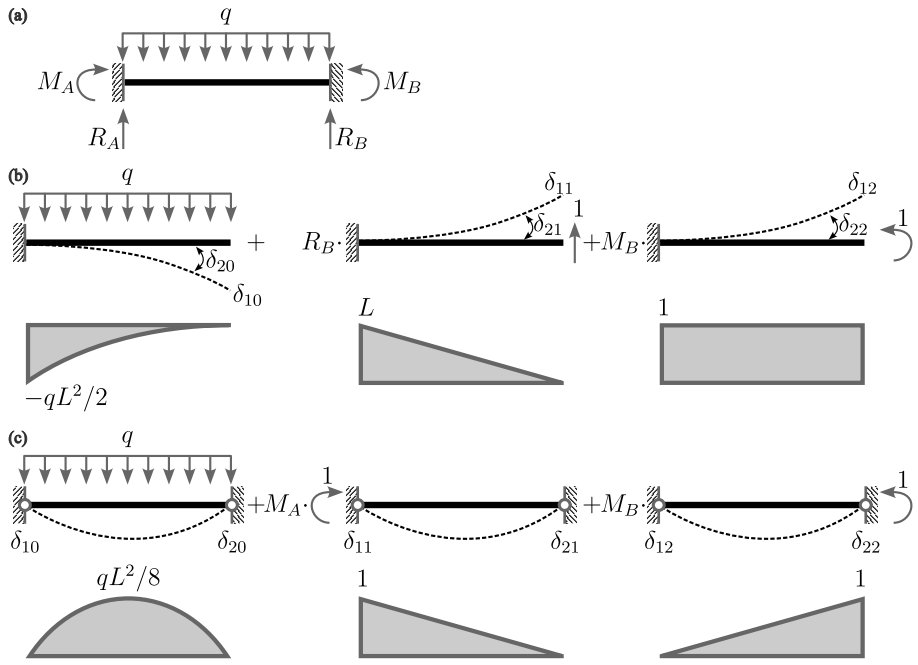

Figure 6.15: Fixed-fixed end beam. (a) Structure, loads, and reactions. (b) Primary structures and bending moment diagram. (c) Alternative primary structures and bending moment diagram.

6.2 Trusses

Previously for indeterminate beams, we identified extra unknowns externally on the boundary of the structure. For trusses, we consider both internally and

externally (and mixed) indeterminate trusses (Figure 6.16). Either externally or internally , the approach is the same with that of indeterminate beams; we determine primary structures and define/solve compatibility conditions.

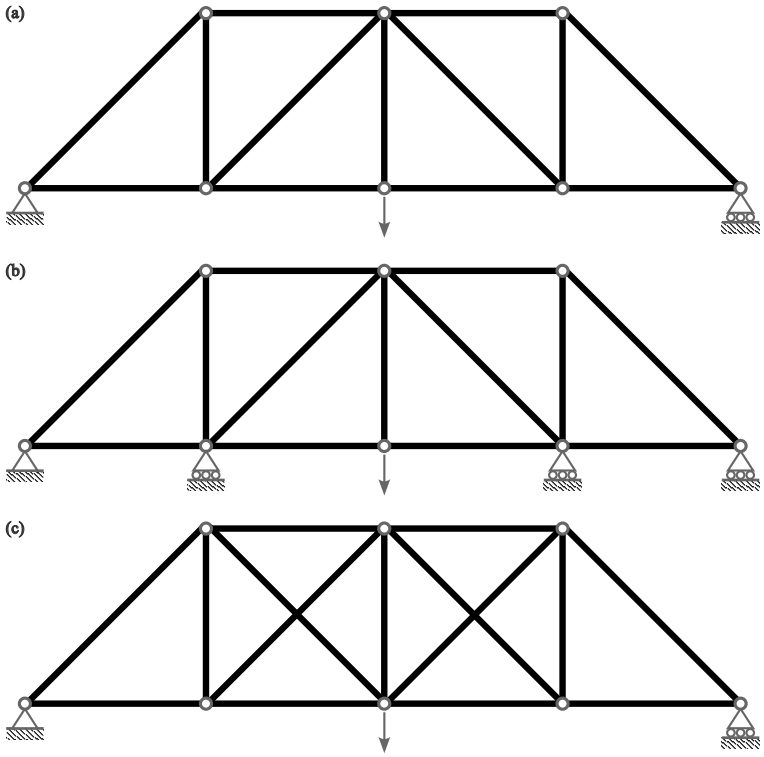

Figure 6.16: Determinate and indeterminate trusses. (a) Determinate truss. (b) Externally indeterminate truss. (c) Internally indeterminate truss.

6.2.1 Simple truss

Consider an indeterminate truss shown in Figure 6.17. When defining the primary structures, we can either release the constraint at support B or a diagonal member (5).

The compatibility condition of the first case reads

$$\delta_0 + R_B \delta_1 = 0. \tag{6.58}$$

Then, the two displacements can be computed via the principle of virtual work (Table 6.1), which gives $R_B = -(2 + 2\sqrt{2})P/(3 + 4\sqrt{2}) \approx -0.56P$. Using the

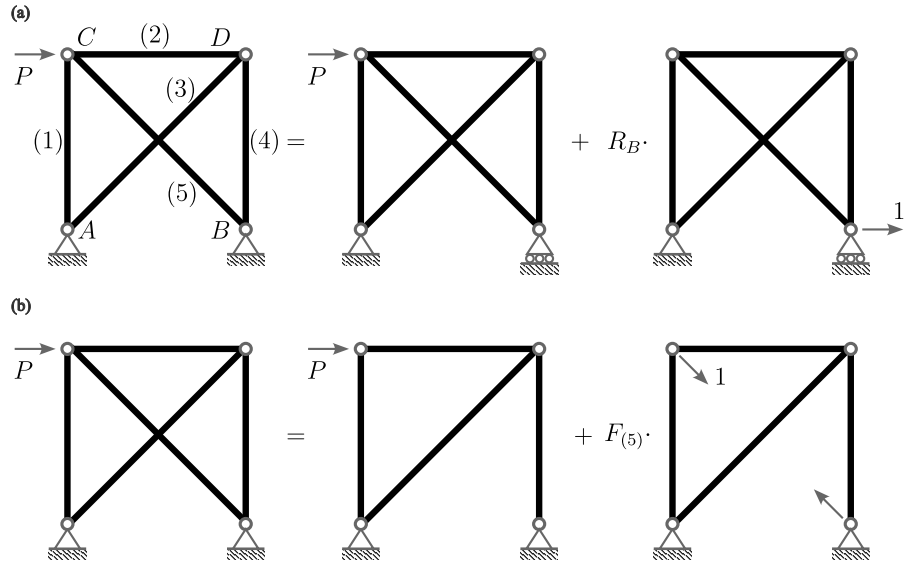

Figure 6.17: Simple truss. (a) Primary structures. (b) Alternative primary structures.

linear superposition, 1we can compute the final member forces as

$$F_{(1)} = F_0 + R_B F_1 = 0.57P, \tag{6.59}$$
$$F_{(2)} = -P + 0.56P = -0.44P, \tag{6.60}$$
$$F_{(3)} = \sqrt{2}P - 0.56\sqrt{2}P = 0.62P, \tag{6.61}$$
$$F_{(4)} = -P + 0.56P = -0.44P, \quad \text{and} \tag{6.62}$$
$$F_{(5)} = 0 - 0.56\sqrt{2}P = -0.79P. \tag{6.63}$$

Table 6.1: Table for the displacement calculation of a simple truss (Figure 6.17(a)).

Member	$L/(EA)$	F_0	F_1	$\delta_0 = \sum F_0 F_1 L/(EA)$	$\delta_1 = \sum F_1^2 L/(EA)$
(1)	1	0	-1	0	1
(2)	1	$-P$	-1	P	1
(3)	$\sqrt{2}$	$\sqrt{2}P$	$\sqrt{2}$	$2\sqrt{2}P$	$2\sqrt{2}$
(4)	1	$-P$	-1	P	1
(5)	$\sqrt{2}$	0	$\sqrt{2}$	0	$2\sqrt{2}$
$\sum$				$(2+2\sqrt{2})PL/(EA)$	$(3+4\sqrt{2})L/(EA)$

Alternatively, the compatibility condition of the second case reads

$$\delta_0 + F_{(5)}\left(\delta_1 + \frac{\sqrt{2}L}{EA}\right) = 0 \quad \text{or} \quad \delta_0 + F_{(5)}\delta_1 = -\frac{F_{(5)}\sqrt{2}L}{EA}. \tag{6.64}$$

The corresponding displacements are computed in Table 6.2. Then, we have $F_{(5)} = -(2 + 2/\sqrt{2})P/(3/2 + \sqrt{2} + \sqrt{2}) \approx -0.79P$ and

$$F_{(1)} = F_0 + F_{(5)}F_1 = 0.56P, \tag{6.65}$$

$$F_{(2)} = -P + 0.79P/\sqrt{2} = -0.44P, \tag{6.66}$$

$$F_{(3)} = \sqrt{2}P - 0.79P = 0.62P, \quad \text{and} \tag{6.67}$$

$$F_{(4)} = -P + 0.79P/\sqrt{2} = -0.44P. \tag{6.68}$$

Table 6.2: Table for the displacement calculation of a simple truss (Figure 6.17(b)).

Member	$L/(EA)$	F_0	F_1	$\delta_0 = \sum F_0F_1L/(EA)$	$\delta_1 = \sum F_1^2L/(EA)$
(1)	1	0	$-1/\sqrt{2}$	0	1/2
(2)	1	$-P$	$-1/\sqrt{2}$	$P/\sqrt{2}$	1/2
(3)	$\sqrt{2}$	$\sqrt{2}P$	1	$2P$	$\sqrt{2}$
(4)	1	$-P$	$-1/\sqrt{2}$	$P/\sqrt{2}$	1/2
$\sum$				$(2 + 2/\sqrt{2})PL/(EA)$	$(3/2 + \sqrt{2})L/(EA)$

6.2.2 Temperature change and fabrication error

A uniform temperature change $\Delta_T \equiv \alpha\Delta TL$ and a fabrication error Δ_E are treated in the same way we did for the support settlement.

Consider a mixed, i.e., internally and externally, indeterminate truss with a fabrication error Δ_E at member (10) (Figure 6.18). With the given choice of primary structures, we have the following compatibility condition:

$$\begin{cases} \delta_{10} + R_B\delta_{11} + F_{(10)}\delta_{12} = 0 \\ \delta_{20} + R_B\delta_{21} + F_{(10)}\delta_{22} = -F_{(10)}\frac{\sqrt{2}L}{EA} - \Delta_E \end{cases}. \tag{6.69}$$

The displacement computations are provided in Table 6.3, which gives

$$\frac{L}{EA}\begin{bmatrix} 3 & -1/\sqrt{2} \\ -1/\sqrt{2} & 2 + 2\sqrt{2} \end{bmatrix}\begin{pmatrix} R_B \\ F_{(10)} \end{pmatrix} = \begin{pmatrix} -5PL/(EA) \\ (2 + 5/\sqrt{2})PL/(EA) - \Delta_E \end{pmatrix}. \tag{6.70}$$

When $\Delta_E = PL/(EA)$, we have $R_B \approx -1.4969P$ and $F_{(10)} \approx 0.7201$.

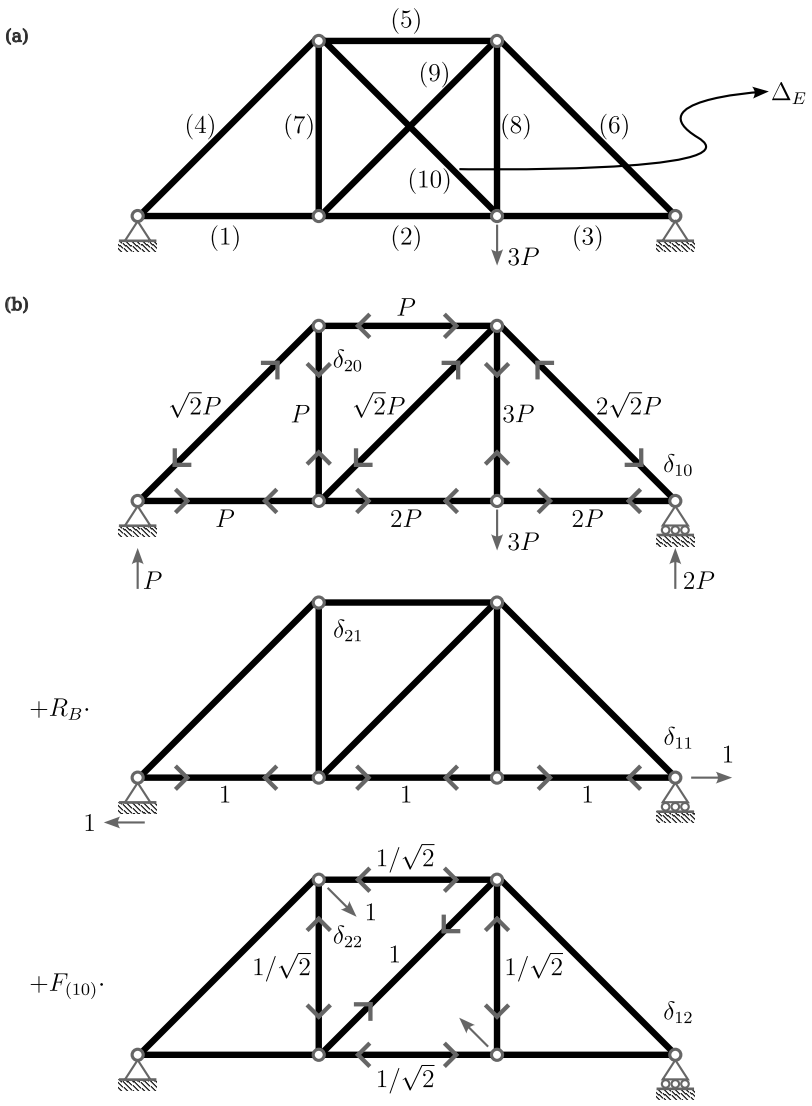

Figure 6.18: Mixed indeterminate truss with a fabrication error. (a) Structure and loads. (b) Primary structures.

Table 6.3: Table for the displacement calculation of a mixed indeterminate truss (Figure 6.18).

Member	$L/(EA)$	F_0	F_1	F_2	δ_{10}	δ_{20}	δ_{11}	$\delta_{21} = \delta_{12}$	δ_{22}
(1)	1	P	1	0	P	0	1	0	0
(2)	1	$2P$	1	$-1/\sqrt{2}$	$2P$	$-2P/\sqrt{2}$	1	$-1/\sqrt{2}$	$1/2$
(3)	1	$3P$	1	0	$2P$	0	1	0	0
(4)	$\sqrt{2}$	$-\sqrt{2}P$	0	0	0	0	0	0	0
(5)	1	$-P$	0	$-1/\sqrt{2}$	0	$P/\sqrt{2}$	0	0	$1/2$
(6)	$\sqrt{2}$	$-2\sqrt{2}P$	0	0	0	0	0	0	0
(7)	1	P	0	$-1/\sqrt{2}$	0	$-P/\sqrt{2}$	0	0	$1/2$
(8)	1	$3P$	0	$-1/\sqrt{2}$	0	$-3P/\sqrt{2}$	0	0	$1/2$
(9)	$\sqrt{2}$	$-\sqrt{2}P$	0	1	0	$-2P$	0	0	$\sqrt{2}$
$\sum$					$5P$	$-(2+5/\sqrt{2})P$	3	$-1/\sqrt{2}$	$2+\sqrt{2}$

6.3 Frames

Analyzing indeterminate frames is not so much different than other type of structures. Simple examples will be presented without detailed explanations, as the underlying theory has already been covered.

6.3.1 Gamma frame

Figure 6.19 shows an indeterminate Gamma-shaped frame with two choices of primary structures. The compatibility equation for the first case is

$$\delta_0 + R_B \delta_1 = 0, \tag{6.71}$$

where δ's are the vertical displacements at node B. For the second case, we have

$$\delta_0 + M_C \delta_1 = 0. \tag{6.72}$$

Here, δ's are the slope discontinuities, i.e., $\theta_L + \theta_R$ (consistent with their respective directions), at node C. Then, we have $M_A = -3PL/64$, $R_A = 35P/64$, and $R_B = 29P/64$, omitting the computation details.

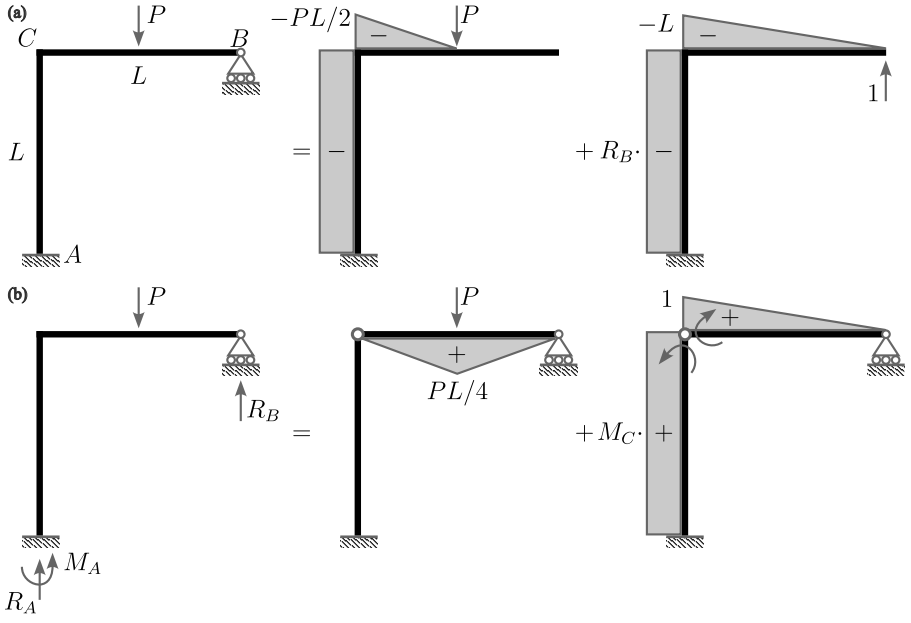

Figure 6.19: Gamma frame. (a) Primary structures and (b) their alternatives with bending moment diagrams.

6.3.2 Portal frame

Next, consider a portal frame with a vertical point load (Figure 6.20). Note that the structure is geometrically symmetric but with an eccentric load. The

corresponding compatibility condition implies the slope continuity at all nodes, i.e.,

$$\begin{cases} \delta_{10} + M_B\delta_{11} + M_C\delta_{12} + M_D\delta_{13} = 0 \\ \delta_{20} + M_B\delta_{21} + M_C\delta_{22} + M_D\delta_{23} = 0 \\ \delta_{30} + M_B\delta_{31} + M_C\delta_{32} + M_D\delta_{33} = 0 \end{cases} \tag{6.73}$$

or

$$\frac{L}{EI}\begin{bmatrix} 4/3 & -1/3 & 1/2 \\ & 1 & -1/6 \\ \text{sym.} & & 2/3 \end{bmatrix}\begin{pmatrix} M_B \\ M_C \\ M_D \end{pmatrix} = -\frac{L}{EI}\frac{Pab}{6L^2}\begin{pmatrix} a+2b \\ 2a+b \\ 0 \end{pmatrix}. \tag{6.74}$$

Then, the bending moments are obtained as

$$\begin{pmatrix} M_B \\ M_C \\ M_D \end{pmatrix} = -\frac{Pab}{42L^2}\begin{pmatrix} 11a+17b \\ 17a+11b \\ -4a-10b \end{pmatrix}. \tag{6.75}$$

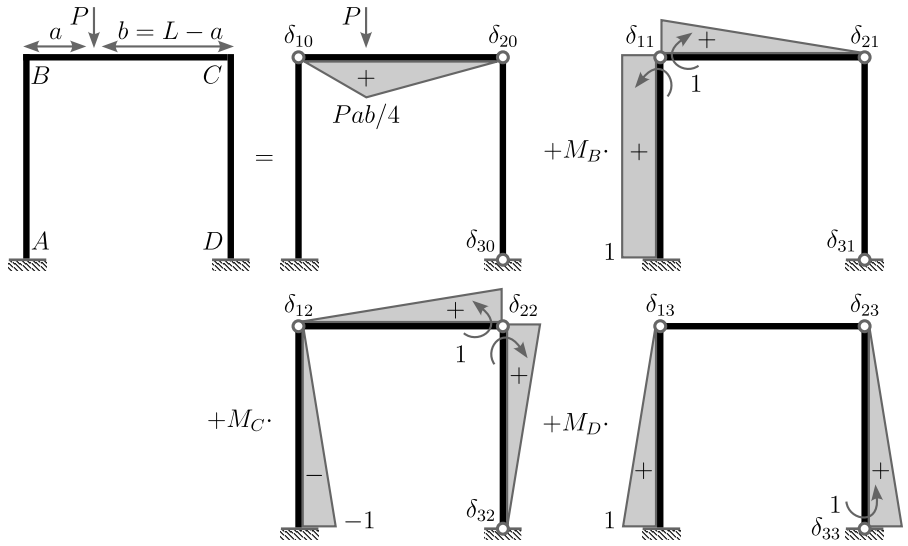

Figure 6.20: Portal frame and its primary structures and bending moment diagrams.

Figure 6.21 demonstrates the deflected shapes of two cases: symmetric and asymmetric loads. Notice that the horizontal member displaces horizontally even when the load is applied vertically. The amount of sidesway is $\Delta = Pab(b-a)/(28EI)$, which vanishes when the system is symmetric, i.e., $a = b$.

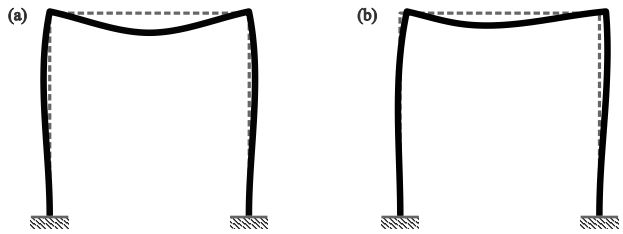

Figure 6.21: Deflected shape of a portal frame. (a) Case $a = b = L/2$; $\Delta = 0$. (b) Case $a = L/4$; a sidesway of $\Delta = Pab(b-a)/(28EI)$ is observed when the system is not symmetric.

6.4 Order of indeterminacy

Before concluding this section, let us rigorously review the concept of the order of indeterminacy. The order of indeterminacy is defined as the difference between the number of unknowns and the number of equations. Specifically, we have

$$\begin{aligned}(\#\text{ of unknowns}) = &(\#\text{ of members}) \times (\#\text{ of internal force per member}) \\ &+ (\#\text{ of reactions}) - (\#\text{ of known quantities}), \qquad (6.76)\\ (\#\text{ of equations}) = &(\#\text{ of members}) \times (\#\text{ of equilibrium equations per member}) \\ &+ (\#\text{ of joints}) \times (\#\text{ of equilibrium equations per joint}) \\ &- (\#\text{ of used equations}). \qquad (6.77)\end{aligned}$$

The member-wise number of internal forces and equilibrium equations for different element types are summarized in Table 6.4.

Table 6.4: Number of internal forces and equilibrium equations (EE).

Element type	# of internal forces	# of EE per element	# of EE per joint
Beam*	4 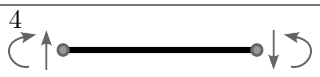	2 $\sum F_x, \sum M$	2 $\sum F_x, \sum M$
Truss	1 	0 (no load within a member)	2 $\sum F_x, \sum F_y$
Frame*	6 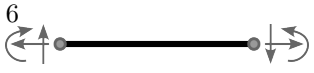	3 $\sum F_x, \sum F_y, \sum M$	3 $\sum F_x, \sum F_y, \sum M$

*When replacing a rigid joint with a hinge, the number of unknowns decreases by the number of members at the joint, and the number of equations decreases by one.

Examples of calculating the order of indeterminacy are compiled in Figures 6.22, 6.23, and 6.24. Note that replacing a rigid joint with a hinge reduces both unknowns (by the number of members at the joint) and equations (by one). Thus, in general, the compatibility condition at the joint reads (Figure 6.25)

$$\delta_1 = \delta_2 = \ldots = \delta_N, \qquad (6.78)$$

which gives $N-1$ equations, and an additional equilibrium equation

$$M_1 + M_2 + \ldots + M_N = 0. \tag{6.79}$$

In the above, the moments M_j and the associated δ_{ij} are oriented identically, and the δ_i are calculated by

$$\delta_i = \delta_{i0} + \sum_{j=1}^{N} M_j \delta_{ij} + \sum_{j=N+1}^{K} X_j \delta_{ij}, \quad i = 1, 2, \ldots, N, \tag{6.80}$$

where, N is the number of members at joint i and K is the order of indeterminacy. In (6.80), the first summation is the contribution from the primary structures associated with the releases at joint i and the second summation is the contribution from the rest of the primary structures.

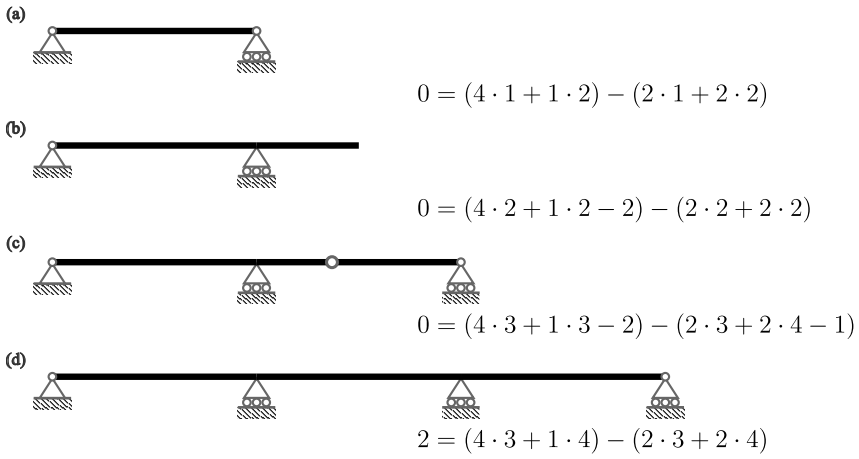

Figure 6.22: Order of indeterminacy calculations for beams. (a) Simple beam. (b) Overhanged beam. (c) Gerber beam. (d) Continuous beam.

Consider the following example of a general frame (Figure 6.26). The order of indeterminancy is calculated as

$$2 = \underbrace{6 \times 3 + 5}_{\text{number of unknowns}} - \underbrace{(3 \times 3 + 3 \times 4)}_{\text{number of equations}}. \tag{6.81}$$

Placing a hinge at the center reduces the order of indeterminancy by two, which gives a determinate structure. The corresponding compatibility condition and the additional equilibrium equation are

$$\delta_1 = \delta_2 = \delta_3 \quad \text{and} \tag{6.82}$$

$$M_1 + M_2 + M_3 = 0. \tag{6.83}$$

In the above, the slopes are defined as

$$\delta_1 = \delta_{10} + \delta_{11} M_1 + \delta_{12} M_2 + \delta_{13} M_3, \tag{6.84}$$

$$\delta_2 = \delta_{20} + \delta_{21} M_1 + \delta_{22} M_2 + \delta_{23} M_3, \quad \text{and} \tag{6.85}$$

$$\delta_3 = \delta_{30} + \delta_{31} M_1 + \delta_{32} M_2 + \delta_{33} M_3, \tag{6.86}$$

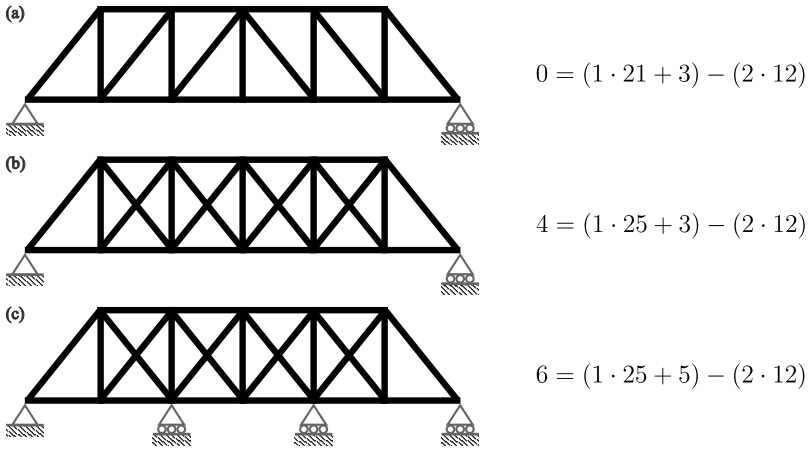

Figure 6.23: Order of indeterminacy calculations for trusses. (a) Determinate truss. (b) Internally indeterminate truss. (c) Internally and externally indeterminate truss.

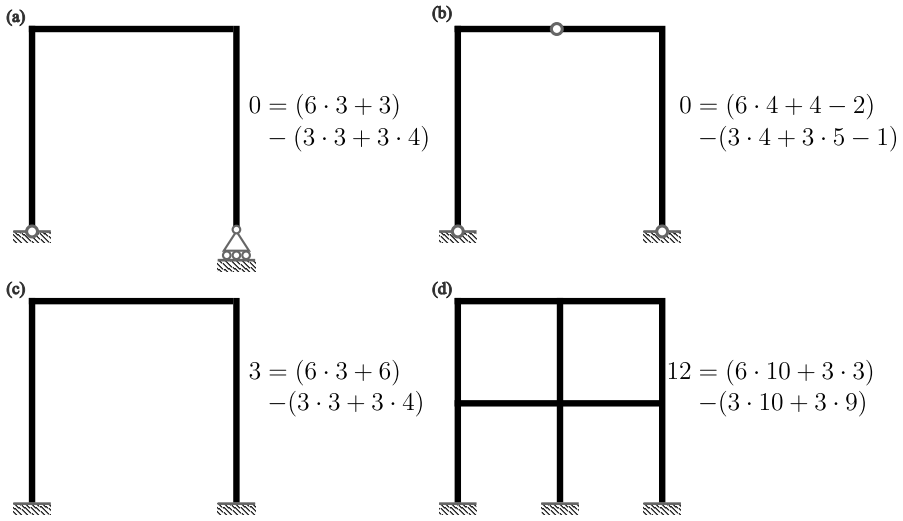

Figure 6.24: Order of indeterminacy calculations for frames. (a) Determinate frame. (b) Frame with a hinge. (c) Portal frame with fixed supports. (d) Complex frame.

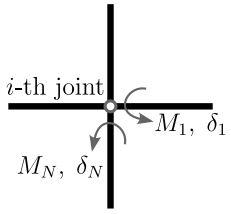

Figure 6.25: General joint compatibility with N members. When M_j, and therefore δ_j, are oriented identically, we have $\delta_1 = \delta_2 = \ldots = \delta_N$ and $M_1 + M_2 + \ldots + M_N = 0$ forming N equations in total.

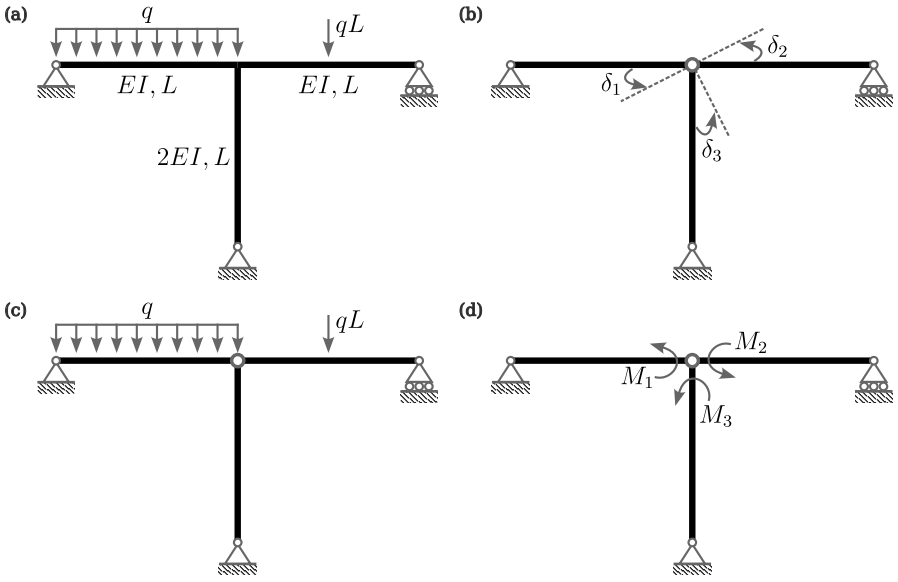

Figure 6.26: General frame. (a) Original structure. (b) Definitions of δ_1, δ_2, and δ_3. (c),(d) Primary structures; M_1, M_2, M_3 are individually applied.

where (Figure 6.27)

$$\delta_{10} = \int_0^L \frac{M_0 M_1}{EI} dx = \frac{qL^3}{24EI}, \tag{6.87}$$

$$\delta_{20} = \int_0^L \frac{M_0 M_2}{EI} dx = -\frac{qL^3}{16EI}, \tag{6.88}$$

$$\delta_{30} = \int_0^L \frac{M_0 M_3}{EI} dx = 0, \tag{6.89}$$

$$\delta_{11} = \int_0^L \frac{M_1 M_1}{EI} dx = \frac{L}{3EI}, \tag{6.90}$$

$$\delta_{22} = \int_0^L \frac{M_2 M_2}{EI} dx = \frac{L}{3EI}, \tag{6.91}$$

$$\delta_{33} = \int_0^L \frac{M_3 M_3}{2EI} dx = \frac{L}{6EI}, \tag{6.92}$$

$$\delta_{12} = \delta_{21} = 0, \tag{6.93}$$

$$\delta_{13} = \delta_{31} = 0, \quad \text{and} \tag{6.94}$$

$$\delta_{23} = \delta_{32} = 0. \tag{6.95}$$

Let $M_3 = -M_1 - M_2$, we have

$$\frac{L}{6EI} \begin{bmatrix} 3 & 1 \\ 1 & 3 \end{bmatrix} \begin{pmatrix} M_1 \\ M_2 \end{pmatrix} = \frac{qL^3}{48EI} \begin{pmatrix} -2 \\ 3 \end{pmatrix}, \tag{6.96}$$

which gives

$$M_1 = -\frac{9qL^2}{64},\ M_2 = \frac{11qL^2}{64},\ \text{and}\ M_3 = -\frac{2qL^2}{64}. \tag{6.97}$$

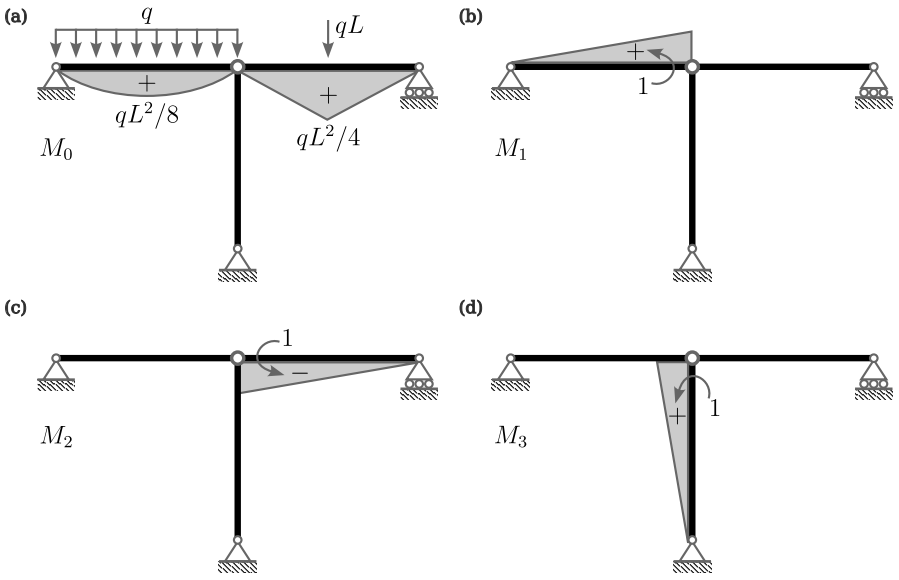

Figure 6.27: General frame. (a) Original structure. (b),(c) Primary structures; M_1, M_2, M_3 are individually applied.

Chapter 7

Influence Lines

7.1 Determinate structures

Influence line is a response function of interest with respect to an arbitrary location of a concentrated load, e.g., a bending moment of a beam at x_o due to a vertical load at an arbitrary location x. Influence line provides a graphical information on how the structure behaves under a continuous change in loading condition, which is useful for finding the maximum response case. Additionally, when an expression for arbitrary x and x_o are given, it provides a general solution method as an operator, thus becomes a *Green's function*.

To understand a Green's function as a general solution method, consider an example of a simple beam under an arbitrary distributed load $q(x)$ (Figure 7.1):

$$\begin{cases} \dfrac{d^2}{dx^2}\left(EI\dfrac{d^2w}{dx^2}\right) = q, \quad x \in (0,L) \\ w|_{x=0} = w|_{x=L} = EI\dfrac{d^2w}{dx^2}\Big|_{x=0} = EI\dfrac{d^2w}{dx^2}\Big|_{x=L} = 0. \end{cases} . \tag{7.1}$$

Next, we multiply by a test function $\overline{w}$ and integrate over a domain; then, perform integration by parts for four times.

$$\begin{aligned} 0 &= \int_0^L \left[\frac{d^2}{dx^2}\left(EI\frac{d^2w}{dx^2}\right) - q\right]\overline{w}dx \\ &= \left[\frac{d}{dx}\left(EI\frac{d^2w}{dx^2}\right)\overline{w}\right]_{x=0}^{x=L} - \left[EI\frac{d^2w}{dx^2}\frac{d\overline{w}}{dx}\right]_{x=0}^{x=L} + \int_0^L \frac{d^2w}{dx^2}EI\frac{d^2\overline{w}}{dx^2}dx - \int_0^L q\overline{w}dx \\ &= \left[\frac{d}{dx}\left(EI\frac{d^2w}{dx^2}\right)\overline{w}\right]_{x=0}^{x=L} - \left[EI\frac{d^2w}{dx^2}\frac{d\overline{w}}{dx}\right]_{x=0}^{x=L} \\ &\quad + \left[\frac{dw}{dx}EI\frac{d^2\overline{w}}{dx^2}\right]_{x=0}^{x=L} - \left[w\frac{d}{dx}\left(EI\frac{d^2\overline{w}}{dx^2}\right)\right]_{x=0}^{x=L} \\ &\quad + \int_0^L w\frac{d^2}{dx^2}\left(EI\frac{d^2\overline{w}}{dx^2}\right)dx - \int_0^L q\overline{w}dx. \end{aligned} \tag{7.2}$$

Now, let us choose $\overline{w}$ such that

$$\begin{cases} \dfrac{d^2}{dx^2}\left(EI\dfrac{d^2\overline{w}}{dx^2}\right) = \delta\left(x - x_o\right), \quad x \in (0, L),\ x_o \in (0, L) \\ \overline{w}|_{x=0} = \overline{w}|_{x=L} = EI\dfrac{d^2\overline{w}}{dx^2}\Big|_{x=0} = EI\dfrac{d^2\overline{w}}{dx^2}\Big|_{x=L} = 0. \end{cases} . \tag{7.3}$$

Then, all boundary terms in (7.2) vanish. Denoting such $\overline{w}$ as $G\left(x; x_o\right)$, we have

$$\begin{aligned} 0 &= \int_0^L w\left(x\right)\delta\left(x - x_o\right)dx - \int_0^L q\left(x\right)G\left(x; x_o\right)dx \\ &\Rightarrow w\left(x_o\right) = \int_0^L q\left(x\right)G\left(x; x_o\right)dx. \end{aligned} \tag{7.4}$$

In this example, the Green's function $G\left(x; x_o\right)$ is the deflection at x for an arbitrary load located at x_o. On the other hand, as a generalized function, the Green's function is an operator that gives a deflection at a point $x = x_o$ for an arbitrary load $q(x)$.

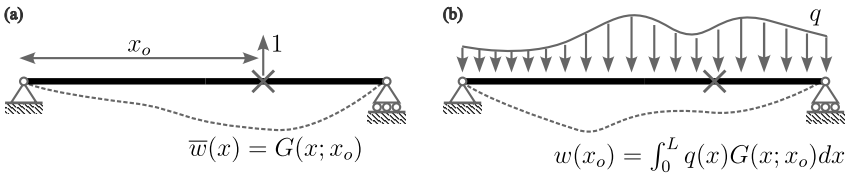

Figure 7.1: Computing deflection using a Green's function. (a) $\overline{w}$ system. (b) w system.

As previously mentioned, an influence line is interested in a certain quantity at a specific location under an arbitrarily positioned unit load. Thus, it can be computed directly from freebody diagrams for a determinate structure.

7.1.1 Simple beam

For example, let us assume that we are interested in the bending moment at the mid-span of a simple beam under an arbitrarily located point load. We can easily compute the influence line using the free-body diagram (Figure 7.2). In this case, the influence line I_M reads

$$I_M = \begin{cases} x/2 & 0 < x \leq L/2 \\ (L - x)/2 & L/2 < x < L \end{cases} . \tag{7.5}$$

Clearly, the bending moment is at its maximum when $x = L/2$.

We can find the maximum moment for more complex loading cases using the linear superposition. Consider an alternative loading case with two point loads $P/2$ and P with a distance between of $L/10$; thus, when we denote the location of $P/2$ as ξ, we have an external load as $(P/2)\delta\left(x - \xi\right) + P\delta\left(x - \xi - \frac{L}{10}\right)$ (Figure 7.3). Then, the moment at x_o is calculated as

$$M\left(x_o\right) = \int_0^L \left[\frac{P}{2}\delta\left(x - \xi\right) + P\delta\left(x - \xi - \frac{L}{10}\right)\right] I_M\left(x\right)dx. \tag{7.6}$$

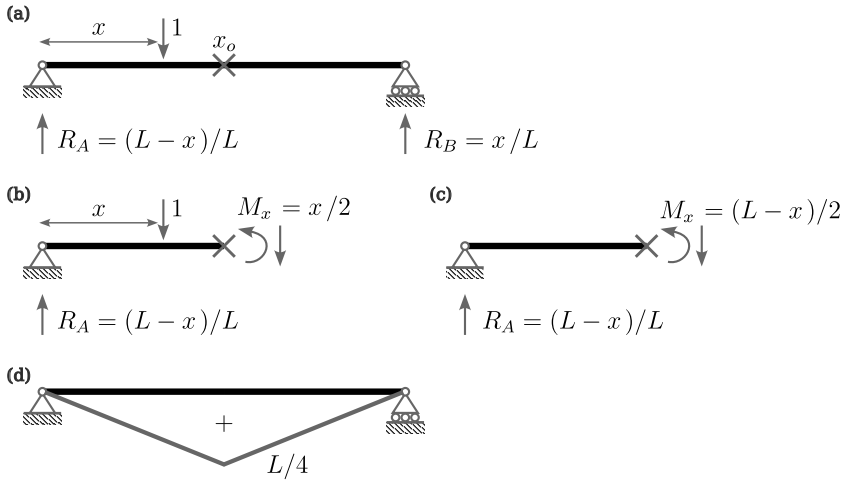

Figure 7.2: Influence line for the bending moment at mid-span. (a) Simple beam with a point load. (b) Freebody diagrams for $0 < x \leq L/2$ and (c) for $L/2 < x < L$. (d) Influence line.

Specifically, we have

$$\begin{cases} M(x_o) = P\frac{1}{2}\left(\xi + \frac{L}{10}\right) \Rightarrow M_{\max}(x_o) = \frac{PL}{20} \text{ at } \xi = 0, & -\frac{L}{10} < \xi \leq 0 \\ M(x_o) = \frac{P}{2}\frac{\xi}{2} + P\frac{1}{2}\left(\xi + \frac{L}{10}\right) \Rightarrow M_{\max}(x_o) = \frac{7PL}{20} \text{ at } \xi = \frac{4L}{10}, & 0 < \xi \leq \frac{4L}{10} \\ M(x_o) = \frac{P}{2}\frac{\xi}{2} + P\left[\frac{L}{2} - \frac{1}{2}\left(\xi + \frac{L}{10}\right)\right] \Rightarrow M_{\max}(x_o) = \frac{7PL}{20} \text{ at } \xi = \frac{4L}{10}, & \frac{4L}{10} < \xi \leq \frac{5L}{10} \\ M(x_o) = \frac{P}{2}\left(\frac{L}{2} - \frac{\xi}{2}\right) + P\left[\frac{L}{2} - \frac{1}{2}\left(\xi + \frac{L}{10}\right)\right] \Rightarrow M_{\max}(x_o) = \frac{13PL}{40} \text{ at } \xi = \frac{5L}{10}, & \frac{5L}{10} < \xi < \frac{9L}{10} \end{cases} \tag{7.7}$$

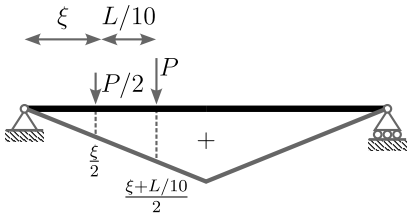

Figure 7.3: Finding the locations of two moving loads maximizing bending moment using an influence line.

On the other hand, if we are interested in the shear force, we can similarly derive the influence line using the freebody diagram (Figure 7.4):

$$I_V = \begin{cases} -x/2 & 0 < x \leq L/2 \\ (L - x)/L & L/2 < x < L \end{cases} . \tag{7.8}$$

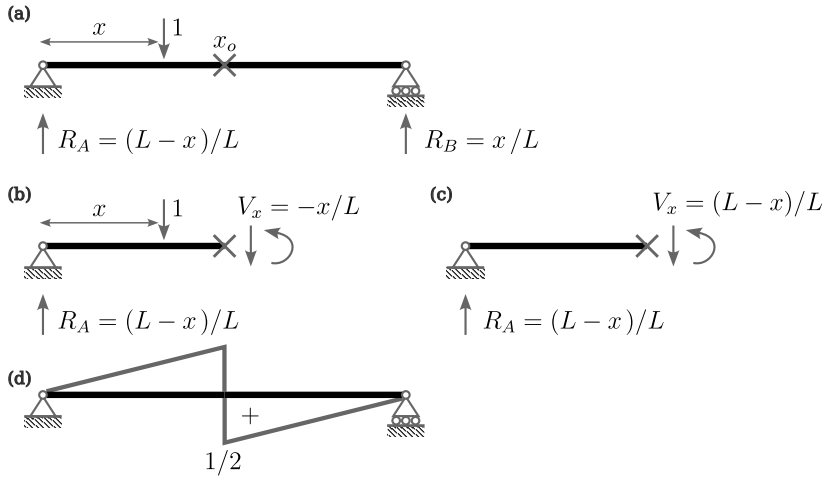

Figure 7.4: Influence line for the shear force at mid-span. (a) Simple beam with a point load. (b) Freebody diagrams for $0 < x \leq L/2$ and (c) for $L/2 < x < L$. (d) Influence line.

7.1.2 Gerber beam

Two examples for a Gerber beam are provided: the shear force at $x_o = L/2$ (Figure 7.5) and the bending moment at a support (Figure 7.6).

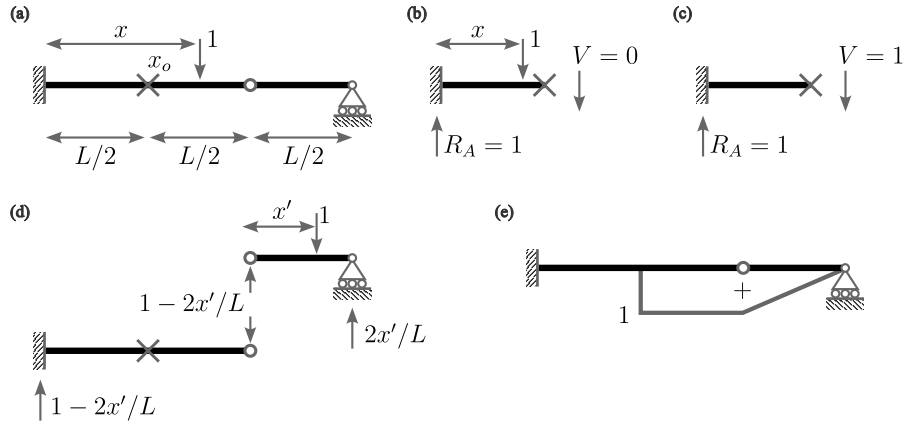

Figure 7.5: Influence line for the shear force at $x_o = L/2$. (a) Gerber beam with a point load. (b) Freebody diagrams for $0 < x \leq L/2$, (c) for $L/2 < x < L$, and (d) for $L < x \leq 3L/2$. (e) Influence line.

With a given influence line in Figure 7.6, we can compute the bending moment at the support for a general loading condition by linear superposition. In Figure 7.7, we consider a distributed load with an arbitrary location, where the bending moment is obtained by an integral of the influence line over the domain of the distributed load.

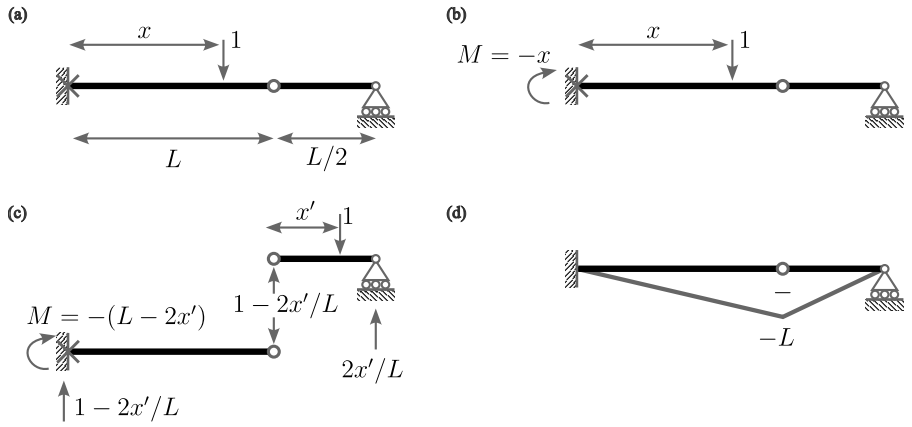

Figure 7.6: Influence line for the bending moment at $x_o = 0$. (a) Gerber beam with a point load. (b) Freebody diagrams for $0 < x \leq L$ and (c) for $L < x < 3L/2$. (d) Influence line.

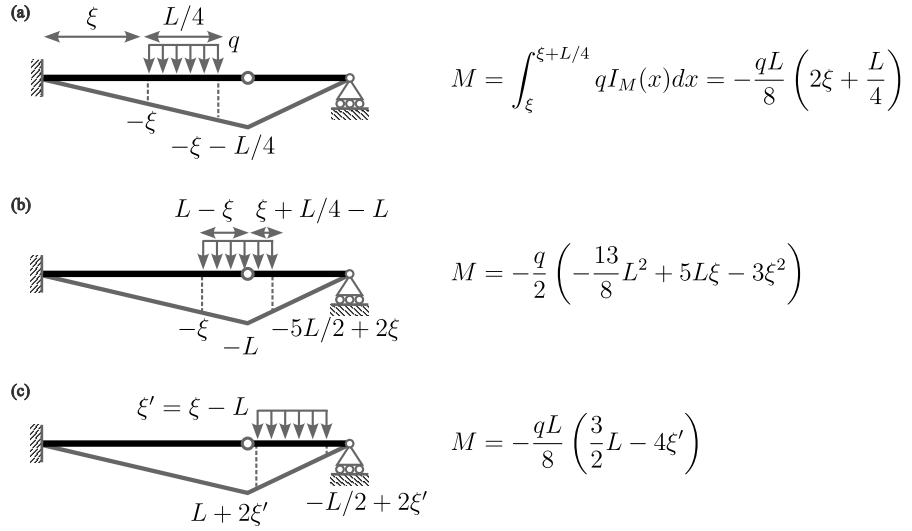

$$M = \int_{\xi}^{\xi+L/4} qI_M(x)dx = -\frac{qL}{8}\left(2\xi + \frac{L}{4}\right)$$

$$M = -\frac{q}{2}\left(-\frac{13}{8}L^2 + 5L\xi - 3\xi^2\right)$$

$$M = -\frac{qL}{8}\left(\frac{3}{2}L - 4\xi'\right)$$

Figure 7.7: Bending moment under a distributed load obtained by an influence line. (a) $0 < \xi \leq 3L/4$. (b) $3L/4 < \xi \leq L$. (c) $L < \xi < 5L/4$.

7.1.3 Indirect load

Here, we are interested in finding an influence line for a bending moment at the center of a beam with a point load indirectly applied: a small simple beam on top of a larger simple beam (Figure 7.8(a)). Figure 7.8(b) is the statically equivalent system, where we can reuse the influence line previously derived (7.5).

$$I_M = \int_0^L \left[\frac{L_o - x}{L_o} \delta\left(\xi - \frac{L - L_o}{2}\right) + \frac{x}{L_o} \delta\left(\xi - \frac{L + L_o}{2}\right) \right] I_M(\xi)\, d\xi \tag{7.9}$$

$$= \frac{L_o - x}{L_o} \frac{L/2 - L_o/2}{2} + \frac{x}{L_o} \frac{L - (L/2 + L_o/2)}{2}$$

$$= \frac{L - L_o}{4}. \tag{7.10}$$

Figure 7.8(c) illustrates the corresponding influence line.

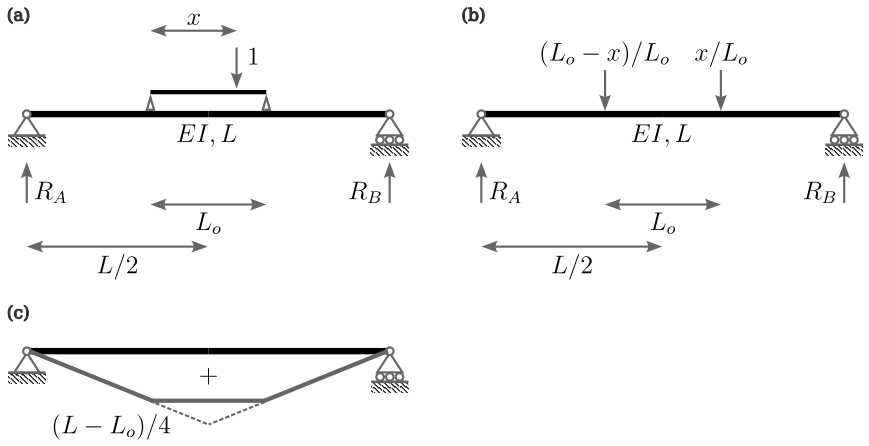

Figure 7.8: Indirect load. (a) Original structure with an indirect load. (b) Statically equivalent system. (c) Influence line.

7.1.4 Truss

Next, consider a truss with an indirect load (Figure 7.9). The reaction forces at the left and right supports are $1 - x/(6L)$ and $x/(6L)$, respectively, where x is the location of the point load.

First, we compute an influence line for the axial force at the diagonal member connecting joint A and B. When x is between 0 and L (Figure 7.9(b)), the method of sections gives

$$0 = \sum F_y = -\frac{\sqrt{2}}{2} F_{AB} + \left(1 - \frac{x}{6L}\right) - 1 \Rightarrow F_{AB} = -\sqrt{2}\frac{x}{6L}. \tag{7.11}$$

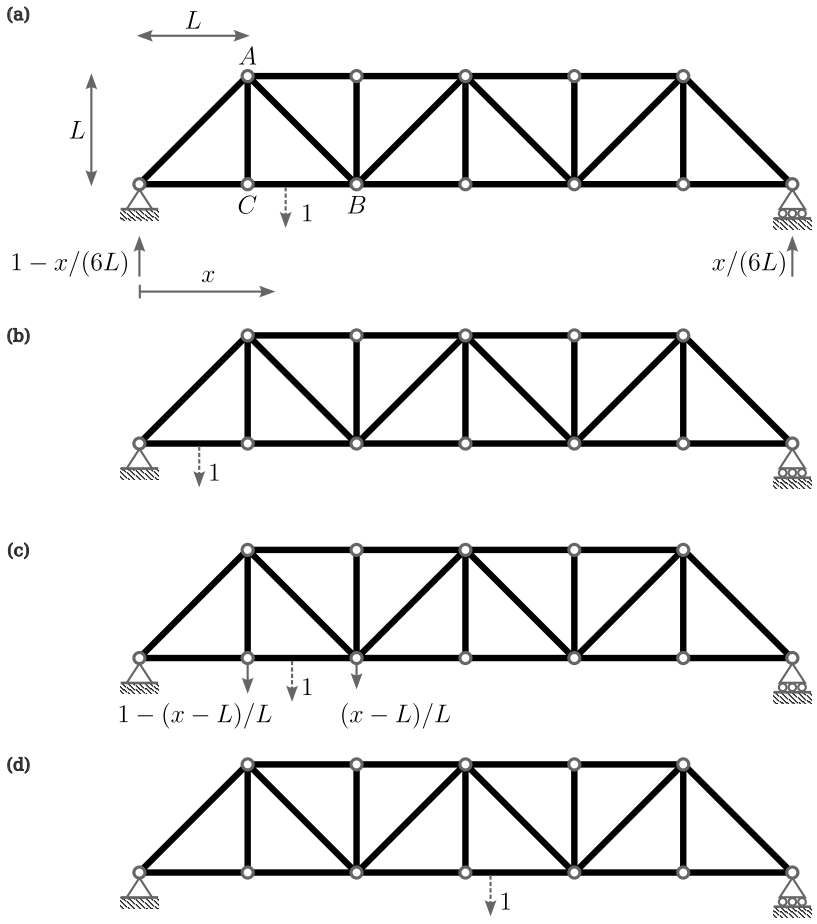

Figure 7.9: Truss with an indirect load. (a) Structure. (b) $0 < x < L$. (c) $L < x < 2L$. (d) $2L < x < 6L$.

For $L < x < 2L$ (Figure 7.9(c)), we have

$$0 = \sum F_y = -\frac{\sqrt{2}}{2} F_{AB} + \left(1 - \frac{x}{6L}\right) - \left(1 - \frac{x-L}{L}\right)$$
$$\Rightarrow F_{AB} = -\sqrt{2}\left(1 - \frac{5x}{6L}\right). \tag{7.12}$$

Finally, for $2L < x < 6L$ (Figure 7.9(c)), we have

$$0 = \sum F_y = -\frac{\sqrt{2}}{2} F_{AB} + \left(1 - \frac{x}{6L}\right) \Rightarrow F_{AB} = \sqrt{2}\left(1 - \frac{x}{6L}\right). \tag{7.13}$$

Second, we repeat the calculations for the bottom member connecting joint C and B. We divide the domain into two sections and evaluate the moment equilibrium about joint A., i.e.,

$$0 = \sum M_A = L \cdot \left(1 - \frac{x}{6L}\right) - (L - x) \cdot 1 - L \cdot F_{CB}$$
$$\Rightarrow F_{CB} = \frac{5x}{6L}, \quad 0 < x < L \quad \text{and} \tag{7.14}$$
$$0 = \sum M_A = L \cdot \left(1 - \frac{x}{6L}\right) - L \cdot F_{CB}$$
$$\Rightarrow F_{CB} = 1 - \frac{x}{6L}, \quad L < x < 6L. \tag{7.15}$$

The corresponding influence lines for the above two cases are sketched in Figure **??**.

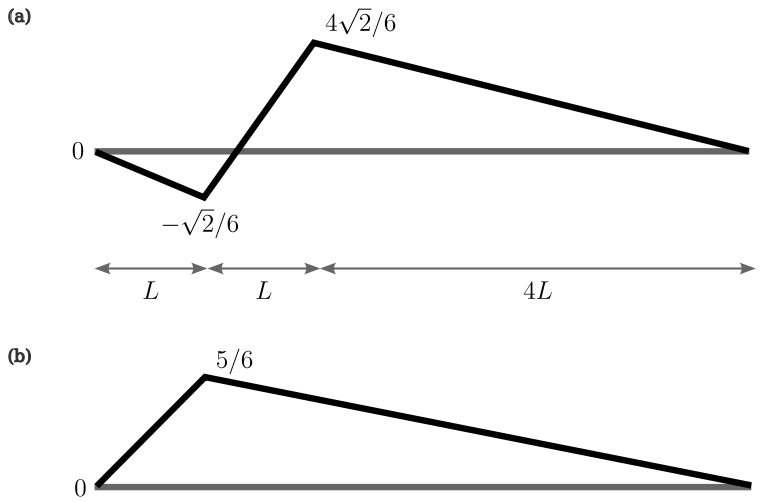

Figure 7.10: Influence line. (a) Member AB. (b) Member CB.

7.2 Müller-Breslau's principle

Müller-Breslau's principle provides an elegant method for estimating influence lines, which is applicable to any type of structure such as beam, truss, and

frame whether statically determinate or indeterminate. The principle is stated as [Utku et al., 1991]:

"The ordinates of the influence line for any stress element (such as axial force, shear, moment, or reaction) of any structure are proportional to those of the deflection curve which is obtained by removing the restraint corresponding to that element from the structure and introducing in its place a corresponding deformation into the primary structure which remains".

Let us revisit the simple beam examples for demonstrations. First, consider an influence line for moment at the middle of a simple beam. Figure 7.11(a) shows the load case in consideration, i.e., a point load at an arbitrary location x with a moment at x_o after releasing the corresponding restraint. On the other hand, we have an alternative load case (Figure 7.11(b)) with a moment at x_o. The Müller-Breslau's principle implies that the influence line (M_1) is proportional with the displacement Δ_2: the solid triangular line in Figure 7.11(b) which is identical with Figure 7.2(d). Such relation is due to the reciprocity, which reads

$$\int_0^L q_1 w_2 d\xi - [V_1 w_2]_{\xi=0}^{\xi=L} + [M_1 \theta_2]_{\xi=0}^{\xi=L} = \int_0^L q_2 w_1 d\xi - [V_2 w_1]_0^{\xi=L} + [M_2 \theta_1]_{\xi=0}^{\xi=L}. \tag{7.16}$$

In this example, we have

$$\int_0^L q_1 w_2 d\xi = \int_0^L -P\delta(\xi - x)\, w_2(\xi)\, d\xi = -P\Delta_2, \tag{7.17}$$

$$[V_1 w_2]_{\xi=0}^{\xi=x_o} + [V_1 w_2]_{\xi=x_o}^{\xi=L} = 0, \tag{7.18}$$

$$[M_1 \theta_2]_{\xi=0}^{\xi=x_o} + [M_1 \theta_2]_{\xi=x_o}^{\xi=L} = M_1\left(\theta_2^L + \theta_2^R\right), \tag{7.19}$$

$$\int_0^L q_2 w_1 d\xi = 0, \tag{7.20}$$

$$[V_2 w_1]_{\xi=0}^{\xi=x_o} + [V_2 w_1]_{\xi=x_o}^{\xi=L} = 0, \quad \text{and} \tag{7.21}$$

$$[M_2 \theta_1]_{\xi=0}^{\xi=x_o} + [M_2 \theta_1]_{\xi=x_o}^{\xi=L} = M_2\left(\theta_1^L + \theta_1^R\right). \tag{7.22}$$

Thus, the reciprocity implies

$$-P_1\Delta_2 + M_1\left(\theta_2^L + \theta_2^R\right) = M_2\left(\theta_1^L + \theta_1^R\right). \tag{7.23}$$

In the above, $\theta_1^L + \theta_1^R = 0$ because the solution w_1 must be admissible. Then, by setting $P_1 = 1$ and $\theta_2^L + \theta_2^R = 1$, we have

$$M_1 = \Delta_2. \tag{7.24}$$

Second, let us consider the shear force at x_o. Similarly, we have (Figure 7.12)

$$-P_1\Delta_2 + V_1\Delta_2' + V_1\Delta_2' = -V_2\Delta_1 + V_2\Delta_1. \tag{7.25}$$

Let $P_1 = 1$ and $\Delta_2' = 1/2$, we have

$$V_1 = \Delta_2. \tag{7.26}$$

Thus, we recovered Figure 7.4(d). Note that the slope of the beam must be the continuous when we break and displace the beam.

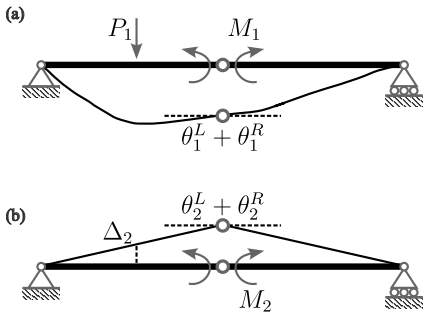

Figure 7.11: Müller-Breslau's principle for calculating an influence line (bending moment). (a) Load case 1. (b) Load case 2.

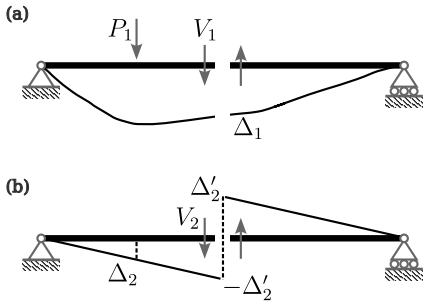

Figure 7.12: Müller-Breslau's principle for calculating an influence line (shear force). (a) Load case 1. (b) Load case 2.

7.3 Indeterminate structures

7.3.1 Two-span beam

Reaction at a support

Influence line for an indeterminate structure is nothing special compared to that of a determinate structure. Consider a following two-span beam, where we are interested in the reaction at the middle support (Figure 7.13). First, we define the primary structures by replacing the middle support with a point load. Then, the corresponding compatibility condition reads

$$d_{L\xi} + R_B \cdot d_{LL} = 0 \Rightarrow R_B = -\frac{d_{L\xi}}{d_{LL}}. \tag{7.27}$$

Then, we can apply the reciprocity relation by

$$\int_0^{2L} \left[-\delta\left(x-\xi\right)\right] d_{xL} dx = \int_0^{2L} \delta\left(x-L\right) d_{x\xi} dx \Rightarrow d_{L\xi} = -d_{\xi L} = -d_{xL}, \tag{7.28}$$

which gives

$$R_B = \frac{d_{xL}}{d_{LL}}. \tag{7.29}$$

The deflection d_{xL} is computed by

$$EI\frac{d^2w}{dx^2} = M = -\frac{PL}{2} \Rightarrow EIw = -\frac{Px^3}{12} + Ax + B, \quad x \in (0, L). \tag{7.30}$$

we apply boundary conditions of

$$w|_{x=0} = 0 \quad \text{and} \quad \theta|_{x=L} = 0, \tag{7.31}$$

which gives

$$EIw = -\frac{Px}{12}\left(x^2 - 3L^2\right). \tag{7.32}$$

Then, the influence line reads

$$I_{R_B} = \frac{d_{xL}}{d_{LL}} = \frac{1}{2}\left[\frac{3x}{L} - \left(\frac{x}{L}\right)^3\right], \quad x \in (0, L), \tag{7.33}$$

where $d_{LL} = w(L) = PL^3/(6EI)$.

Bending moment within a member

Here, we are interested in finding an influence line for a bending moment within a member of a two-span beam (Figure 7.14). Similarly to previous examples, we define the primary structure by releasing the constraint corresponds to the bending moment at the location of interest. The corresponding compatibility condition reads

$$\theta_0^L + \theta_0^R + M_m\left(\theta_1^L + \theta_1^R\right) = 0 \Rightarrow M_m = -\frac{\theta_0^L + \theta_0^R}{\theta_1^L + \theta_1^R}, \tag{7.34}$$

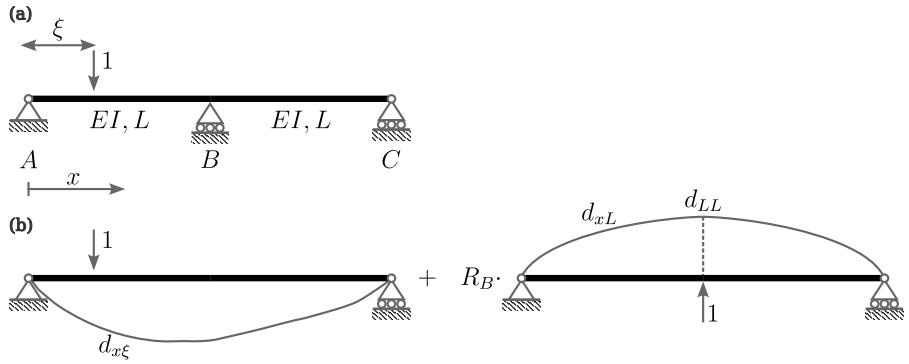

Figure 7.13: Influence for an indeterminate structure. (a) Original structure. (b) Primary structure.

which enforces the slope continuity of the original structure. Then, the Müller-Breslau's principle implies

$$\int_0^{2L} \left[-\delta\left(x-\xi\right)\right] d_{xm} dx = 1 \cdot \theta_0^L\big|_{x=L/2} - 1 \cdot \left(-\theta_0^R\right)\big|_{x=L/2}$$
$$\Rightarrow \theta_0^L + \theta_0^R = -d_{\xi m} = -d_{xm}. \tag{7.35}$$

Thus, the influence line becomes

$$I_M = \frac{d_{xm}}{\theta_1^L + \theta_1^R}. \tag{7.36}$$

First, the deflections of the suspended span ($x \in (0, L/2)$) and the overhanged span ($x \in (L/2, L)$) are computed by

$$EI\frac{d^2 w_S}{dx^2} = \frac{2x}{L} \Rightarrow EIw_S = \frac{L^2}{3}\left[\left(\frac{x}{L}\right)^3 + A\left(\frac{x}{L}\right) + B\right] \quad \text{and} \tag{7.37}$$

$$EI\frac{d^2 w_O}{dx^2} = \frac{2x}{L} \Rightarrow EIw_O = \frac{L^2}{3}\left[\left(\frac{x}{L}\right)^3 + C\left(\frac{x}{L}\right) + D\right]. \tag{7.38}$$

The deflection of the right span ($x \in (L, 2L)$) reads

$$EI\frac{d^2 w_R}{dx^2} = 4 - \frac{2x}{L}$$
$$\Rightarrow EIw_R = \frac{L^2}{3}\left[-\left(\frac{x}{L}\right)^3 + 6\left(\frac{x}{L}\right)^2 + E\left(\frac{x}{L}\right) + F\right]. \tag{7.39}$$

The boundary (and the interface) conditions are

$$w_S|_{x=0} = 0, \tag{7.40}$$
$$w_S|_{x=L/2} = w_O|_{x=L/2}, \tag{7.41}$$
$$w_O|_{x=L} = 0, \tag{7.42}$$
$$\frac{d}{dx}w_O\bigg|_{x=L} = \frac{d}{dx}w_R\bigg|_{x=L}, \tag{7.43}$$
$$w_R|_{x=L} = 0, \quad \text{and} \tag{7.44}$$
$$w_R|_{x=2L} = 0. \tag{7.45}$$

Then, the deflection reads

$$EIw = \begin{cases} \dfrac{L^2}{3}\left[\left(\dfrac{x}{L}\right)^3 + 3\left(\dfrac{x}{L}\right)\right] & x \in (0, L/2) \\ \dfrac{L^2}{3}\left[\left(\dfrac{x}{L}\right)^3 - 5\left(\dfrac{x}{L}\right) + 4\right] & x \in (L/2, L) \\ \dfrac{L^2}{3}\left[-\left(\dfrac{x}{L}\right)^3 + 6\left(\dfrac{x}{L}\right)^2 - 11\left(\dfrac{x}{L}\right) + 6\right] & x \in (L, 2L) \end{cases} . \quad (7.46)$$

Here, we can calculate the slope discontinuity by $\theta_1^L + \theta_1^R = 8L/(3EI)$. Finally, the influence line is

$$I_M = \begin{cases} \dfrac{L}{8}\left[\left(\dfrac{x}{L}\right)^3 + 3\left(\dfrac{x}{L}\right)\right] & x \in (0, L/2) \\ \dfrac{L}{8}\left[\left(\dfrac{x}{L}\right)^3 - 5\left(\dfrac{x}{L}\right) + 4\right] & x \in (L/2, L) \\ \dfrac{L}{8}\left[-\left(\dfrac{x}{L}\right)^3 + 6\left(\dfrac{x}{L}\right)^2 - 11\left(\dfrac{x}{L}\right) + 6\right] & x \in (L, 2L) \end{cases} . \quad (7.47)$$

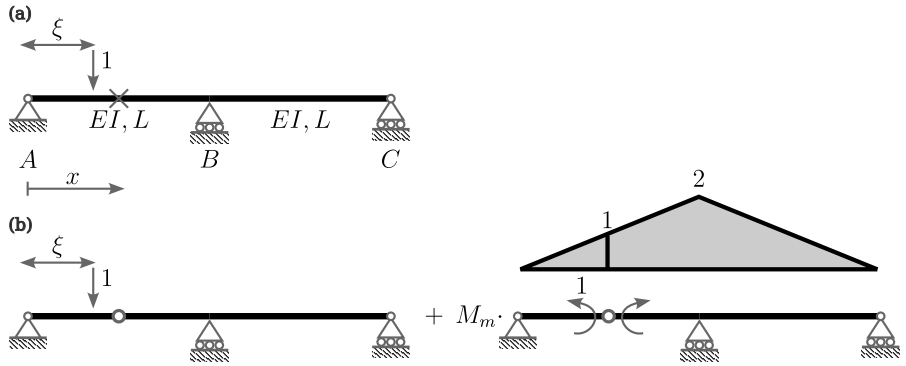

Figure 7.14: Bending moment within a member. (a) Original structure. (b) Primary structure.

Shear force within a member

Next, we consider a shear force at the same location (Figure 7.15). The compatibility condition reads

$$d_0 + V_M d_1 = 0 \Rightarrow V_M = -\frac{d_0}{d_1}. \quad (7.48)$$

Here, the above equation implies deflection continuity. Then, the reciprocity yields

$$\begin{aligned} &\int_0^{2L} \left[-\delta\left(x - \xi\right)\right] d_{xm} dx = -1 \cdot \left(-w_0^L\right)\big|_{x=L/2} + 1 \cdot w_0^R\big|_{x=L/2} \\ &\Rightarrow d_0 = -d_{\xi m} = -d_{xm}. \end{aligned} \quad (7.49)$$

Integrating the bending moment, we have

$$EIw_S = \frac{L^3}{6}\left[\left(\frac{x}{L}\right)^3 + A\left(\frac{x}{L}\right) + B\right] \quad x \in (0, L/2), \tag{7.50}$$

$$EIw_O = \frac{L^3}{6}\left[\left(\frac{x}{L}\right)^3 + C\left(\frac{x}{L}\right) + D\right], \quad x \in (L/2, L), \quad \text{and} \tag{7.51}$$

$$EIw_R = \frac{L^3}{6}\left[-\left(\frac{x}{L}\right)^3 + 6\left(\frac{x}{L}\right)^2 + E\left(\frac{x}{L}\right) + F\right], \quad x \in (L, 2L). \tag{7.52}$$

The boundary conditions are

$$w_S|_{x=0} = 0, \tag{7.53}$$

$$\left.\frac{d}{dx}w_S\right|_{x=L/2} = \left.\frac{d}{dx}w_O\right|_{x=L/2}, \tag{7.54}$$

$$w_O|_{x=L} = 0, \tag{7.55}$$

$$\left.\frac{d}{dx}w_O\right|_{x=L} = \left.\frac{d}{dx}w_R\right|_{x=L}, \tag{7.56}$$

$$w_R|_{x=L} = 0, \quad \text{and} \tag{7.57}$$

$$w_R|_{x=2L} = 0. \tag{7.58}$$

Then, the deflection reads

$$EIw = \begin{cases} \dfrac{L^3}{6}\left[\left(\dfrac{x}{L}\right)^3 - 5\left(\dfrac{x}{L}\right)\right] & x \in (0, L/2) \\ \dfrac{L^3}{6}\left[\left(\dfrac{x}{L}\right)^3 - 5\left(\dfrac{x}{L}\right) + 4\right] & x \in (L/2, L) \\ \dfrac{L^3}{6}\left[-\left(\dfrac{x}{L}\right)^3 + 6\left(\dfrac{x}{L}\right)^2 - 11\left(\dfrac{x}{L}\right) + 6\right] & x \in (L, 2L) \end{cases}. \tag{7.59}$$

In the above, the deflection discontinuity is computed as $d_1 = 2L^3/(3EI)$, which gives

$$I_V = \begin{cases} \dfrac{1}{4}\left[\left(\dfrac{x}{L}\right)^3 - 5\left(\dfrac{x}{L}\right)\right] & x \in (0, L/2) \\ \dfrac{1}{4}\left[\left(\dfrac{x}{L}\right)^3 - 5\left(\dfrac{x}{L}\right) + 4\right] & x \in (L/2, L) \\ \dfrac{1}{4}\left[-\left(\dfrac{x}{L}\right)^3 + 6\left(\dfrac{x}{L}\right)^2 - 11\left(\dfrac{x}{L}\right) + 6\right] & x \in (L, 2L) \end{cases}. \tag{7.60}$$

Alternatively, the influence line for the shear force can be computed from (7.47) using a freebody diagram (Figure 7.16). The equilibrium equation for $x \in (0, L/2)$ is

$$-\frac{L}{2} \cdot V_m - x \cdot 1 + M_m = 0, \tag{7.61}$$

while, for $x \in (L/2, 2L)$,

$$-\frac{L}{2} \cdot V_m + M_m = 0. \tag{7.62}$$

The influence lines for the moment and shear are sketched in 7.17.

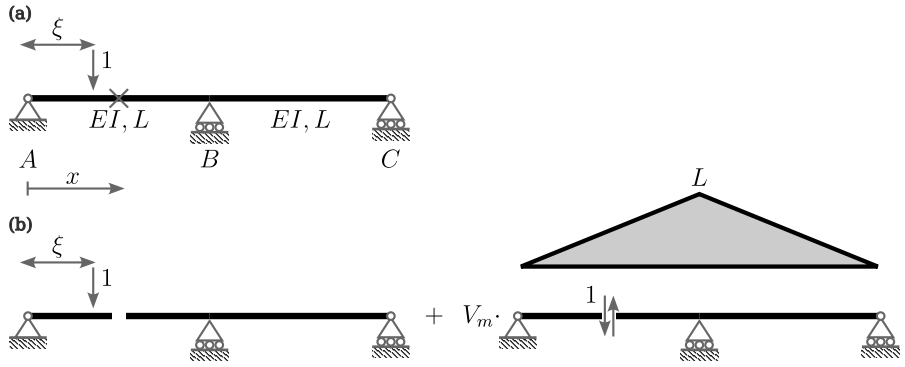

Figure 7.15: Shear force within a member. (a) Original structure. (b) Primary structure.

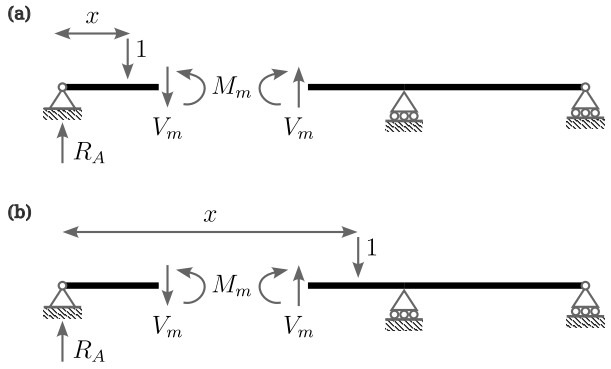

Figure 7.16: Freebody diagram for calculating V_m. (a) $x \in (0, L/2)$. (b) $x \in (L/2, 2L)$.

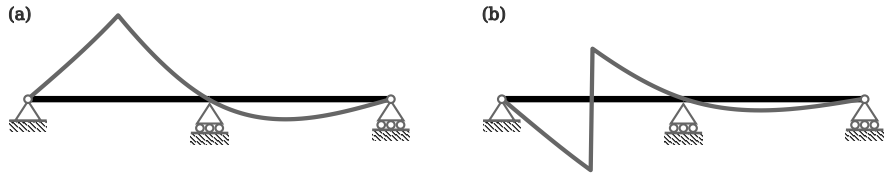

Figure 7.17: Influence lines. (a) Moment (7.47). (b) Shear force (7.60).

7.3.2 Three-span beam

Here, we are interest in calculating an influence line for the bending moment at support B of a three-span beam. The order of indeterminacy is three for the given structure; however, it is not illegal to define primary structures as shown in Figure 7.18. The corresponding compatibility equation reads

$$\theta_0^L + \theta_0^R + M\left(\theta_1^L + \theta_1^R\right) = 0 \Rightarrow M = -\frac{\theta_0^L + \theta_0^R}{\theta_1^L + \theta_1^R}. \tag{7.63}$$

Then, the reciprocity $\int_0^L q\overline{w}dx + \left[M\overline{\theta}\right]_0^L = \int \overline{q}wdx + \left[\overline{M}\theta\right]_0^L$ implies

$$\begin{aligned}&\int_0^{3L} \left[-\delta\left(x-\xi\right)\right] d_{xB}dx = 1\cdot\theta_0^L\big|_{x=L} - 1\cdot\left(-\theta_0^R\right)\big|_{x=L}\\ &\Rightarrow \theta_0^L + \theta_0^R = -d_{\xi B} = -d_{xB}.\end{aligned} \tag{7.64}$$

Thus, we have

$$M = \frac{d_{xB}}{\theta_1^L + \theta_1^R}. \tag{7.65}$$

In the above, we need to analyze another indeterminate structure to find d_{xB} and $\theta_1^L + \theta_1^R$.

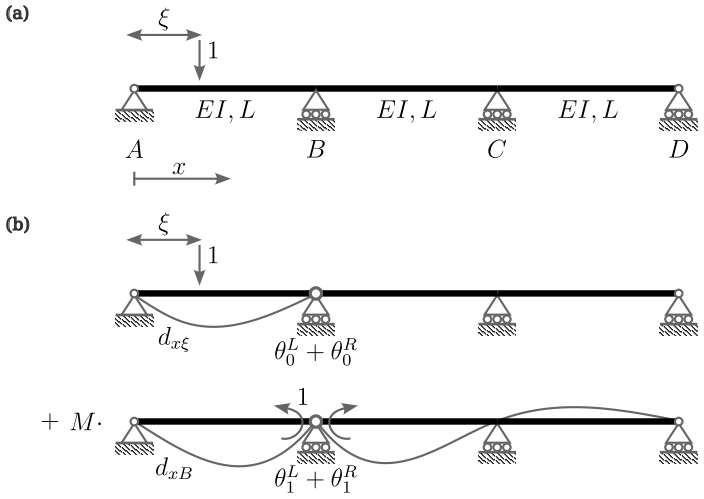

Figure 7.18: Influence for an indeterminate structure. (a) Original structure. (b) Primary structure.

The deflection curve d_{xB} at the left span ($x \in (0, L)$) is easily obtained as (Figure 7.19(a))

$$EIw = \frac{L^2}{6}\left[\left(\frac{x}{L}\right)^3 - \frac{x}{L}\right]. \tag{7.66}$$

The slope at support B becomes

$$\theta_1^L = \frac{L}{3EI}. \tag{7.67}$$

On the other hand, we need to solve an indeterminate structure for $x \in (L, 3L)$ (Figure 7.19), where the compatibility condition reads

$$\delta_0 + M_C \delta_1 = 0. \tag{7.68}$$

Here, we have $\delta_0 = L/(6EI)$ and $\delta_1 = 2L/(3EI)$, which gives $M_C = -1/4$. Introducing $x_1 = (x-L)/L$ and $x_2 = (x-2L)/L$, the bending moment becomes

$$EI\frac{dw^2}{dx^2} = \begin{cases} -\dfrac{5}{4}x_1 + 1 & x_1 \in (0,1) \\ \dfrac{1}{4}x_2 - \dfrac{1}{4} & x_2 \in (0,1) \end{cases}. \tag{7.69}$$

Integrating twice ($Ldx_1 = dx$ and $Ldx_2 = dx$) and applying boundary conditions, we have

$$EIw = \begin{cases} \dfrac{L^2}{24}\left(-5x_1^3 + 12x_1^2 - 7x_1\right) & x_1 \in (0,1) \\ \dfrac{L^2}{24}\left(x_2^3 - 3x_2^2 + 2x_2\right) & x_2 \in (0,1) \end{cases}. \tag{7.70}$$

Then, we have $\theta_1^R = 7L/(24EI)$, which gives $\theta_1^L + \theta_1^R = 5L/(8EI)$. In summary, the influence line reads

$$M = \begin{cases} \dfrac{4L}{15}\left[\left(\dfrac{x}{L}\right)^3 - \left(\dfrac{x}{L}\right)\right] & x \in (0, L) \\ \dfrac{L}{15}\left[-5\left(\dfrac{x-L}{L}\right)^3 + 12\left(\dfrac{x-L}{L}\right)^2 - 7\left(\dfrac{x-L}{L}\right)\right] & x \in (L, 2L) \\ \dfrac{L}{15}\left[\left(\dfrac{x-2L}{L}\right)^3 - 3\left(\dfrac{x-2L}{L}\right)^2 + 2\left(\dfrac{x-2L}{L}\right)\right] & x \in (2L, 3L) \end{cases}. \tag{7.71}$$

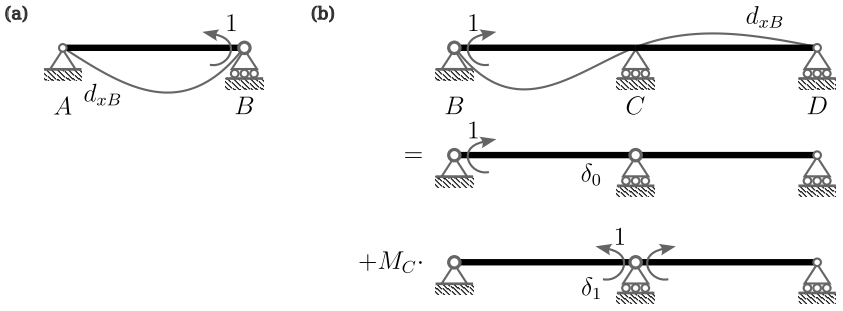

Figure 7.19: Displacement calculation. (a) Left span. (b) Right span.

Bibliography

[Gel'Fand and Shilov, 1964] Gel'Fand, I. M. and Shilov, G. E. (1964). *Generalized Functions: Properties and Operations*, volume 1. Academic Press, New York and London.

[Lee, 2022a] Lee, H. S. (2022a). Lecture notes for structural analaysis 1. Seoul National University.

[Lee, 2022b] Lee, H. S. (2022b). Lecture notes for structural analaysis 2. Seoul National University.

[Stone and Goldbart, 2009] Stone, M. and Goldbart, P. (2009). *Mathematics for physics: a guided tour for graduate students*. Cambridge University Press.

[Utku et al., 1991] Utku, S., Norris, C., and Wilbur, J. (1991). *Elementary Structural Analysis*. McGraw-Hill international editions: Civil engineering series. McGraw-Hill.